Coordination Chemistry Reviews 388 (2019) 406–439

Contents lists available at ScienceDirect

Coordination Chemistry Reviews

journal homepage: www.elsevier.com/locate/ccr

Review

Exohedral functionalization of endohedral metallofullerenes: Interplay between inside and outside ☆

Peng Jin [a,*], Ying Li [a], Saneliswa Magagula [b], Zhongfang Chen [b,*]

[a] School of Materials Science and Engineering, Hebei University of Technology, Tianjin 300130, China
[b] Department of Chemistry, University of Puerto Rico, San Juan, PR 00931, USA

ARTICLE INFO

Article history:
Received 26 December 2018
Received in revised form 21 February 2019
Accepted 22 February 2019
Available online 21 March 2019

In celebration of the 100th anniversary of Nankai University.

Keywords:
Fullerenes
Endohedral metallofullerenes
Chemical functionalization

ABSTRACT

Endohedral metallofullerenes (EMFs) are fullerene cages enclosing various metallic species. The functionalization of EMFs has remarkably blossomed in recent years, in contrast to early efforts that were mainly devoted to their geometric and electronic structures as well as optical and magnetic properties. This review presents an exhaustive survey of the important functionalization approaches of EMFs, mainly focusing on the progress since 2014. The involved reactions include silylation and germylation, Diels–Alder reaction, Bingel–Hirsch reaction, 1,3-dipolar cycloaddition, carbene addition, benzyne addition, free radical reaction, hydroxylation, dimerization, coordination reaction, noncovalent complexation, as well as numerous miscellaneous reactions. We summarize the major factors that affect the reactivity and regioselectivity, focusing particularly on the intriguing interplay between the exohedral groups and internal species. This work highlights the established role of current theoretical studies in further understanding the reactivity and regioselectivity of functionalization reactions. Finally, we discuss potential applications of exohedrally modified EMFs.

Contents

☆ This paper belongs to the special issue entitled "Coordination Chemistry goes multidisciplinary: The Centennial Celebration of Nankai University".

* Corresponding authors.
E-mail addresses: china.peng.jin@gmail.com (P. Jin), zhongfangchen@gmail.com (Z. Chen).

https://doi.org/10.1016/j.ccr.2019.02.028
0010-8545/

1. Introduction

Endohedral metallofullerenes (EMFs), with metallic species (atoms or clusters) imprisoned in carbon cages, are novel metal–carbon hybrid molecules with interesting core–shell structures [1–6]. In the last three decades, the unique and tunable physicochemical properties of EMFs have garnered research interest from various fields such as photovoltaics, materials science and biomedicine.

An EMF molecule is commonly denoted by $M@C_{2n}$, where the symbol @ indicates that the left metallic species are within the right carbon cage [7]. EMFs all feature substantial charges (up to 6*e*) donated by the enclosed metal atom/cluster to the fullerene framework, and are thus commonly described by an ionic model $M^{q+}@C_{2n}{}^{q-}$ [8–11].

The mutual stabilization of the metal core and carbon shell endows EMFs a rather unique capability to encapsulate metal atoms/clusters into the fullerene cage and stabilize the otherwise unstable carbon cages. Various reactive metallic species with a maximum atom number of seven (Sc_4O_3 [12]) have been successfully captured in EMFs due to the confinement effect and effective metal-cage interaction. Therefore, the interior space of fullerenes can serve as an ideal platform to study novel cluster structures. The stability of empty fullerenes is governed by the well-known isolated pentagon rule (IPR) [13], which states that each of the twelve pentagons of a stable carbon cage should only have five hexagons as near neighbors. However, the transfer of electrons can efficiently convert an antiaromatic 8π-electron pentalene subunit of a non-IPR fullerene cage to a local Hückel aromatic 10π-electron motif [14], thus the metal-to-cage charge transfer may partly alleviate the high strain and instability caused by fused pentagons. Encapsulation can therefore serve as an efficient approach to achieve non-IPR fullerenes [15].

To date, more than two hundred EMF molecules have been experimentally characterized. The interior metal mainly originates from Groups I to V on the periodic table and is dominated by Sc, Y and lanthanides with the cages covering a wide size range. In the last two years, Th- or U-based actinide EMFs have emerged as budding stars with unique structures and properties [16–23].

EMFs are generally classified according to their encased composition. Monometallofullerenes (mono-EMFs, e.g., $La@C_{82}$ [7]) and dimetallofullerenes (di-EMFs, e.g., $La_2@C_{80}$ [24]) are two classical types. Trimetallic nitride template (TNT) EMFs, typified by $Sc_3N@C_{80}$, represent a large family of the cluster fullerenes. Notably, $Sc_3N@C_{80}$ can be obtained in rather high yield, only surpassed by C_{60} and C_{70}. Following the accidental production of $Sc_3N@C_{80}$ in 1999 [25,26], various pure or mixed metal nitride EMFs containing two or even three different metals have been extensively reported [3]. Metal carbides ($M_{2,3,4}C_{1,2}$, e.g., $Sc_2C_2@C_{84}$ [27]), hydrogenated metal carbides ($M_{3,4}C_2H$, e.g., $Sc_3CH@C_{80}$ [28]), metal cyanides ($M_{1,3}CN$, e.g., $Sc_3CN@C_{80}$ [29,30]), metal carbide/cyanide alloyed clusters (M_3C_2CN, e.g., $Sc_3C_2CN@C_{80}$ [31]), metal oxides ($M_{2,4}O_{1,2,3}$, e.g., $Sc_4O_2@C_{80}$ [32]), metal sulfides (M_2S, e.g., $Sc_2S@C_{82}$ [33]), and even pure tri-metal clusters (M_3, e.g., $Sm_3@C_{80}$ [34]) have all been successfully encased in fullerene cages.

The rapid progress in isolation and purification of various EMFs greatly facilitated the broad research on their diverse properties. Compared with early efforts mostly devoted to the geometric and electronic structures as well as optical and magnetic properties, their chemical functionalization has remarkably blossomed in recent years for several reasons: (1) it benefits the purification and separation of EMFs from fullerene mixtures; (2) it provides an effective approach to stabilize the highly reactive small-bandgap EMFs and make them obtainable; (3) the functionalized derivatives are easy to crystallize and can help structural characterization of the parent EMFs by using X-ray crystallography; (4) external functional groups can be introduced, which can finely modulate the physical and chemical properties of EMFs to engender diversely applicable functional materials; (5) it assists in increasing the solubility of EMFs by obtaining corresponding water-soluble derivatives that have potential applications in biomedicine; (6) the location, configuration and dynamic behavior of the internal metallic species can be effectively regulated for the design of novel nanodevices and; (7) the relative position and orientation of fullerene molecules can be precisely controlled *via* exohedral modification to achieve self-assembled nano systems with well-ordered structures. In previous years, several excellent review articles focusing on the functionalization of EMFs have been published [35–44]. Since the last dedicated contribution in 2014 [42], however, significant strides have been made in this field, and a timely and comprehensive summary is thus highly desirable to guide the future development of EMFs functionalization.

Herein, we present an extensive survey on the exohedral functionalization of EMFs, mainly focusing on the new developments in the last five years. Some early works missed in other reviews are also covered. The structure for the remainder of the paper is as follows: Section 2 introduces the molecular structures of representative EMFs. Section 3 summarizes all kinds of reported functionalization reactions, including both experimental and theoretical progress. Section 4 briefly introduces the potential applications of the modified EMFs in different fields, followed by Section 5—concluding remarks.

2. Structures of typical EMFs

For convenience, we first introduce the structures of EMFs frequently encountered in functionalization reactions. These include $La@C_{2v}(9)$-C_{82}, $La_2@D_2(10611)$-C_{72}, $La_2@D_{3h}(5)$-C_{78}, $La_2@I_h(7)$-C_{80}, $Sc_3N@D_3(6140)$-C_{68}, $Sc_3N@D_{3h}(5)$-C_{78}, $Sc_3N@D_{5h}(6)$-C_{80}, $Sc_3N@I_h(7)$-C_{80}, $Sc_3C_2@I_h(7)$-C_{80}, $Sc_2C_2@C_s(6)$-C_{82}, $Sc_2C_2@C_{3v}(8)$-C_{82} and $Sc_2C_2@C_{2v}(9)$-C_{82} (Fig. 1). The fullerene isomers are named by the size and point group symmetry of the cage as well as the number assigned by the spiral algorithm (when an IPR cage is concerned, it is numbered by only counting all the IPR isomers) [45]. For example, $La@C_{2v}(9)$-C_{82} indicates that a lanthanum atom is encapsulated by the ninth C_{82} isomer obeying IPR, which has a C_{2v} cage symmetry.

Since its first isolation in 1991, $La@C_{82}$ has been widely recognized as the prototypical EMF molecule [7], and its major isomer bears a $C_{2v}(9)$-C_{82} outer cage. The jailed La atom is off-center positioned along the C_2 axis of cage, and resides under a hexagon ring [46,47]. The metal formally transfers 3*e* to the outer cage, resulting in an electronic structure of $La^{3+}@C_{82}^{3-}$. There are 24 nonequivalent carbon atoms for reactions in $La@C_{2v}(9)$-C_{82} due to the intact cage symmetry upon metal doping.

$La_2@C_{72}$ was first prepared and isolated in 1998 [48] and later found to have a non-IPR cage structure by nuclear magnetic resonance (NMR) measurements [49]. Theoretical calculations [50,51] and X-ray structural characterization of its carbene adducts [52,53] show that it has a $D_2(10611)$-C_{72} cage isomer featuring a

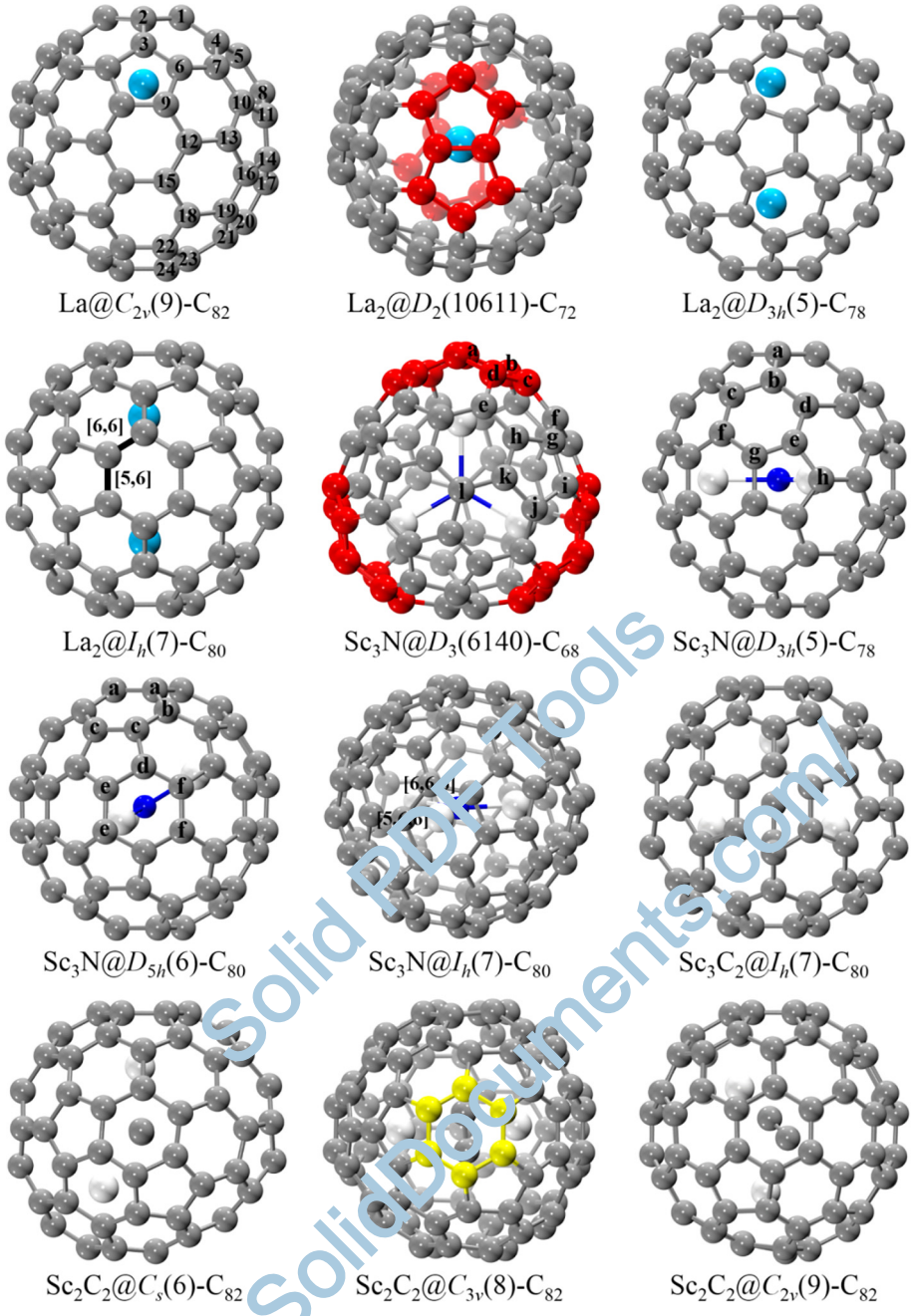

Fig. 1. Structures of typical EMFs marked with different carbon sites or bond types (fused pentagons in non-IPR ones are highlighted in red).

pair of fused pentagons at each of the two poles, which coordinates with a La atom along the C_2 axis. The electronic structure of La_2@D_2(10611)-C_{72} can be described as $(La^{3+})_2$@C_{72}^{6-}. It has 18 different types of carbon for exohedral functionalization due to the high D_2 symmetry.

La_2@D_{3h}(5)-C_{78} was isolated and preliminarily characterized with the aid of NMR and UV-vis-NIR spectra in 2004 [54]. Later, X-ray diffraction analysis on its adamantylidene (Ad) adduct confirmed its cage structure [55]. Theoretical calculations suggest its electronic structure as $(La^{3+})_2$@C_{78}^{6-} [54]. The two La atoms, situated on the C_3 axis, lead to eight types of cage carbon in total.

La_2@C_{80} [24] was identified to have an I_h(7)-C_{80} framework with a $(La^{3+})_2$@C_{80}^{6-} electronic configuration by experimental and theoretical studies [56–60]. Interestingly, even at room temperature, the two La ions can readily circulate in the cage due to the rather low energy barrier and flat electrostatic potential inside C_{80}^{6-} [57,61]. The I_h-C_{80} cage surface has two kinds of C–C bonds: one is the [6,6] bond shared by two hexagonal rings, and the other is the [5,6] bond between one pentagonal ring and one hexagonal ring. Note that the reactive [6,6] pyracylene-type bond is absent in the I_h-C_{80} cage, implying its distinctive chemical behavior.

Sc_3N@C_{80} was first obtained in 1999 and has the same I_h(7)-C_{80} cage framework as that of La_2@I_h-C_{80}. It has an important isomer – Sc_3N@D_{5h}(6)-C_{80}, discovered in 2003, which has six types of carbon atoms [62–64]. The D_{5h} isomer can be converted to an I_h one by splitting the cage along its σ_h plane into two parts, rotating the top one by 36°, and then reconnecting them. They both have a planar, rather flexible Sc_3N cluster with a closed-shell $(Sc^{3+})_3N^{3-}$@C_{80}^{6-} electronic structure. A year after the discovery of Sc_3N@C_{80}, Sc_3N@C_{68} was isolated and confirmed to bear a

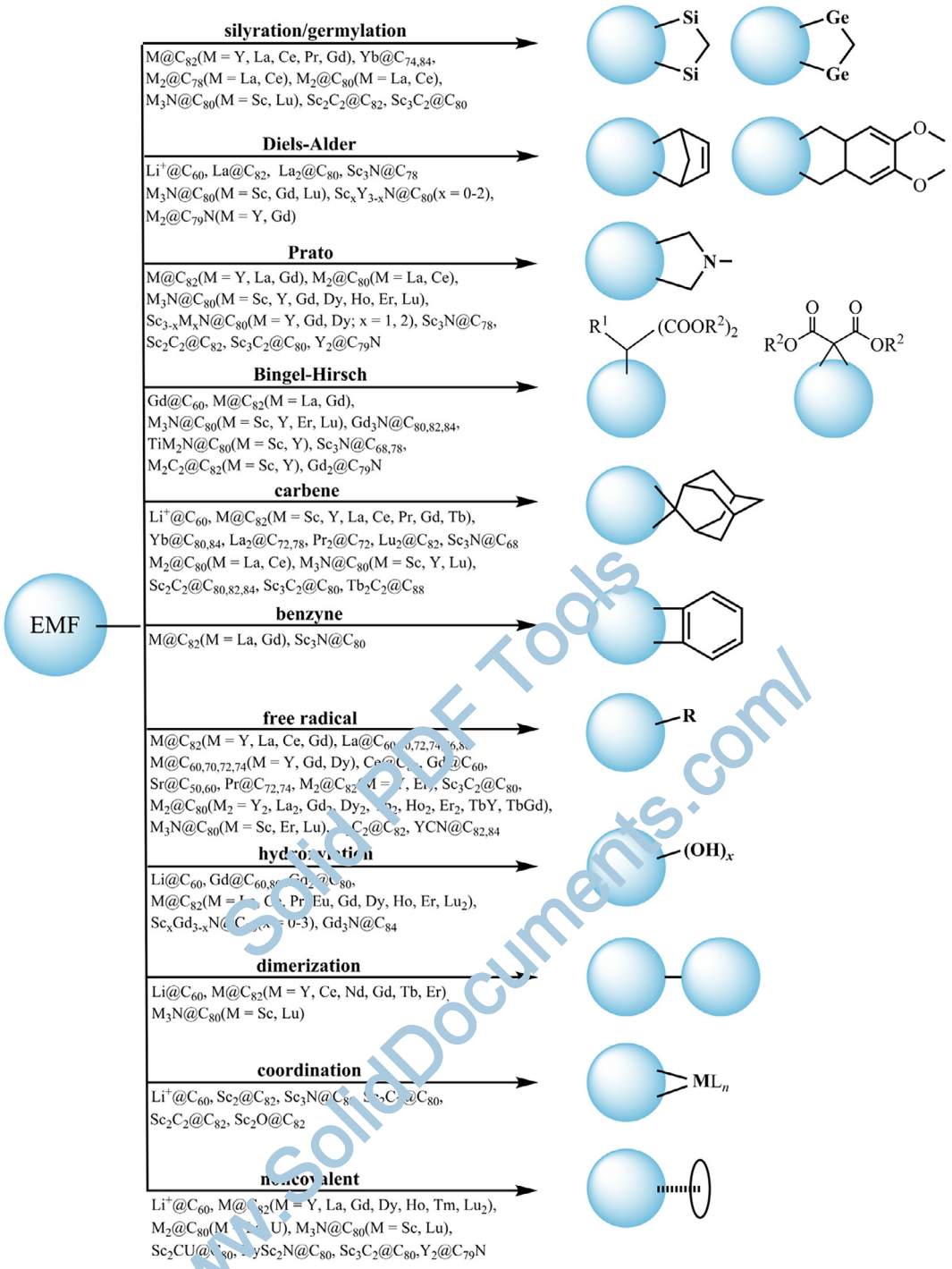

Scheme 1. Typical functionalization reactions of EMFs.

non-IPR D_3(6140)-C_{68} outer cage with three pairs of fused pentagons [65,66]. The Sc_3N cluster is planar with each Sc atom coordinated to the [5,6] bonds of equatorial pentalene moieties. It has 12 kinds of carbon atoms with a $(Sc^{3+})_3N^{3-}@C_{68}^{6-}$ electronic configuration. Another important TNT EMF is $Sc_3N@D_{3h}(5)$-C_{78}, which was isolated and unambiguously characterized in 2001 [67]. The three Sc ions are fixed on the horizontal mirror plane of the cage and point to the [6,6] bonds of three pyracylene patches. Therefore, it has eight nonequivalent carbon atoms due to the preserved D_{3h} symmetry with a $(Sc^{3+})_3N^{3-}@C_{78}^{6-}$ electronic configuration [68].

Metal carbide clusterfullerenes (MCCFs) were discovered during the breakthrough reassignment of Sc_2C_{86} (assumed to be $Sc_2@C_{86}$) as $Sc_2C_2@D_{2d}(23)$-C_{84} in 2001 [27]. Similarly, Sc_3C_{82} is $Sc_3C_2@I_h(7)$-C_{80} rather than the long-believed $Sc_3@C_{82}$ structure with an equivalent Sc trimer [69,70]. The inner Sc_3C_2 cluster adopts a planar or trifoliate configuration and can rotate freely inside the cage. Theoretical calculations suggested that it has an open-shell radical nature with $(Sc^{3+})_3(C_2)^{3-}@C_{80}^{6-}$ electronic configuration [71]. Three Sc_2C_{84} isomers have been isolated thus far and confirmed to be MCCFs: $Sc_2C_2@C_s(6)$-C_{82} [72], $Sc_2C_2@C_{3v}(8)$-C_{82} [73,74] and $Sc_2C_2@C_{2v}(9)$-C_{82} [75]. The Sc_2C_2 cluster prefers to adopt a butterfly shape

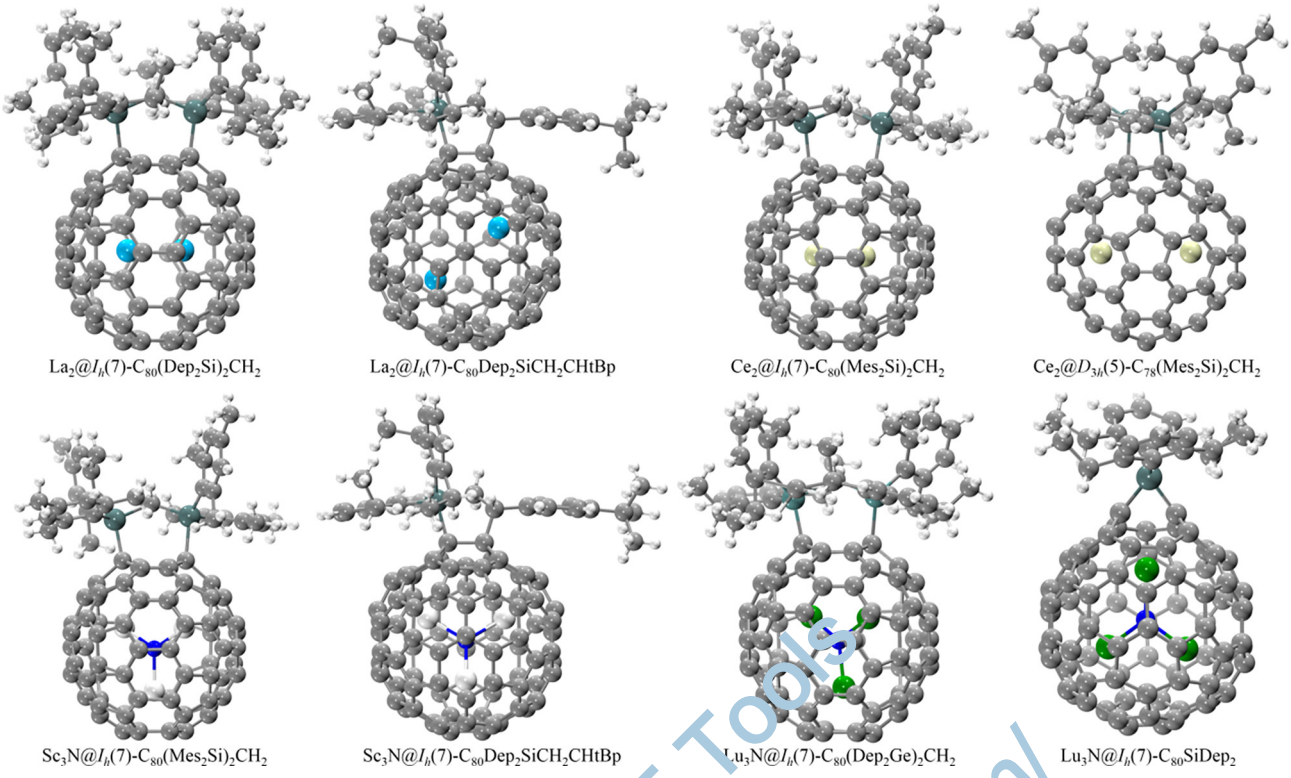

Fig. 2. Silylation and germylation of EMFs. Products structures from Refs. [89,93–95,98,99,101,103].

and formally donates four electrons to the C_{82} cage, giving rise to an electronic structure of $(Sc^{3+})_2(C_2)^{2-}@C_{82}^{4-}$. The most abundant $Sc_2C_2@C_{3v}(8)$-C_{82} features a sumanene-type hexagon with high local strain (highlighted by yellow in Fig. 1), which is very reactive towards various reagents.

3. Functionalization reactions

The exohedral functionalization of EMFs involves plenty of reactions. Scheme 1 summarizes the typical functionalization reactions.

3.1. Silylation and germylation

The chemical transformation of EMFs was first introduced by using activated organosilicon compounds to afford bis-silylated derivatives [76]. In 1995, Akasaka et al. first found that $La@C_{2v}(9)$-C_{82} in toluene solution can react with 1,1,2,2-tetrakis(2,4,6-trimethylphenyl)-1,2-disilirane[$(Mes_2Si)_2CH_2$; Mes = 2,4,6-trimethylphenyl] when photo-irradiated or heated to afford a $La@C_{82}(Mes_2Si)_2CH_2$ monoadduct [77]. The high reactivity of $La@C_{82}$ mainly stems from its strong electron donating/accepting ability (indicated by smaller ionization potential (IP) and larger electron affinity (EA) [78] or low oxidation and reduction potentials [79]). Similar to the Si-Si σ bond in disilirane, the strained Ge-Ge bond in digermirane may also serve as an electron donor to react with EMFs. Indeed, $La@C_{82}$ reacted photochemically with 1,1,2,2-tetrakis(2,6-diethylphenyl)-1,2-digermirane [$(Dep_2Ge)_2CH_2$, Dep = 2,6-diethylphenyl], and yielded at least three isomeric monoadducts [80,81]. Notably, the reaction also occurred thermally even at a temperature as low as 20 °C due to the lower oxidation potential of digermirane.

So far, silylation/germylation has been realized for the mono-EMFs $M@C_{82}$ (M = Y, La, Ce, Pr, Gd) [77,80–87]; divalent $Yb@D_{3h}(1)$-C_{74} and $Yb@C_2(13)$-C_{84} [88]; di-EMFs $M_2@D_{3h}(5)$-C_{78} (M = La, Ce) [54,89,90], $M_2@I_h(7)$-C_{80} (M = La, Ce) [91–95] and $Ce_2@D_{5h}(6)$-C_{80} [96]; and clusterfullerene $M_3N@I_h(7)$-C_{80} (M = Sc, Lu) [97–105], $Sc_2C_2@C_{3v}(8)$-C_{82} [99] and $Sc_3C_2@I_h(7)$-C_{80} [106]. The structures of their corresponding adducts have been characterized by single crystal X-ray crystallographic analysis (Fig. 2).

Following their early study on the photoreaction of $Lu_3N@I_h(7)$-C_{80} with disilirane [100], Akasaka et al. recently reported that the digermirane more readily reacts with $Lu_3N@I_h(7)$-C_{80} in toluene to afford bis-germylated $Lu_3N@I_h$-$C_{80}(Dep_2Ge)_2CH_2$ adduct in 59% yield under the same condition [101]. The enhanced reactivity stems from its higher HOMO (highest occupied molecular orbital) energy level and stronger donor character than disiliranes as well as weaker steric clash around the Ge-Ge bond. The exact structures of $Lu_3N@I_h$-$C_{80}(R_2Si)_2CH_2$ (R = Mes and Dep) and $Lu_3N@I_h$-$C_{80}(Dep_2Ge)_2CH_2$ were revealed by single-crystal X-ray analysis to have the additions at the [1,4] sites. Their inner Lu atoms are disordered, but all oriented away from the addition site. It is worth noting that $Lu_3N@I_h$-$C_{80}(Dep_2Ge)_2CH_2$ is reportedly the first crystallographically characterized germylated fullerene (Fig. 2). The thermal reactions of $Lu_3N@I_h$-C_{80} with disilirane and digermirane all failed as in the $Sc_3N@I_h$-C_{80} case [97] due to the similar LUMOs (lowest unoccupied molecular orbital) of the two EMF molecules [64]. Very recently, they further isolated and characterized the liable 1,2 adducts previously observed in the photoreactions of disilirane with $Sc_3N@I_h$-C_{80} [97,98] and $Lu_3N@I_h$-C_{80} [100,101] by using spectroscopic and electrochemical measurements as well as density functional theory (DFT) calculations [105]. The obtained $M_3N@I_h$-C_{80} $(Mes_2Si)_2CH_2$ (M = Sc, Lu) products may both have the [5,6] addition pattern. Theoretical calculations reveal that they are higher in energy than the 1,4 counterparts, consistent with the observed isomerization of the 1,2-adducts to the 1,4-ones.

On the other hand, they also conducted the photochemical reactions between $M_3N@I_h(7)$-C_{80} (M = Sc, Lu) and silirane (silacyclopropane) containing 4-*tert*-butyl-2,6-dimethylphenyl (Dmt) or Dep substituents, and obtained three isomeric carbosilylated

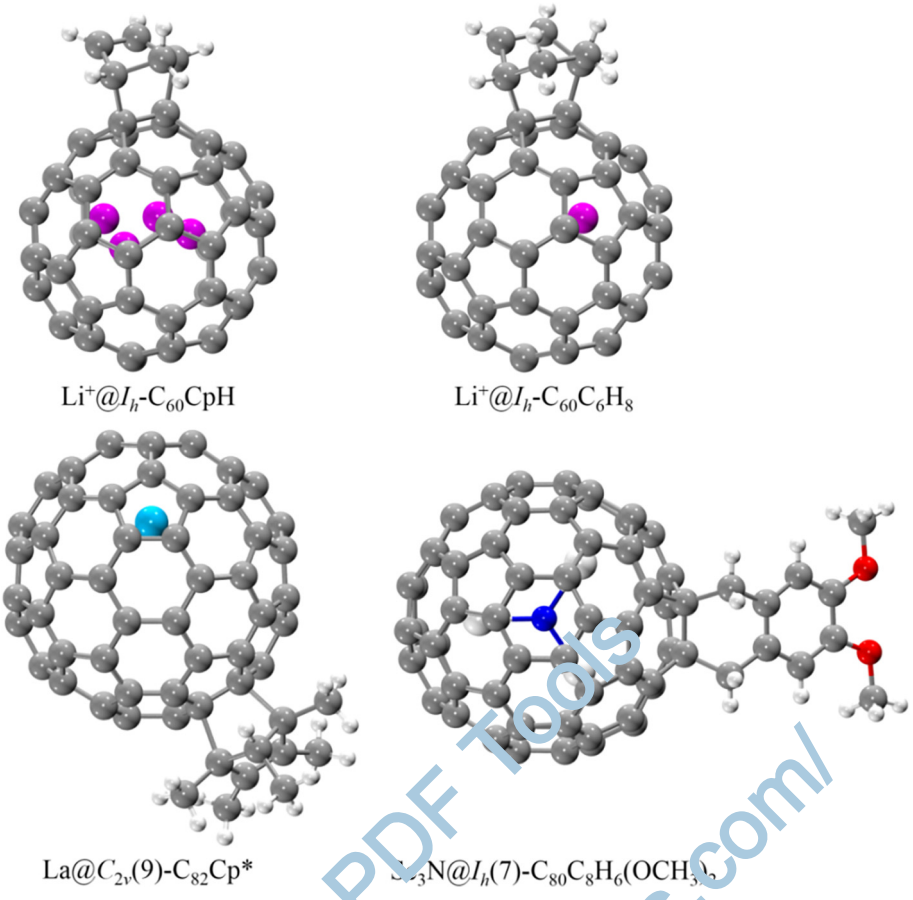

Fig. 3. Product structures for Diels–Alder reactions of EMFs from Refs. [109–111,113]. Counteranions are omitted for clarity.

derivatives including two [5,6]- and one [6,6]-adducts, respectively [102–104]. Among them, the crystal structure of a [5,6]-$Sc_3N@I_h$-$C_{80}Dep_2SiCH_2CHtBp$ (tBp = 4-*tert*-butylphenyl) was firmly established by X-ray crystallographic analysis, in which the internal Sc atoms are disordered, whereas the N atom is fixed (Fig. 2).

Numerious studies reveal that the reduction potentials of EMFs play a critical role in dictating their chemical reactivity toward electron-donating siliranes and germiranes [107]. The classical EMFs are generally more reactive than clusterfullerenes due to their lower reduction potentials and higher electron affinities [97]. Changing either the metal or the outer cage can dramatically alter the chemical reactivity [77,84,86]. The charge state could also affect the chemical reactivity of EMFs, and oxidation and reduction can effectively increase and decrease reactivity of the EMF toward the nucleophilic disilirane, respectively [87]. The flexible metal motion in pristine di-EMFs may be hindered by the exohedral addition [93,94]. Besides the bis-silylation, carbosilylation is efficient to introduce silicon into carbon systems as well, and one can finely tune the electronic properties of EMFs by attaching different numbers of silyl groups [95].

3.2. Diels–Alder cycloaddition

The Diels-Alder (DA) reaction is the [4+2] cycloaddition between a dienophile and a conjugated diene. The Woodward-Hoffmann rules point out that the reaction occurs between the LUMO of the former and the HOMO of the latter, and a small energy gap between them generally makes the cycloaddition more favorable. The reaction generates a six-membered ring linked to the fullerene cage surface.

As the first DA reaction of EMFs and also the first organic derivatization of TNT EMFs, Dorn et al. reported in 2002 the thermal reaction between $Sc_3N@I_h(7)$-C_{80} and excess diene precursor 1,3-dimethoxyisochroman-3-one to afford a $Sc_3N@C_{80}C_8H_6(OCH_3)_2$ monoadduct [108]. Subsequent X-ray crystallographic characterization showed that the addition occurred at a [5,6] junction, which protruded from the cage surface with an elongated C–C separation of 1.626 Å (Fig. 3) [109]. Afterwards, the reported DA reactions extended to $Li^+@C_{60}$ [110,111], $La@C_{2v}(9)$-C_{82} [112–116], $La_2@I_h(7)$-C_{80} [116], $Sc_3N@D_{3h}(5)$-C_{78} [117], $M_3N@C_{80}$ (M = Sc, Gd, Lu) [64,108,109,118], $Sc_xY_{3-x}N@I_h(7)$-C_{80}(x = 0–2) [119], and $M_2@C_{79}N$ (M = Y, Gd) [120].

Recently, Takano et al. reported the [4+2] cycloaddition reaction of $La@C_{2v}(9)$-C_{82} or $La_2@I_h(7)$-C_{80} with reactive *o*-quinodimethanes generated *in situ* by the thermolysis of sultine 4,5-benzo-3,6-dihydro-1,2-oxathiin 2-oxide and its derivative [116]. Spectroscopic analysis suggest that both [5,6]- and [6,6]-adducts were obtained for $La_2@C_{80}$, whereas the addition of $La@C_{82}$ occurs at the same **C21-C23** site (Fig. 1) as that of cyclopentadiene (Cp)/1,2,3,4,5-pentamethylcyclopentadiene (Cp*) [112,113].

$Li^+@C_{60}$ is expected to exhibit high reactivity with diene due to its lowered LUMO energy level and activation energy by Li^+ encapsulation than those of C_{60} and $La@C_{82}$ [121]. Indeed, the DA reaction of Cp with $[Li^+@C_{60}]PF_6^-$ occurs very smoothly at room temperature with an equilibrium constant more than 10^3-fold that of C_{60} [110]. Among the obtained $[Li^+@C_{60}Cp_{1,2}]PF_6^-$ mono- and bis-adducts, the monoadduct was successfully isolated and characterized by X-ray diffraction (XRD). Likewise, the reaction between $[Li^+@C_{60}]PF_6^-$ and 1,3-cyclohexadiene at 303 K proceeded about 2400 times faster than that of empty C_{60} and afforded a very stable

monoadduct [111]. As indicated by the X-ray crystallographic data, both additions occurred at the [6,6] bond (Fig. 3).

More M@C_{60}-based DA reactions come from theoretical studies. Recent DFT calculations revealed that the encapsulation of various metal cations (M = Li^+, Na^+, K^+, Rb^+, Cs^+, and Ca^{2+}) makes the DA cycloaddition of Cp to C_{60} both kinetically and thermodynamically more favorable [122]. The DFT study on the DA reaction between M@C_{60} (M = Li^+, Na^+, K^+, Be^{2+}, Mg^{2+}, Al^{3+} and Cl^-) and 1,3-cyclohexadiene further reveals that the encapsulation of a cation and an anion enhances and reduces the reactivity, respectively [123]. Interestingly, compared to the usual concerted mechanism, a stepwise pathway involving a zwitterionic intermediate was suggested for M = Be^{2+}, Mg^{2+} and Al^{3+} probably due to the highly polarized C_{60} cage. Enhanced reactivity upon cation encapsulation was also found for the reactions between Li^+@C_{60}, Mg^{2+}@C_{60} and 2,4-butadiene [124] owing to the significantly reduced energy gap between the HOMO of diene and the LUMO of fullerene.

Smaller fullerene cages are also considered in the computations. Ravinder and Subramanian investigated the role of metal encapsulation on the DA reaction between Na^+@C_{32} and *cis*-1,3-butadiene by DFT calculations [125]. C_{32} and Na^+@C_{32} favor the attack at a [5,5] bond both thermodynamically and kinetically, with the latter exhibiting a dramatically decreased activation energy than the former (10.02 vs. 1.08 kcal mol^{-1}). The charge transfer from the cage to Na^+ cation and the significantly lowered HOMO and LUMO levels upon the encapsulation may account for the higher reactivity of Na^+@C_{32}.

For the TNT EMFs with cages smaller than $Sc_3N@I_h(7)$-C_{80}, Zhang et al. recently reported that the DA reaction between $Sc_3N@D_{3h}(5)$-C_{78} and *o*-quinodimethane yielded four $Sc_3N@C_{78}(CH_2)_2C_6H_4$ monoadducts with possible addition sites suggested by calculations [117].

In recent years, Swart and Solà et al. systematically investigated the DA reactions of 1,3-*cis*-butadiene with X@C_{78} (X = Sc_3N, Y_3N, Ti_2C_2) [126–130] and X@C_{80}(X = La_2, Y_3, Sc_3N, Y_3N, Gd_3N, Lu_3N, Sc_3C_2, Sc_3CH, Sc_3NC, Sc_4C_2, Sc_4O_2, Sc_4O_3) [131,132] by analyzing both the thermodynamics and kinetics via careful DFT calculations. The additions to all nonequivalent bonds of the fullerene cages are thoroughly surveyed, and various metal orientations are considered for the C_{80}-based EMFs due to the flexible metal motion. EMFs exhibit less regioselectivity and are generally less reactive toward butadiene than their hollow counterparts mainly due to the higher-lying LUMOs caused by the metal-to-cage charge transfer. The LUMOs alter the structure of the carbon framework, which activates certain types of unreactive bonds, and deactivates others.

Recently, Yang et al. theoretically studied the addition of 1,3-butadiene with small non-IPR $D_3(6140)$-C_{68} fullerene and its $Sc_3N@D_3(6140)$-C_{68} derivative [133]. Since the metals are fixed nearby the pentalenes, the two molecules both have 18 nonequivalent C–C bonds (Fig. 1) and same symmetry. The additions to [5,5] **a-a** and [5,6] **a-b** bonds of empty C_{68} are favored thermodynamically and kinetically, respectively. The endohedral exhibits lower reactivity and regioselectivity mainly due to the intramolecular charge transfer, and the addition at the [5,5] **a-a** bond is both thermodynamically and kinetically most favored. Computational results suggest that $Sc_3N@C_{68}$ may be more reactive toward *o*-quinodimethane than 1,3-butadiene based on its larger reaction energy and lower energy barrier.

The DA reaction of mixed-metal clusterfullerenes (MMCFs) $Sc_xY_{3-x}N@I_h(7)$-C_{80}(x = 0–3) with *o*-quinodimethane was investigated very recently [119]. For $Sc_3N@C_{80}$, $Sc_2YN@C_{80}$ and $ScY_2N@C_{80}$, only one [5,6]-monoadduct was isolated. $Y_3N@C_{80}$, with the largest endocluster yields one [5,6]- and one [6,6]-monoadducts probably due to the decreased energy difference between its two adducts.

So far, DA addition to MCCFs has not been realized. The reaction of 1,3-butadiene with $Sc_2C_2@C_{3v}(8)$-C_{82} was predicted by DFT calculations to occur at the [6,6] bond of the sumanene-type hexagon in terms of both thermodynamics and kinetics [134]. The high regioselectivity is accounted for by the shortest bond length, relatively large POAV (π-orbital axis vector) [135] value and appropriate LUMO shape at the addition site. The possible DA reaction of a computationally characterized $La_2C_2@C_1(153491)$-C_{94} isomer was also proposed [136].

Besides the above mono-addition reactions, very recently, the anthracene bis-cycloaddition of La@D_{5h}-C_{70} was also investigated by DFT calculations [137].

In summary, the encapsulation of metal clusters may induce two opposite effects on the fullerene reactivity [126]. On one hand, the resultant geometric deformation enhances the strain energy of the carbon framework and therefore increases the reactivity. On the other hand, the metal-to-cage charge transfer reduces the EA of the cage and lowers the chemical reactivity. The efficient isolation of considerable quantities of high-purity TNT EMFs from hollow fullerenes and classical EMFs in a short period of time was achieved based on their diverse reactivities toward the DA additions [138].

3.3. Prato reaction

Various (metallo)fulleropyrrolidines can be prepared by Prato reaction, namely the 1,3-dipolar cycloaddition occurring between (metallo)fullerenes and azomethine ylides (formed *in situ* from aldehydes and *N*-substituted glycines). This [3+2] cycloaddition features the formation of a heterocyclic five-membered ring on the cage surface.

In 2004, Akasaka and co-workers first reported the Prato reaction of EMFs [139]. After heating a toluene solution containing La@$C_{2v}(9)$-C_{82} and excess *N*-methylglycine as well as paraformaldehyde at 100 °C for 30 min, they successfully synthesized and isolated a monoadduct and a bisadduct of La@C_{82} metallofulleropyrrolidines. So far, the experimentally realized EMFs include La@$C_{2v}(9)$-C_{82} [139,140], La@$C_s(6)$-C_{82} [141], M@C_{82} (M = Y, Sc) [142,143], $M_2@I_h(7)$-C_{80} (M = La, Ce) [144–146], $Sc_3N@D_{3h}(5)$-C_{78} [147], $M_3N@C_{80}$ (M = Sc, Y, Gd, Dy, Ho, Er, Lu) [64,148–172], $Sc_{3-x}M_xN@I_h$-C_{80}(M = Y, Gd, Dy; *x* = 1, 2) [173–177], $Sc_2C_2@C_s(6)$-C_{82} [72], $Sc_2C_2@C_{3v}(8)$-C_{82} [178], $Sc_2C_2@C_{2v}(9)$-C_{82} [75], $Sc_3C_2@I_h$-C_{80} [179–182] and $Y_2@C_{79}N$ [183].

Unlike La@$C_{2v}(9)$-C_{82}, it has been hard to study the reactivity of La@$C_s(6)$-C_{82}, partly due to its low-symmetry, which causes poor regioselectivity and consequent low yields in addition reactions [184,185]. Recently, Akasaka and co-workers conducted its Prato reaction by employing an azomethine ylide as 1,3-dipole and *o*-dichlorobenzene (*o*-DCB) as the solvent [141]. By adding a droplet of toluene into the solution before refluxing, they remarkably improved the reaction selectivity, and obtained two adducts in relatively high conversion yields. Surprisingly, the mass spectra of the two products exhibit a molecular ion peak at 1285 *m/z*, suggesting that they are 1,3-dipolar cycloadducts with an unexpected additional H atom. Subsequent NMR measurements for the main product confirmed this simultaneous hydrogenation. The adducts thus have a closed-shell configuration and are ESR silent. The hydrogen atom was considered to stem from the toluene and its addition occurred after that of the azomethine ylide. After a careful theoretical investigation on several isomer candidates, the reaction sites with large POAV values and spin density were proposed for the cycloaddition and hydrogenation. The products represent the first EMFs containing a cage surface-direct-linking hydrogen atom.

The only new study on the Prato reaction of di-EMFs is from theoretical prediction. Recently, the exact structure of $Sc_2@C_{66}$ [186] was confirmed to bear a $C_{2v}(4059)$-C_{66} cage [187]. Subsequent DFT calculations suggest that $Sc_2@C_{2v}(4059)$-C_{66} may exhibit

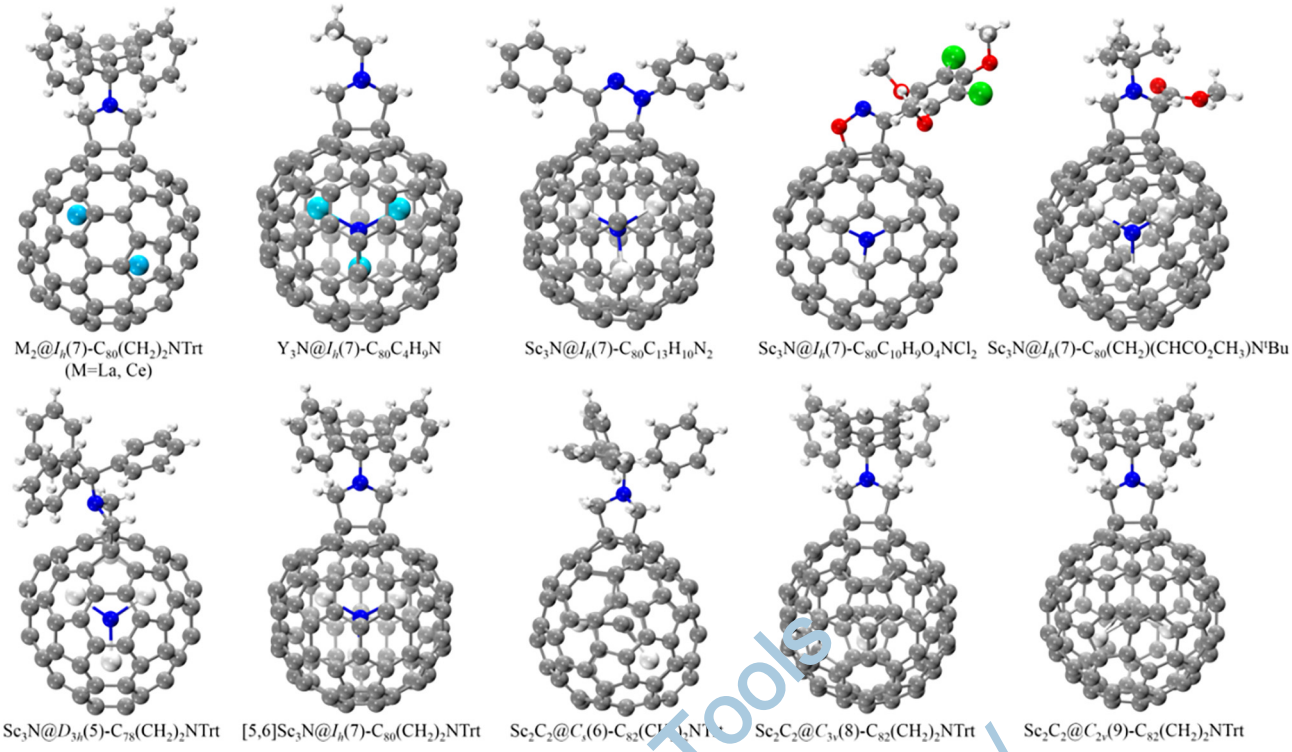

Fig. 4. Product structures for Prato reactions of EMFs from Refs. [72,75,144,147,150,152–154,158,178] (Trt = triphenylmethyl).

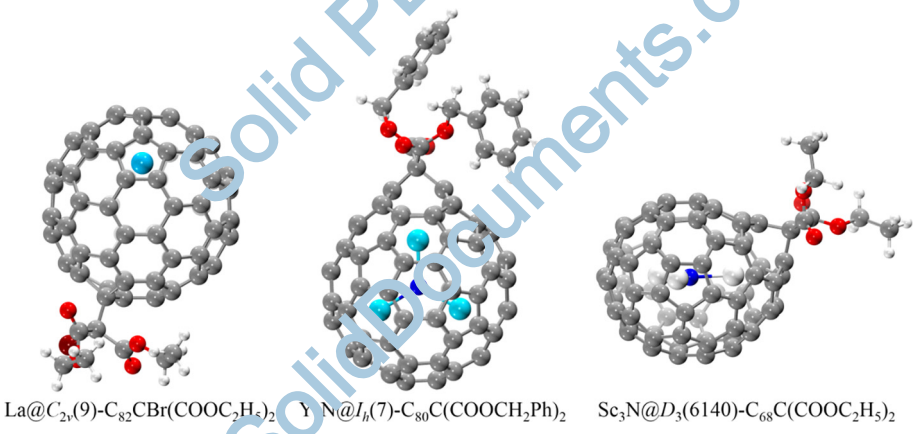

Fig. 5. Product structures for Bingel–Hirsch reactions of EMFs from Refs. [195,201,203].

high reactivity but low regioselectivity toward the Prato reaction [188].

In contrast to the most pyrrolidino-ring Prato derivatives, Lu et al. recently synthesized a rather stable pyrazole-ring fused derivative of $Sc_3N@I_h(7)$-C_{80} by using diphenylnitrilimine (DPNI, generated *in situ* from N-phenylbenzenecarbohydrazonoyl chloride in the presence of triethylamine) as the reagent at elevated temperatures [153]. For the stable pyrazole-ring fused monoadduct $Sc_3N@C_{80}(C_{13}H_{10}N_2)$, UV–vis-NIR spectrometry and single-crystal data show that the reaction occurs at a [5,6] junction, exhibiting a local close-cage structure (Fig. 4). The internal metal cluster slightly deviates from planarity, with two Sc atoms facing the carbon atoms in para position to the attacked carbons. The free Sc_3N motion in I_h-C_{80} is severely hampered upon the exohedral functionalization.

Later, they further reported the 1,3-dipolar cycloaddition reaction of $Sc_3N@I_h$-C_{80} with 3,5-dichloro-2,4,6-trimethoxybenzonitrile oxide [154]. Regarding the obtained $Sc_3N@I_h$-$C_{80}(C_{10}H_9O_4NCl_2)$ derivative, XRD studies revealed that the isoxazoline ring is fused to the cage at a [5,6] bond (Fig. 4). Visible-near-IR spectra and electrochemical measurements show that the electronic structures and redox properties of $Sc_3N@I_h$-C_{80} are altered by chemical modification. Since isoxazoline derivatives are well known to have biological activities, the corresponding derivatives of EMFs may show promising biological applications.

The paramagnetic properties of functionalized EMFs are intriguing. Very recently, $M_3N@I_h(7)$-C_{80}(M = Sc, Y, Dy) was linked to the nitroxide radical via Prato reaction and afforded [5,6] and [6,6] adducts [163]. The ESR intensity of the [5,6] $Dy_3N@C_{80}$ adduct is higher than that of the [6,6] one due to different distances and

relative positions between the nitroxide radical and $Dy_3N@C_{80}$, which lead to stronger dipole–dipole interaction in the latter. The spin-paramagnet interactions between $Dy_xSc_{3-x}N@C_{80}$ ($x = 1, 2$) and the nitroxide radical were also investigated [173]. The adducts may have potential applications as a molecular compass with position-sensitive magnetoreception ability.

Osuna and Yamakoshi et al. systematically studied the different effects of endohedral clusters and three types of exohedral functional groups (glycine derivatives with bis-ester, bis-ether, and ethyl substituents) on the regioisomeric ratios of the $M_3N@C_{80}$ (M = Sc, Lu, Y, Gd) fulleropyrrolidines [170]. Although both the metal cluster size and exohedral groups affect the [6,6] to [5,6] isomerization rates, the [6,6]/[5,6] regio ratio depends only on the former, namely 0:100, ca. 10:90 and 50:50 for M = Sc/Lu, Y, and Gd, respectively. The isomerization was confirmed to proceed *via* a [1,5]-sigmatropic rearrangement rather than a retrocycloaddition one by experiment and DFT calculated energy barriers.

The metal motion is also tunable by exohedral functionalization. Recently, Wang et al. performed a systematic study on the internal dynamic behaviour of $Sc_3N@I_h$-C_{80} with the aid of ^{45}Sc NMR spectroscopy, and found that the inner cluster motion can be finely tuned by chemically modifying the cage [171]. $Sc_3N@C_{80}$ fulleropyrrolidine and $Sc_3N@C_{80}$-PCBM (PCBM = phenyl-C_{81}-butyric acid methyl ester), which are a [5,6]-closed isomer (from Prato reaction) and a [6,6]-open metallofulleroid (from carbene addition) respectively, exhibit distinct ^{45}Sc NMR spectral patterns different from that of pristine $Sc_3N@C_{80}$ (a single 190 ppm peak at room temperature). At 273 K, two distinctive signals for the former and a broad one for the latter were observed, indicating a more hindered metal motion in the former. The NMR spectra at low temperatures clearly show two lines with an intensity ratio of 1:2, indicating two of the three Sc atoms are equal. It also shows that the Sc_3N cluster in $Sc_3N@C_{80}$-PCBM may have oscillating motions, which is consistent with the single crystal structures of $M_3N@C_{80}$-PCBM (M = Sc, Y) [172].

The single molecule magnet (SMM) $DySc_2N@C_{80}$ and its [5,6]-C_4H_9N derivative synthesized *via* the Prato reaction exhibit different magnetic properties with the hysteresis loop of the latter wider than that of the former [176]. Interestingly, both of them can be entrapped in the cage-shaped pores of a metal–organic framework (MOF-177) and show an increased remanent magnetization at zero field. The strong π–π interactions between $DySc_2N@C_{80}$ and the pores of the MOF are responsible for the suppressed quantum tunneling of magnetization. The behavior of the Prato mono-adduct of $DySc_2N@C_{80}$ on a gold surface was also studied by molecular dynamics simulations [189]. Very recently, $DySc_2N@I_h(7)$-C_{80} and $Dy_2ScN@I_h(7)$-C_{80} were successfully functionalized with thioether –S-CH_3 group via Prato reaction [177]. The low-temperature SMM properties of the obtained [5,6]-monoadducts are obviously improved and worsened compared to $DySc_2N@I_h(7)$-C_{80} and $Dy_2ScN@I_h(7)$-C_{80}, respectively. The self-assembled monolayers formed by their deposition onto the Au(1 1 1) surface show magnetic hysteresis at 2 K.

Systematic theoretical calculations at the DFT level were conducted for the Prato reaction of the recently discovered $LaSc_2N@C_s(hept)$-C_{80}, whose cage contains one heptagon fused to two pentalene units, 11 pentagons and 28 hexagons [190,191]. Among the 64 inequivalent C–C bonds, $LaSc_2N@C_s(hept)$-$C_{80}(CH_2)_2NH$ cycloadduct (even bis-adduct) thermodynamically tends to form at the [5,5] bonds in the heptagon-pentagon-fused region, probably due to the large POAV value. A similar addition pattern was also theoretically suggested for $Sc_3N@D_3(6140)$-C_{68}, implying an enhanced Prato reactivity of [5,5] bonds of non-IPR EMFs.

There are very few reports on the effects of exohedral functionalization on the nonlinear optical properties of EMFs. By using time-dependent DFT methods, Wang et al. studied the multiphoton absorption of *N*-methyl-2-ferrocenyl-[5,6]-pyrrolidine-$Sc_3N@I_h(7)$-C_{80}, and found red-shifted peaks and increased cross sections in comparison with pristine $Sc_3N@C_{80}$ [192].

Very recently, Wang et al. covalently linked the triptycene rotor to $Sc_3C_2@C_{80}$ to construct an intriguing coupled system between spin flip and molecular rotor [182]. Temperature-dependent EPR measurements revealed that the spin relaxation and spin-metal hyperfine couplings of the EMF part could be remotely controlled by the rotation of the triptycene rotor. Such controllable molecular paramagnetism induced by chemical functionalization may find great applications in the design of future nanodevices.

In summary, the metal position, motion and spin density distribution could be affected by the exohedral addition [144,145,159,171,193]. The encased metal cluster could control the reactivity and addition pattern of TNT EMFs [156,167]. The size of endohedral clusters may affect the product isomer distribution [169,170,174,175]. Endohedral clusters could affect the electrochemical properties of EMF derivatives [162]. 1,3-Dipolar reactions can also be applied in the construction of applicable systems [140]. The corresponding *retro*-cycloaddition reactions were also reported, and may be a promising non-HPLC approach to separate EMFs from hollow fullerenes [164–166].

3.4. Bingel–Hirsch reaction

The Bingel–Hirsch (BH) reaction is an important nucleophilic [2 + 1] cycloaddition to generate a three-membered ring on the fullerene surface. Typically, the dehydrogenation of bromomalonate with 1,8-diazabicyclo[5.4.0]undec-7-ene (DBU) first forms a carbanion, which then attacks a double bond of fullerene to generate the intermediate. The intermediate then converts to the cyclopropanated derivatives. The product is either closed-cage methanofullerene or methanofulleroid.

The first reported BH addition to EMFs ($Gd@C_{60}$) appeared in 2003 [194]. To date, the reaction has been successfully extended to $M@C_{2v}(9)$-C_{82} (M = La, Gd) [195–200], $M_3N@I_h(7)$-C_{80}(M = Sc, Y, Er, Lu) [195,196,201–204], $Sc_3N@D_{5h}$-C_{80} [205], $Gd_3N@C_{2n}$($2n$ = 80, 82, 84) [206–208], $TiM_2N@I_h$-C_{80} (M = Sc, Y) [209,210], $Sc_3N@D_3$-$_h$(5)-C_{78} [211], $Sc_3N@D_3(6140)$-C_{68} [212], $M_2C_2@C_s$-C_{82} (M = Sc, Y) [213], and $Gd_2@C_{79}N$ [120] (Fig. 5).

For mono-EMFs, Bickelhaupt and Solà et al. carried out an exhaustive DFT investigation involving all 65 possible pathways of the BH reaction between dimethyl bromomalonate and $La@C_{2v}(9)$-C_{82} through all 24 nonequivalent reaction sites [214]. They found that the BH reaction is not as regioselective as the DA reaction, and proposed that the attack at bond **C2-C3** leads to the fulleroid product, whereas the initial attacks at **C2**, **C19**, **C21**, and **C23** result in the four singly bonded ones.

Similar to the mono-EMFs, the reported BH reaction of di-EMFs is also limited to a recent theoretical study on $Sc_2@C_{2v}(4059)$-C_{66} [188]. The reaction would occur at a [6,6] junction close to the unsaturated linear triquinanes under kinetic control and lead to a closed methanofullerene product.

Recently, an azidomalonate monoadduct of $Sc_3N@C_{80}$ was synthesized via BH reaction and covalently connected with a [5:1] hexakisadduct of C_{60} (with a terminal alkyne group) using a copper–catalyzed "click" reaction to generate the first EMF-based dumbbell [204].

Yang et al. have found that, although $TiSc_2N@I_h$-C_{80} is different from unreactive $Sc_3N@I_h$-C_{80} by replacing one Sc with a Ti atom, it reacts with diethyl bromomalonate at room temperature in the presence of DBU to afford two isolable monoadducts [209]. Zhao et al.'s recent DFT calculations further suggest that they are kinetically favored [6,6,6] and thermodynamically favored [5,6,6] regioisomers, respectively [215]. Similarly, $TiY_2N@I_h$-C_{80} was found to be more reactive than $Y_3N@I_h$-C_{80}, and its BH derivative is a singly

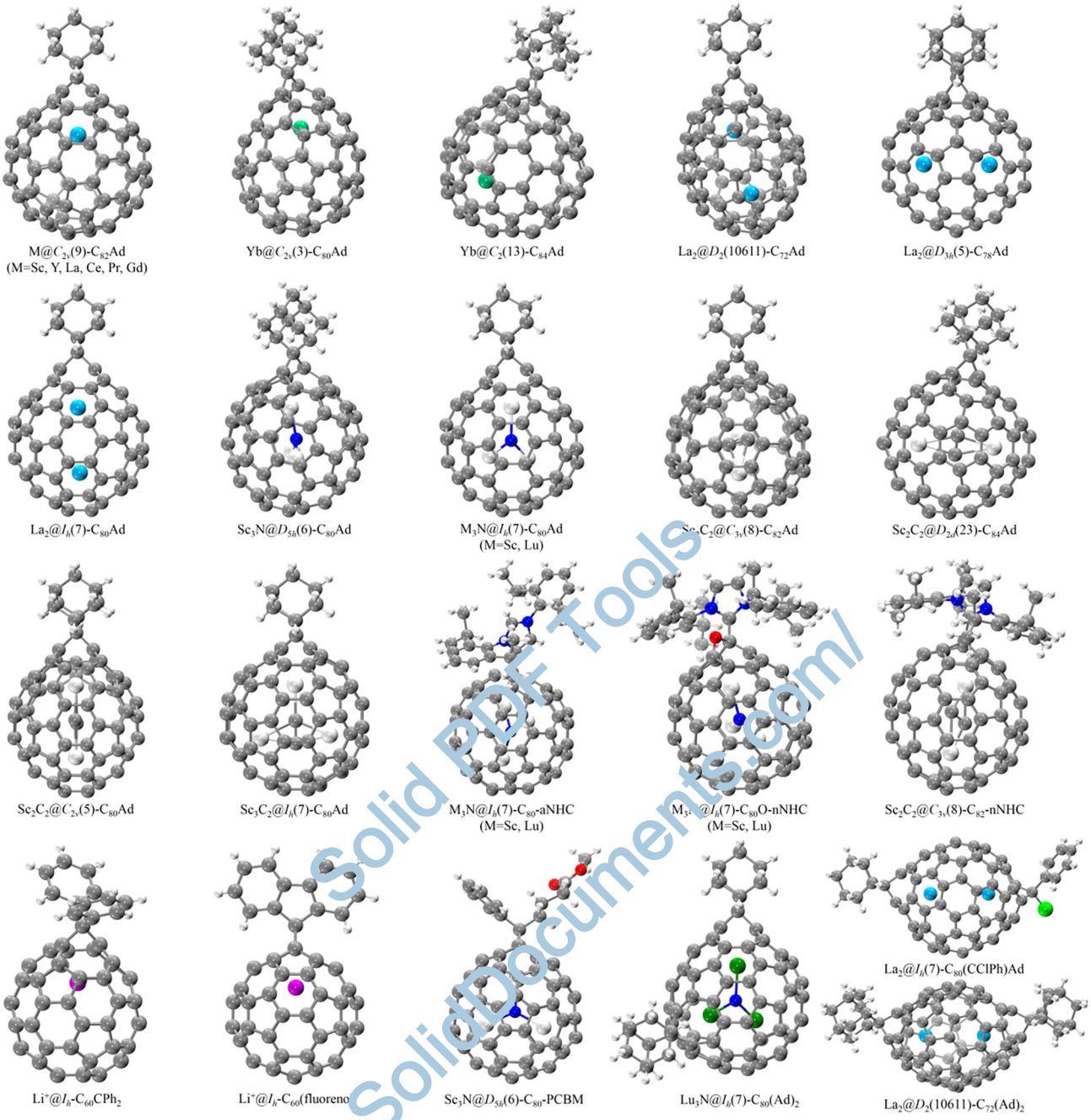

Fig. 6. Product structures for carbene addition reactions of EMFs from Refs. [52,53,55,69,73,224,225,227,235,236,239,240,243–247,249].

bonded product similar to that of $La@C_{82}$ [195] rather than the common cyclopropane adducts of $Sc_3N@I_h$-C_{80} [210]. The addition site is a [5,6,6] junction, which has the lowest electron density and large local strain. The comparable adducts for $TiY_2N@C_{80}$ and $La@C_{82}$ imply a common addition mechanism due to their similar radical nature, which can greatly stabilize the singly bonded intermediate anion first generated in the reaction by oxidization and thus impede the formation of cyclopropane.

The BH reaction of the nonconventional $LaSc_2N@C_s$(hept)-C_{80} to afford CH_2 adduct was theoretically suggested [191] to have a similar addition preference to the [6,6] bond adjacent to pentalene units as that of $Sc_3N@C_{68}$ [203] and $Gd_3N@C_{82,84}$ [208]. The regioselectivity can be rationalized by the largest LUMO coefficients of the related carbon atoms in pristine $LaSc_2N@C_s$(hept)-C_{80}, whose sites are favorable for the formation of $[LaSc_2N@C_{80}CH_2Br]^-$ intermediates.

In summary, the BH reactivity depends on the metal type [156]. In addition to the complete change of the metal species, partial substitution may also considerably affect the reactivity and even addition pattern [209,210]. The reactivity may substantially decrease with increasing cage size [206,207]. The local cage aromaticity may determine the chemical reactivity and regioselectivity of EMFs [205,216–218]. Significantly, insoluble EMFs can be utilized through preparing the corresponding Bingel adducts, and could be employed as a magnetic resonance imaging (MRI) contrast agent [219,220].

3.5. Carbene addition

Carbenes are the reactive intermediates featuring a neutral divalent carbon atom with two unshared valence electrons. The

carbene additions are important for both synthesizing new derivatives and clarifying the chemical reactivity of fullerenes/EMFs [221].

In 1995, Suzuki et al. first conducted the reaction between La@C_{82} with excess diphenyldiazomethane (Ph_2CN_2) in a toluene solution at 60 °C [222]. They observed several peaks in the FAB mass spectrum corresponding to the La@$C_{82}(CPh_2)_n$ (n = 1–3) adducts. To date, carbene addition has been applied to Li^+@C_{60} [223–225], M@C_{2v}(9)-C_{82} (M = Sc, Y, La, Ce, Pr, Gd, Tb) [80,222,226–234], La@C_s(6)-C_{82} [184], Yb@C_{2v}(3)-C_{80} [235], Yb@C_2(13)-C_{84} [236], M_2@D_2(10611)-C_{72} (M = La, Pr) [52,53,237], La_2@D_{3h}(5)-C_{78} [55], M_2@I_h(7)-C_{80} (M = La, Ce) [238–240], Lu_2@C_{3v}(8)-C_{82}, Lu_2@C_{2v}(9)-C_{82} [241], M_3N@C_{80} (M = Sc, Y, Lu) [241–246], Sc_3N@D_3-C_{68} [246], Sc_2C_2@C_{2v}(5)-C_{80} [247,248], Sc_2C_2@C_{3v}(8)-C_{82} [73,249], Sc_3C_2@I_h(7)-C_{80}[69,250], Sc_2C_2@D_{2d}(23)-C_{84} [251] and Tb_2C_2@D_2(35)-C_{88} [252].

Since 2004, Akasaka and co-workers have carried out a series of room-temperature photochemical reactions between M@C_{82} (M = Sc, Y, La, Ce, Gd) and 2-adamantane-2,3-[3H]-diazirine (AdN_2) [184,227–231]. All the metal ions are positioned inside the cavity provided by the bond cleavage upon Ad addition. Recently, Lian et al.'s X-ray crystallography (for the major one of two isolated isomers) revealed that, although the internal Pr atom in the photochemically-yielded Pr@C_{2v}(9)-C_{82}Ad adduct is disordered, it mainly resides in the same cavity as well (Fig. 6) [232,233].

The first spiroannelated Li^+@C_{60} derivative, [6,6]-[Li^+@C_{60}(fluoreno)]$TFSI^-$ (TFSI = bis(trifluoromethanesulfonyl)imide), was recently synthesized by the reaction of 9-diazofluorene and [Li^+@C_{60}]$TFSI^-$ [224]. The crystal structure shows that Li^+ dispersedly occupies three different positions, implying weak metal-cage coordination interactions at the addition sites due to the through-space periconjugation in the derivative (Fig. 6). The room-temperature reaction of [Li^+@C_{60}]($TFSI^-$) with 1 equiv of Ph_2CN_2 in dichloromethane afforded the mono-diphenylmethano compounds [5,6]- and [6,6]-[Li^+@$C_{61}Ph_2$]$TFSI^-$ and bisadducts [225]. Single crystals confirm that the two monoadducts are [5,6]-open and [6,6]-closed structures. The former kinetic product can be converted to the latter thermal product via thermal treatment ([5,6] one shown in Fig. 6). It is the first successful crystal structure characterization of the [5,6]-open methano[60]fullerene (fulleroid) structure.

Pristine Pr_2@D_2(10611)-C_{72} was synthesized and isolated recently [237]. Its photochemical reaction with excess AdN_2 yields a major mono-adduct and minor bis-adduct. DFT calculations suggested that the mono-addition most likely takes place at a [5,6] bond in the pentagon adjacencies.

The Ad additions to Sc_3N@D_{5h}(6)-C_{80} and M_3N@I_h(7)-C_{80} (M = Sc, Lu) were achieved recently via the photochemical reactions with 2-adamantyl-2,3′-[3H]-diazirine [243]. For M_3N@I_h-C_{80}, the major and minor isomers are [6,6]-open fulleroid and [5,6]-open fulleroid, respectively. The reaction led to three major monoadducts (all are [6,6]-open) for Sc_3N@D_{5h}-C_{80}, showing high regioselectivity. Single-crystal XRD analyses unambiguously determined the exact structures of all the seven Ad monoadducts (one [6,6] isomer for M_3N@I_h-C_{80} and Sc_3N@D_{5h}-C_{80} shown in Fig. 6). The stepwise Ad addition to the more reactive Lu_3N@I_h-C_{80} affords several bisadducts, one of which was successfully characterized by XRD to feature the second Ad group close to one Lu atom (Fig. 6). The addition pattern was rationalized by calculating the relative energies of isomers, charge density and local strain of the cage carbons.

In contrast to the various carbon-based Lewis bases such as N-heterocyclic carbene (NHC), carbon-based Lewis acids are scarce and have been recently extended to hollow fullerenes such as C_{60} and C_{70} [253–255]. Interestingly, despite bearing a negatively charged outer cage, Lu et al. found that Sc_3N@I_h-C_{80} exhibits excellent Lewis acidity and it can react with 1,3-bis(diisopropylphenyl)-imidazol-2-ylene at 90 °C to afford a Lewis acid-base pair [244]. Differing from the common [1+2] cycloaddition of carbene, single crystal X-ray data show that the abnormal carbene (with C5 as its active center) is singly connected (C–C bond length: 1.515 Å) to an otherwise inert [6,6,6] junction with the Sc_3N plane perpendicular to the N-heterocyclic ring (Fig. 6). Theoretical calculations reveal that the unprecedented addition pattern is kinetically controlled as a result of the steric hindrance between the congested diisopropylphenyl groups of the normal NHC and large C_{80} cage. The high regioselectivity is due to the low electron density and relatively large LUMO distribution at the [6,6,6] site [256]. This is the first example of carbon-based Lewis acid-base pair formed by EMFs.

Normal NHC adducts of M_3N@I_h-C_{80} (M = Sc, Lu) were recently achieved by introducing a tiny amount of oxygen in the same reaction (Fig. 6) [245]. Joint experimental and computational studies reveal that the oxygen may first be activated by the carbene to generate a dioxirane product, which then reacts with Sc_3N@I_h-C_{80} to form a Sc_3N@$C_{80}O$ intermediate. The intermediate reacts with NHC to yield the final normal NHC-Sc_3N@I_h-$C_{80}O$ product. It is very interesting that the attachment of an oxygen atom to the cage framework leads to a totally different NHC adduct. It is noteworthy that the NHC addition was further extended to MCCFs such as Sc_2C_2@C_{3v}(8)-C_{82} by Lu et al., and a normal C2-binding [6,6,6] monoadduct was obtained despite it bearing a larger carbon cage than Sc_3N@I_h(7)-C_{80} with stronger steric clash (Fig. 6) [249]. Quite recently, they further conducted the reactions between the less strained 3-diisopropylphenyl-1H-imidazol-3-ium-2-ide and Lu_3N@I_h(7)-C_{80}, Lu_2@C_{3v}(8)-C_{82}, or Lu_2@C_{2v}(9)-C_{82} [241]. X-ray

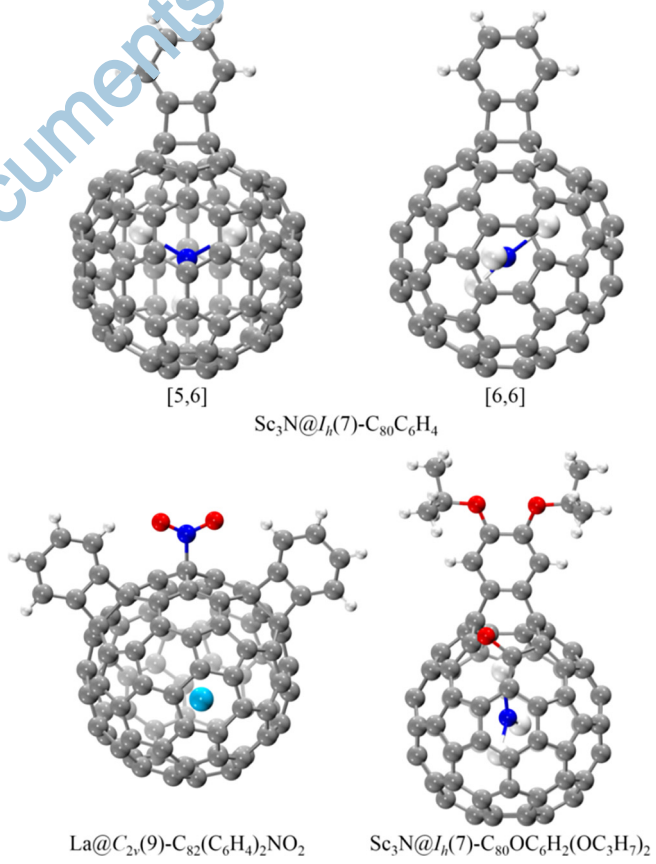

Fig. 7. Product structures for [2+2] cycloaddition of benzyne to EMFs from Refs. [258–260].

data revealed that $Lu_3N@C_{80}$ also gives rise to a normal-bonding epoxide adduct under ambient conditions, whereas an abnormal-bonding adduct is obtained in a pure argon atmosphere. In contrast, each $Lu_2@C_{82}$ yields one normal adduct regardless of the reaction conditions. DFT calculations thus clarify that the high regioselectivity and addition types are mainly determined by the molecular orbitals and electrostatic interactions of the carbon cages rather than the previously assumed steric clash.

Recently, the first derivatives of diterbium fullerenes were achieved *via* the photochemical reaction of Tb_2C_{90} (the structure was tentatively assigned to $Tb_2C_2@D_2(35)$-C_{88}) with 2-admantane-2,3-[3H]-diazirine, and an Ad monoadduct was successfully isolated [252]. Its similar optical absorption spectrum as that of pristine one suggests that the Ad addition takes place at the [6,6] ring junctions with local open-cage structure.

For the reported reactions, high regioselectivity is frequently found due to strong metal-cage interactions [184,227–231]. Charge density distribution, local cage stain and relative energies are often analyzed to explain the observed high regioselectivity, and the carbon atoms close to the metal are possible reaction sites. The different amounts of metal-to-cage charge transfer could lead to diverse reactivity and regioselectivity [235,236]. Since direct XRD structural characterization is difficult due to the rapid rotation of spherical EMFs in the crystal lattice, one may employ their corresponding carbene derivatives, whose crystallizations are more feasible [69,73,247,248].

3.6. Benzyne cycloaddition

The [2+2] cycloaddition of benzyne is well known for empty fullerenes. The first application to EMFs is reported by Lu et al. in 2004 for $Gd@C_{2v}$-C_{82}, and two $Gd@C_{82}(C_6H_4)$ monoadducts dominate the reaction products [257]. The reported cases are limited to $M@C_{2v}(9)$-C_{82} (M = La, Gd) [257,258] and $Sc_3N@I_h$-C_{80} [259,260] thus far.

The cycloaddition of benzyne to $Sc_3N@I_h$-C_{80} afforded two stable monoadducts and multiple adducts with up to 10 benzene addends [259]. One monoadduct is a symmetric [5,6] isomer, whereas the other is an unsymmetrical [6,6] one (Fig. 7). Recent DFT calculations reveal that the [5,6] isomer is thermodynamically more favorable that the [6,6] one [261]. The two cycloaddition patterns lead to diverse metal cluster dynamics, with a more flexible mode in the [6,6] isomer [262]. Their monoanion radicals were generated by the reaction between the two cycloadducts and cobaltocene $Co(Cp)_2$, and show very different hyperfine patterns in ESR spectra and spin density distribution for the metal cluster. The benzyne adduct may be further functionalized by porphyrin and tetrathiafulvalene to achieve variable electronic properties [261].

A deep understanding of complicated reactions surely needs theoretical insights. Very recently, systematic DFT calculations were performed by Yang et al. to disclose the reaction mechanism of [2+2] cycloaddition of benzyne with $M_3N@C_{80}$ (M = Sc, Y) [263]. The benzyne ring is first singly linked to the [5,6,6] or [6,6,6] site to form a singlet diradical intermediate, which is rather flexible and readily rotates on the cage surface to reside over the [5,6] or [6,6] bond. It then undergoes a ring-closing step to form the major [5,6] or minor [6,6] adducts. $Y_3N@C_{80}$ may exhibit higher reactivity due to a lower reaction barrier and larger reaction energy than $Sc_3N@C_{80}$. The yields of the two adducts become competitive and both of them may exhibit a two-atom-bridging open-cage structure. Therefore, the open or close of the cage can be controlled by only altering the internal metal species. The regioselectivity is explained in terms of the local strain of EMFs. Li et al. found that the structure, electronic and optical properties of $M_3N@C_{80}$(M = Sc, Y) may be affected by the addition of a benzyne group [264].

3.7. Radical reaction

Generally, in the radical reactions, an even and odd number of addends are singly bonded to the diamagnetic and paramagnetic EMFs, respectively, to achieve a closed-shell electronic configuration. The high reactivity of reactions leads to a low selectivity. The involved EMFs are $Sr@C_{50,60}$ [265], $M@C_{60}$ (M = La, Gd) [266], $M@C_{2n}$ (M = Y, Gd or Dy; $2n$ = 60, 70, 72, or 74) [267], $La@D_{5h}$-C_{70} [268], $M@C_2(10612)$-C_{72} (M = La, Pr) [269–273], $M@D_{3h}$-C_{74}(M = La, Pr) [273–277], $La@C_{76}$ [273], $La@C_{2v}(3)$-C_{80} [278], $Ce@C_{80}$ [279], $M@C_{82}$ (M = Y, La, Ce, Gd) [185,279–288], $M_2@C_{80}$ (M_2 = Y_2, La_2, Gd_2, Dy_2, Tb_2, Ho_2, Er_2, TbY, TbGd) [283,288–292], $M_2@C_{82}$ (M = Y, Er) [288,293], $M_3N@C_{80}$ (M = Sc, Er, Lu) [265,294–304], $Y_2C_2@C_s(6)$-C_{82} [305], $Sc_3C_2@I_h(7)$-C_{80} [70], $YCN@C_s(6)$-C_{82} [306], $YCN@D_{2d}(23)$-C_{84} and $YCN@C_2(13)$-C_{84} [307].

Recently, five isomers of $M@C_{82}CH_2$-3,5-$C_6H_3Me_2$ (M = La or Ce) were synthesized *via* photoirradiation of $M@C_{82}$ in the presence of mesitylene [287]. XRD analysis reveals that the 3,5-dimethylbenzyl group in one $Ce@C_{82}CH_2$-3,5-$C_6H_3Me_2$ isomer (Fig. 8) is added to the same **C10** site as that of the benzyl adduct of $La@C_{82}$ [280]. One isomer for each metal is suggested to have addition at the **C23** site due to their similarity in absorption spectra with $La@C_{82}CBr(COOEt)_2$ [195]. DFT calculations suggest the addition sites based on large spin density and positive charge. Significantly, the paramagnetic shifts of the ^{1}H NMR peaks (due to the anisotropic magnetism of the Ce-f electron) can be employed to probe the location of other adduct isomers to be **C9**, **C14** and **C18**.

Exohedral modification may greatly alter the bonding state of the trapped species to achieve covalent metal–metal bonds [308,309]. Generally, to obtain a closed-shell adduct, an odd and even number of benzyl radicals are needed to attach open-shell and closed-shell EMFs respectively. However, in a recent report on the photo-irradiation reaction of benzyl bromide with $La_2@I_h$-C_{80}, an open-shell $La_2@I_h$-$C_{80}CH_2C_6H_5$ monoadduct was unexpectedly achieved [289]. XRD revealed that the benzyl mono-addition takes place at a [5,6,6] cage carbon (Fig. 8). The average internal La-La separation is comparable to that of the metal–metal covalent bond in the $La_2@C_{80}^-$ anion (3.71 Å vs. 3.723 Å), confirming the formation of a direct La-La bond. EPR measurements and DFT calculations revealed that the σ-bonding orbital of the La_2 pair accepts an unpaired electron. The localized spin density on the metals thus causes the extreme stability of this fullerene radical. The formation of the fullerene radical dramatically modified the vis/NIR absorption spectrum owing to the introduction of an unpaired electron. The first reduction and oxidation potentials are negatively shifted by 510 and 410 mV, respectively. Stable benzyl monoadducts $M_2@I_h(7)$-$C_{80}(CH_2Ph)$ (M_2 = Y_2, Gd_2, Tb_2, Dy_2, Ho_2, Er_2, TbY, TbGd) were soon synthesized [290,291]. As the $La_2@I_h$-C_{80} adduct, EPR and DFT calculations indicate that they all bear an unpaired electron located between the two metal atoms, resulting in the formation of a single-electron metal–metal bond. Significantly, the strong interactions between the unpaired electron and metal ions in $Dy_2@C_{80}(CH_2Ph)$ and $Tb_2@C_{80}(CH_2Ph)$ give rise to single-molecule magnetism with a rather high blocking temperature of magnetization.

Very recently, Hada et al. theoretically proposed the stable structures of $Gd_2@I_h$-C_{80}-CF_3 and $Gd_2@I_h$-C_{80}-$C_3N_3Ph_2$ adducts, and predicted the magnetic properties of their corresponding $Dy_2@I_h$-C_{80} derivatives [310].

Missing small-gap metallofullerenes can be stabilized and obtained with CF_3 modification. Recently, Shinohara et al. used a modified arc-discharge method to effectively produce a series of trifluoromethyl derivatives of insoluble EMFs with the aid of polytetrafluoroethene [267]. The $M@C_{2n}(CF_3)_{1,3}$ (M = Y, Gd or Dy; $2n$ = 60, 70, 72, or 74) derivatives can be dissolved in common organic solvents and subjected to further separation/purification.

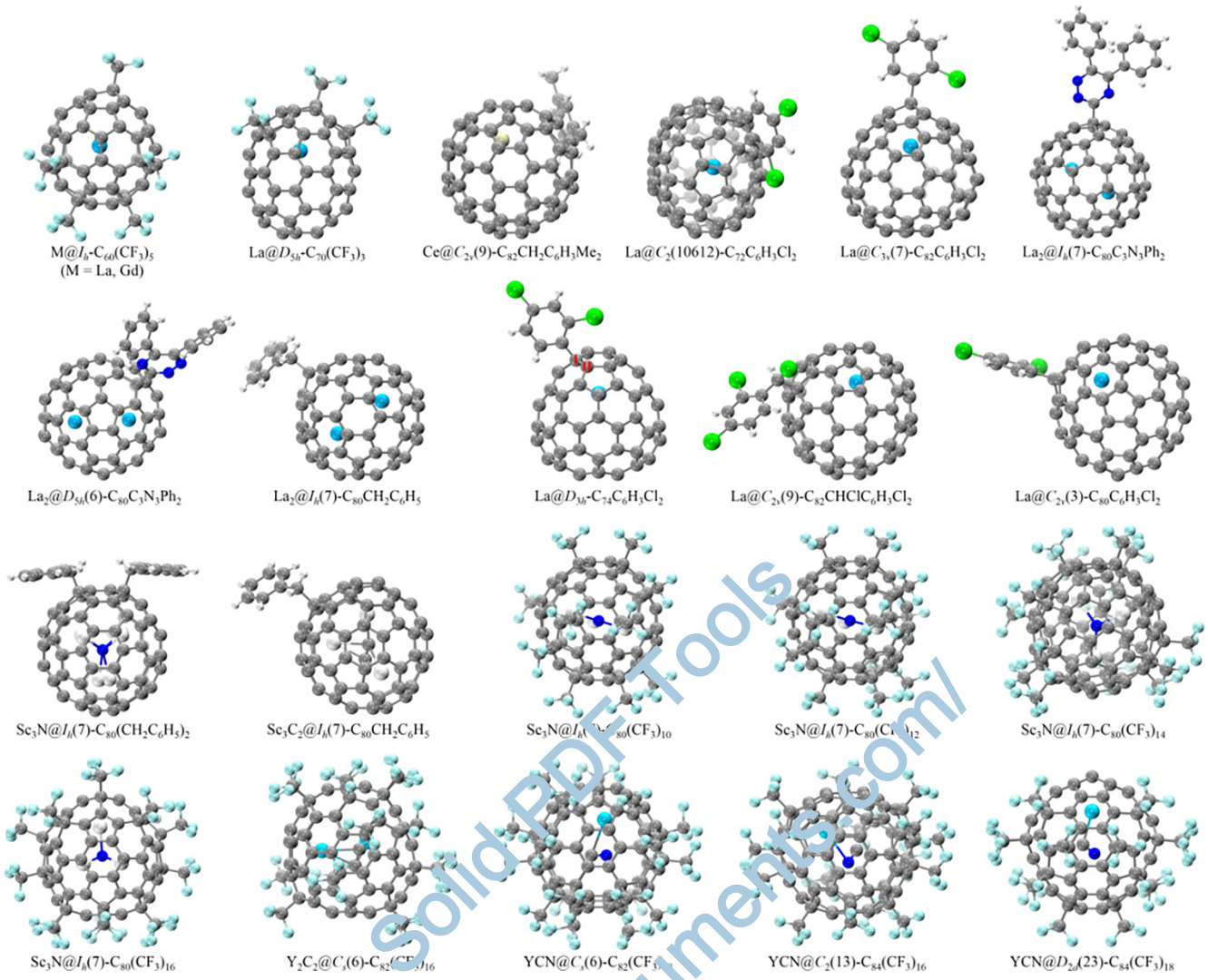

Fig. 8. Radical reactions of EMFs. Product structures from Refs. [70,263,280,286,269,275,278,286,287,289,292,294,297,303,305,306,307].

They also observed the existence of $Y_2@C_{80}CF_3$. DFT calculations show that $Y_2@I_h$-C_{80} has a triplet ground state and exhibits high chemical reactivity towards CF_3 addition due to its unpaired electron on the cage. Similar chemical properties were also suggested for $M_2@I_h$-C_{80} (M = Gd, Lu) by theoretical calculations [311]. The same *in situ* trifluoromethylation method was recently used to isolate the long-sought small-bandgap La@C_{70} [268]. Single-crystal XRD for one of the two obtained isomers revealed that La@$C_{70}(CF_3)_3$ is the first D_{5h}-C_{70}-based rare-earth EMF with the La atom and three CF_3 substituents residing on the same side of the C_{70} long axis (Fig. 8). DFT calculations found that it is greatly stabilized owing to the enlarged HOMO-LUMO gap upon trifluoromethylation. DFT calculations predicted that Y@C_{2v}(4348)-C_{66} could be greatly stabilized by trifluoromethylation [312]. Recent calculations for La@$C_{80}(CF_3)_m$ ($m \leq 5$) also found that the attachment of an odd number (m = 1, 3 or 5) of CF_3 radicals is energetically favored due to the stabilization of extra electrons (3e donated by La) on the cage and achievement of closed-shell configurations [313]. Indeed, small-gap M@C_{60} endohedrals can be macroscopically obtained in their trifluoromethylated forms Gd@$C_{60}(CF_3)_{3,5}$ and La@$C_{60}(CF_3)_{3,5}$ due to the widened energy gap (one M@$C_{60}(CF_3)_5$ isomer shown in Fig. 8) [266].

Recently, the addition reactions of 1,2,4-trichlorobenzene (TCB) to Pr@C_{72} and Pr@C_{74} were continually reported by Zhao et al. and one isomer for each was successfully prepared and isolated [272,277]. Their structures should be Pr@$C_2(10612)$-$C_{72}(C_6H_3Cl_2)$ and Pr@D_{3h}-$C_{74}(C_6H_3Cl_2)$ respectively based on the similar UV–vis-NIR spectra as that of La@$C_{72}(C_6H_3Cl_2)$ and La@$C_{74}(C_6H_3Cl_2)$ as well as theoretical calculations.

However, it was argued that TCB is not an ideal radical precursor due to the simultaneous yield of three regioisomers, namely 2,4-, 2,5-, and 3,4-dichlorophenyl radicals. When iodobenzene was used, the insoluble missing La@C_{2n} ($2n$ = 72–76) was successfully extracted as corresponding phenyl adducts La@$C_2(10612)$-$C_{72}(C_6H_5)$, La@D_{3h}-$C_{74}(C_6H_5)$ (I, II) and La@$C_{76}(C_6H_5)$ (I, II) with remarkably reduced isomer number [273].

In general, fullerenyl radicals are rather reactive and hard to be isolated. Recently, Akasaka and co-workers reported the synthesis of isolable stable fullerenyl radicals by the thermal reaction of $La_2@I_h$-C_{80} or $La_2@D_{5h}$-C_{80} with excess 3-chloro-5,6-diphenyltriazine in 1,2-dichlorobenzene (1,2-DCB) solution [292]. The mass spectra indicate the formation of radical coupled products $La_2@C_{80}$-$C_3N_3Ph_2$, which are air-stable. EPR spectra similar to that of the $La_2@C_{80}$ anion radical as well as calculated SOMO distribution suggest that the unpaired electron is confined in the La-La σ-bonding orbital within the protective cage, accounting for the remarkable stability of the radical products. The electronic configuration is thus $(La_2)^{5+}@(C_{80}\text{-}C_3N_3Ph_2)^{6-}$. X-ray analysis of the

two $La_2@C_{80}$-$C_3N_3Ph_2$ products shows that both additions took place at the [5,6,6] carbon site (Fig. 8). In addition, $La_2@I_h$-C_{80}-$C_3N_3Ph_2$ can further react with toluene under thermal conditions to afford a diamagnetic benzylated derivative $La_2@I_h$-C_{80}–$(C_3N_3Ph_2)(CH_2Ph)$ in solution, which will dimerize to form a diradical in the crystal structure with the unpaired electrons again localized in the metal moieties (Fig. 10).

Addition pattern may also affect cluster conformation. Yang et al. obtained four isomeric trifluoromethyl derivatives $Y_2C_2@C_s(6)$-$C_{82}(CF_3)_{16}$ very recently [305]. Interestingly, despite being trapped in the same C_{82} cage, the Y_2C_2 cluster exhibits varied butterfly-shaped geometry dependent on the addition pattern of the exohedral CF_3 groups (one shown in Fig. 8). This phenomenon is well understood: different trifluoromethylation patterns determine various relative positions of two cage pentagons coordinating with the two Y atoms, thus resulting in different internal cluster structures. They also reported that the trifluoromethylation of the monometallic cyanide cluster fullerene $YCN@C_s(6)$-C_{82} with gaseous CF_3I at 430 °C afforded a mixture of $YCN@C_s(6)$-$C_{82}(CF_3)_{14\text{-}20}$ [306]. X-ray diffraction reveals two isolated products: $YCN@C_s(6)$-$C_{82}(CF_3)_{16}$ and $YCN@C_s(6)$-$C_{82}(CF_3)_{18}$, whose additions both occur at 11 pentagons with the Y-coordinated pentagon remaining intact (Fig. 8). DFT calculations suggest that the CF_3 groups enhance the localized electron density within the conjugated patch coordinating with the metal atom. They further obtained $YCN@D_{2d}(23)$-$C_{84}(CF_3)_{18}$ and three isomers of $YCN@C_2(13)$-$C_{84}(CF_3)_{16}$ using a similar procedure [307]. An XRD study revealed that the Y atom is coordinated by one and two neighboring pentagons in $YCN@C_2(13)$-$C_{84}(CF_3)_{16}$ and $YCN@D_{2d}(23)$-$C_{84}(CF_3)_{18}$ (one isomer shown in Fig. 8), respectively, suggesting that only these pentagons should escape from CF_3 addition. However, the isomer III of $YCN@C_2(13)$-$C_{84}(CF_3)_{16}$ (Fig. 8) is special and features a second pentagon free from the CF_3 attachment. Note that the resultant different CF_3 distribution led to a much smaller endohedral Y-C-N angle (90° vs. 160° in others) in this isomer, indicating a pronounced communication between the inner and outer moieties.

Significantly, directly fluorinated EMFs such as $Sc_3N@C_{80}F_n$ (n = 1, 2) and even small Sr@C_{50}F and Sr@C_{60}F can be obtained under gas-phase conditions of metallofullerene plasma synthesis [265].

Experimental studies for the radical reaction of mixed-metal and metal oxide clusterfullerenes have not been reported. However, calculations reveal that the addition of multiple trifluoromethyl groups to $Sc_xY_{3-x}N@I_h$-C_{80} (x = 1–3) and $Sc_4O_2@C_{80}$ could decrease their HOMO-LUMO gap energies [314–317].

The radical addition can change the electronic structure of the internal cluster and subsequently affect its configuration [70]. The additions could influence the cluster conformation [305–307] and motion [297–300]. The addition sites could have large local cage stain and high spin density because of the neighboring metal atom, thus confirming the critical role of metals in regioselective derivatization.

3.8. Polyhydroxylation

Hydrophilic groups are used to solubilize the EMFs and improve their biocompatibility for application in medical science. The simplest and most efficient modification method is polyhydroxylation to yield various metallofullerenols. Among them, extensive studies are focused on Gd-metallofullerenols (Fig. 9). Gadolinium holds a half-filled 4f subshell ($4f^7$) with strong paramagnetic properties. The extremely stable carbon cage can prevent metallic species leakage under physiological conditions and enlarge the surface of the Gd ion. The polyhydroxyls transmit the paramagnetic effect of the Gd ion to the bulk water by fast proton exchange. Therefore, the conflict between toxicity and relaxation efficiency is perfectly solved in Gd-metallofullerenols, which are thus very attractive MRI contrast agents. Compared with various commercial Gd^{3+} ion-chelated compounds, exohedrally modified gadofullerenes feature much higher spin coupling between inner Gd and outer water protons. They not only exhibit 10–40 times improvement as MRI contrast agents, but also have excellent biosafety [318]. The efficiency of an MRI contrast agent is gauged by its proton relaxivity, r_1. The relaxivities are highly dependent on the functional group type and aggregate size.

In 1997, Chang et al. prepared the first water-soluble EMF derivatives, gadolinium fullerenols $Gd@C_{82}(OH)_{\sim 20}$, *via* the reaction of gadolinium fullerenes with potassium [319]. $Gd@C_{82}(OH)_{20}$ exhibits an excellent r_1 relaxivity of 47.0 ± 1.0 mM^{-1} s^{-1} at room temperature, much higher than the common contrast agents such as Gd(DOTA), Gd(DTPA), Gd(HP-DO3A) and Gd(DTPA-BMA). Thereafter, various types of Gd-metallofullerenols were reported, most of which were based on $Gd@C_{82}$. Herein, for the sake of clarity, we ignore the tedious description of the synthesis procedure, and only summarize all types of reported polyhydroxylated EMFs species in Table 1.

With the increasing number of OH groups, the isomer number of adducts grows dramatically, which severely impedes the experimental purification and characterization. Thus, systematic theoretical calculations play a critical role in disclosing the formation mechanism and exact addition pattern of OH groups on the EMF cage surfaces. Owing to high symmetry, $Gd@C_{2v}$-C_{82} and its hydroxylated derivative are theoretically predicted to favor simultaneous attack by four hydroxyls [320]. For the lowest-energy $Gd@C_{82}(OH)_x$ (x = 4–24), the OH groups are homogeneously distributed and they reside at either *para*-position of the hexagon rings or the *meta*-position of the pentagon rings and tend to enclose more uncovered hexagons. The binding energy of each OH unit essentially increases with the increasing number of hydroxyls.

The formation of $Gd@C_{60/82}$ metallofullerenols using O_2 or H_2O_2 as oxidizing agents under alkaline aqueous conditions was investigated by means of DFT calculations [321]. The O_2 oxidation energetically favors generating hydroxyls and carbonyls on the cage surface, whereas the H_2O_2 one most likely forms hydroxyl, carbonyl, hemiacetal and deprotonated *vic*-diol groups.

DFT calculations suggest that $La@C_{60}(OH)_{32}$ and $La@C_{82}(OH)_{20}$ favor the formation of small isolated OH domains and a segregated

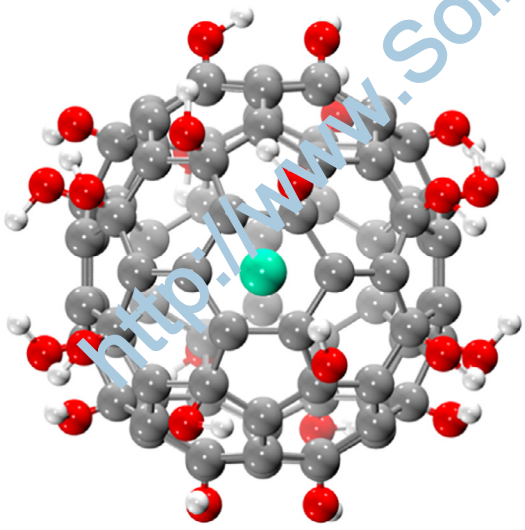

Fig. 9. Schematic representation of a Gd-metallofullerenol.

Table 1
Summary of reported metallofullerenols.

Classical EMFs	Ref.	Classical EMFs	Ref.	Clusterfullerenes	Ref.
$Li@C_{60}(OH)_{18}$	[327]	$Gd@C_{82}(OH)_{16}O_6(NHCH_2CH_2COOH)_8$	[328]	$Sc_3N@C_{80}OH$	[329]
$Gd@C_{60}(OH)_x$	[330]	$Gd@C_{82}(OH)_{18}$	[331]	$Sc_3N@C_{80}(OH)_{10}O_{10}$	[332]
$Gd@C_{80}(OH)_{22}$	[333]	$Gd@C_{82}(OH)_{18}O_8$	[334]	$Sc_3N@C_{80}(OH)_{33}(CH_2CH_2COOH)_{19}$	[335]
$La@C_{82}(OH)_x$	[336,337]	$Gd@C_{82}(OH)_{20}$	[319]	$Gd_3N@C_{80}OH$	[329]
$Ce@C_{82}(OH)_x$	[336]	$Gd@C_{82}(OH)_{20}O_2$	[338]	$Gd_3N@C_{80}(OH)_{10}O_{12}(NH_2)_7(NO_2)_2$	[339]
$Pr@C_{82}(OH)_{10}O_{10}$	[340]	$Gd@C_{82}(OH)_{21}O_7$	[338]	$Gd_3N@C_{80}(OH)_{21}O_{11}$	[341]
$Gd@C_{82}(OH)_2$	[342]	$Gd@C_{82}(OH)_{22}$	[343–345]	$Gd_3N@C_{80}(OH)_{26}(CH_2CH_2COOM)_{16}$(M = Na, H)	[335,346]
$Gd@C_{82}(OH)_5(NHCH_2COOH)_9$	[343]	$Gd@C_{82}(OH)_{24}(CH_2CH_2COOH)_{22}$	[347]	$Gd_3N@C_{80}(OH)_{30}$	[348]
$Gd@C_{82}(OH)_6(NHCH_2CH_2SO_3H)_8$	[343]	$Gd@C_{82}(OH)_{26}$	[349]	$Gd_3N@C_{80}(OH)_{30}(CH_2CH_2COOH)_{20}$	[350]
$Gd@C_{82}(OH)_{12}$	[351]	$Gd@C_{82}(OH)_{30}$	[352]	$Gd_3N@C_{80}$-R_x, R = $[N(OH)(CH_2CH_2O)_nCH_3]_x$, n = 1, 3, 6 and X = 10–22)	[353]
$Gd@C_{82}(OH)_{12}(C(COOH)_2)_3(DOTA)_1$	[354]	$Gd@C_{82}(OH)_{30}O_8$	[355]	$Gd_3N@C_{80}$[DiPEG$(OH)_x$]	[356,357]
$Gd@C_{82}(OH)_{12}(C(COOH)_2)_8(DOTAM)_1$	[354]	$M@C_{82}(OH)_{40}$(M = Eu, Gd, Dy, Er, Lu_2)	[358–361]	$ScGd_2N@C_{80}(OH)_{26}O_{12}$	[355]
$Gd@C_{82}(OH)_{13}(NHCH_2CH_2COOH)_6$	[349]	$Dy@C_{82}(OH)_x$	[336]	$Sc_2GdN@C_{80}(OH)_{26}O_{12}$	[355]
$Gd@C_{82}O_{14}(OH)_{14}(NH_2)_6$	[362]	$^{166}Ho_{1,2}@C_{82}(OH)_x$	[363]	$Gd_3N@C_{84}(OH)_{28}O_6$	[341]
$Gd@C_{82}(OH)_{15}O_{14}(C_6H_5C(CH_2)_3COOH$	[364]	$Er@C_{82}(OH)_x$	[336]		
$Gd@C_{82}(OH)_{16}$	[365]	$Gd_2@C_{80}(OH)_{18}O_8$	[334]		
$Gd@C_{82}(OH)_{16}O_{10}$	[366]	$Gd_2@C_{80}(OH)_{22}$	[333]		
$Gd@C_{82}(OH)_{16}O_2(C(PO_3Et_2)_2)_{10}$	[200]				

OH array on one side respectively, on the cage surface with hydrogen bonds between neighboring OH groups [322]. The different addition patterns affect the metal position, and the La atom is apt to be attached to the internal cage surface and resides close to the electron-rich uncovered regions. When positively charged (+2, +4, +6, +8), some C–C bonds may be broken and lead to enable holes in the C_{60} framework, whereas no C–C bond breakage was found for the C_{82} cage. In all cases, the inner La atom is rather stable and does not escape from the polyhydroxylated cage.

It was theoretically proposed that only the EMF multi-adducts with large first excitation energy and HOMO-LUMO gap are chemically inert and can survive in experiments. They are easily identified: their sp^2 carbons should form local aromatic ionic patches isolated by sp^3 carbons [323,324]. In addition, the global molecular aromaticity may also affect the energy stability of polyhydroxylated derivatives [325].

Theoretical calculations could also give insights into potential biofunction of metallofullerenols. For instance, Gao et al.'s recent molecular dynamics simulations and DFT calculations reveal that $Gd@C_{82}(OH)_{13,21}$ can reside in the same pocket of the dimer of tumor necrosis factor-α (TNF-α) as a SPD304 inhibitor [326]. The calculated binding free energies suggest that they have larger affinities and may be employed as new inhibitors of TNF-α.

3.9. Dimerization reaction

There are only a few reports on the dimerization of EMFs and their derivatives, and the former includes $Li@C_{60}$ [367], $M@C_{82}$ (M = Y, Ce, Nd, Gd, Tb, Er) [368–378], and $M_3N@I_h$-C_{80} (M = Sc, Lu) [379–381], whereas the latter include the BH bisadduct of $La@C_{82}$ [197], $La@C_{82}$-C_5Cp^* [113] and $La_2@I_h$-C_{80}-$C_3N_3Ph_2$ [292].

Recent studies show that the metallic species determine the reactivity towards dimerization. In contrast to $M@C_{2v}(9)$-C_{82} (M = Sc, Y, La, Gd, Sm, Yb) which all retain monomer form in their co-crystals with Ni(OEP), $Ce@C_{2v}(9)$-C_{82} dimerizes via a C–C single bond in a centrosymmetric fashion (Fig. 10) [375]. The reaction site holds the highest POAV value among all the cage carbons. DFT calculations reveal that the dimer is energetically more favorable than the two monomers by 22.6 kcal mol^{-1}. With the similar geometry and metal-to-cage electronic transfer for $M@C_{82}$(M = Sc, Y, La, Ce), it is interesting to further understand the underlying reaction behind their remarkable reactivity difference.

Cage isomerization also affects the reactivity towards dimerization. For example, $Y@C_s(6)$-C_{82} forms a dimeric structure via a C–C single bond in the crystalline state, whereas $Y@C_{2v}(9)$-C_{82} does not dimerize under identical conditions [376]. In the single crystal structure (Fig. 10), the Y atom resides under a [6,6] bond and deviates slightly from the mirror plane of the cage. Dimerization takes place at a carbon site far from the metal with rather high spin density, endowing the $C_s(6)$ cage with considerable radical character to facilitate the radical coupling reaction. The situation is a sharp contrast to the even distribution of spin density on the cage carbon of $Y@C_{2v}(9)$-C_{82}. Similar phenomena were also observed for $Er@C_s(6)$-C_{82} and $Er@C_{2v}(9)$-C_{82}, and only the former dimerizes in the crystalline state due to the localized high spin density at the addition site, although identical crystallization conditions were used for both of them [377].

$Li^+@C_{60}^-$ radical anion was recently isolated by the electrochemical reduction of ionic $Li^+@C_{60}$ salt [367]. Although $Li@C_{60}$ exists mainly as a monomer in solution, it can form a stable dimer in *trans* conformation in the co-crystal with nickel octaethylporphyrin by coupling of the spin center on the cage (Fig. 10). The metal resides close to a carbon atom adjacent to the bridging site due to the electrostatic attraction.

The cage orientation may determine the dimerization reactivity. Koshino et al. reported the dimerization reaction of $Er@C_{82}$ within the narrow space of nanotubes [378]. By using HRTEM, they observed that more intermolecular bonds are formed when the EMF molecules are packed with their apse lines along the tube axis and in a head to tail contact.

The mixed triazine/benzyl derivative of EMF, namely $La_2@I_h$-C_{80}-$C_3N_3Ph_2$, can react with toluene under thermal conditions to afford a diamagnetic benzylated derivative $La_2@I_h$-C_{80}–$(C_3N_3Ph_2)(CH_2Ph)$ in solution, which dimerizes to form a diradical in the crystal with the unpaired electrons localized on the metals (Fig. 10) [292].

Heterodimers such as $Li@I_h$-C_{60}-$Y@C_{2v}(9)$-C_{82}, $Li@C_{60}$-$Y_2@I_h(7)$-C_{80} and $Y@C_{2v}(9)$-C_{82}-$Y_2@I_h(7)$-C_{80} were also theoretically designed [382]. They are linked via a weak C–C single bond, and exhibit

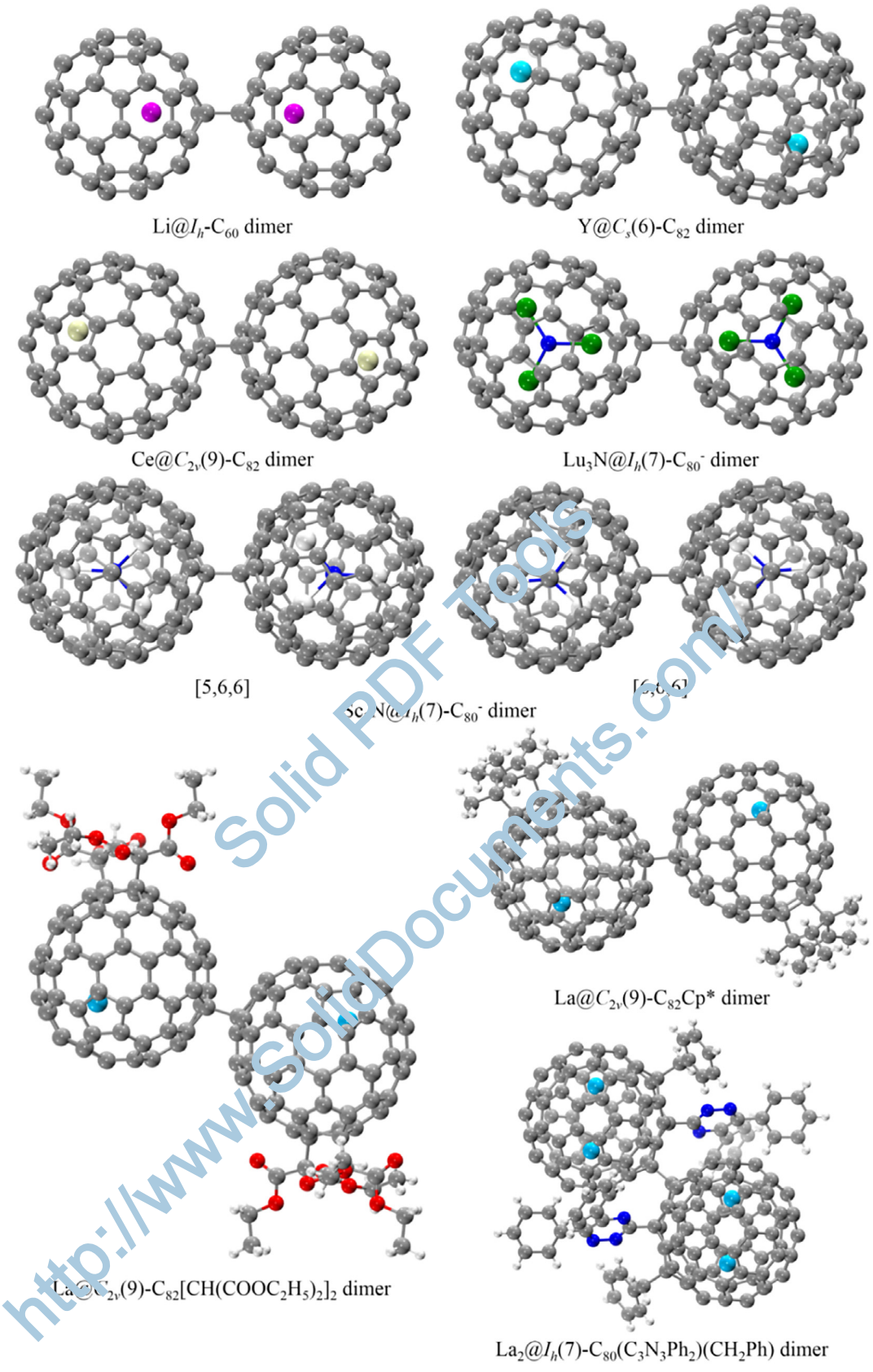

Fig. 10. Product structures for dimerization reactions of EMFs from Refs. [113,197,292,367,375,376,380,381].

enhanced first hyperpolarizability than their respective monomers. Therefore, dimerization could effectively improve the nonlinear optical properties of EMFs.

The anionic TNT EMFs may be more prone to dimerize. Recent systematic DFT calculations by Popov et al. focused on the possible dimerization reactions of several anionic TNT EMFs and their derivatives [383,384]. They found that the most stable dimers of non-IPR $Sc_3N@D_3(6140)$-C_{68}^-, $Y_3N@C_2(22010)$-C_{78}^- and $Y_3N@C_s(51365)$-C_{84}^- could all be obtained by connecting the peripheral carbon atoms of the pentalene units. In the most stable dimeric structure of $Sc_3N@C_{80}^-$, the bridge carbon atoms are at the [5,6,6] sites, which are between the coordination sites of two equivalent Sc atoms and near the Sc_3 plane. As a matter of fact, the [5,6,6] and [6,6,6] dimers can form simultaneously due to their slight energy difference, as confirmed by the single crystal $\{cryptand[2,2,2](Na^+)\}_2(Sc_3N@I_h\text{-}C_{80}^-)_2{\cdot}2.5C_6H_4Cl_2$ salt (Fig. 10) [380]. They both exhibit *trans*-orientation with intercage C–C bond lengths of 1.642 and 1.636 Å, respectively. The most stable $(Sc_3N@I_h\text{-}C_{80}(CF_3)_2)_2^{2-}$ favors the [6,6,6] carbons far from the CF_3 groups as the binding sites, which also reside between two Sc atoms and close to the metal plane. The dimerization of [5,6] *N*-methyl pyrrolidine adduct $Sc_3N@I_h\text{-}C_{80}(C_3H_7N)^-$ may occur at the [6,6,6] site next to the pentagon ring where the pyrrolidine unit is attached, whereas that of the [6,6] adduct may be related to the [5,6,6] site far from the pyrrolidine ring. In contrast to $Sc_3N@C_{80}^-$, $Y_3N@I_h\text{-}C_{80}^-$ favors the dimeric bonding via [6,6,6] carbon atoms. The most stable [5,6] $Y_3N@I_h\text{-}C_{80}(C_3H_7N)^-$ dimer is very similar to that of $Sc_3N@I_h\text{-}C_{80}(C_3H_7N)^-$. For the [6,6] $Y_3N@I_h\text{-}C_{80}(C_3H_7N)^-$ dimer, however, the two monomeric units are bonded via [6,6,6] carbon atoms with one Y atom in each monomer pointing directly to the bridging site as a result of releasing the strain experienced by the large Y_3N cluster in the C_{80} cage. In addition, $Y_3N@D_3(19)$-C_{86} most likely prefers the [6,6,6] site for the dimerization, and the most stable $(Y_3N@D_2(35)$-$C_{88})_2$ has the [5,6,6] carbon atoms as the bridging site. From the above, the authors concluded that the carbon atoms with the largest spin density distribution in the anion-radicals are generally the bonding sites in the corresponding dimers if other factors such as steric hindrance are ignored. In contrast to the cases of empty fullerenes, the dianionic EMF dimers formed via [5,6,6] sites are energetically comparable with those by [6,6,6] ones. The dimers may become more stable in solvent and the results correlate well with the observed irreversible reduction steps for the nonderivatized ones in electrochemical studies.

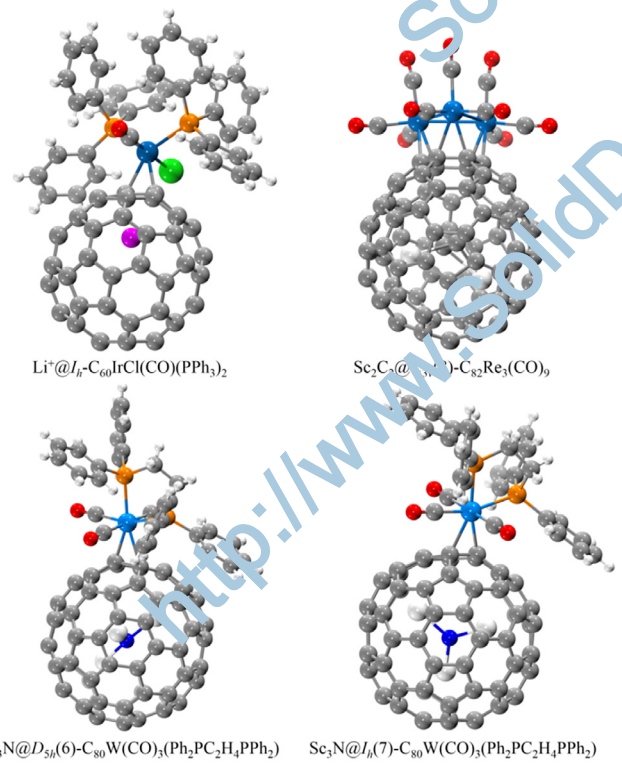

Fig. 11. Coordination reactions of EMFs. Product structures from Refs. [388,390,391].

The relative stability and orientation of the dimer can be controlled by the nature of the endohedral cluster. Voevodin et al. reported that the anionic $Lu_3N@C_{80}$ fullerenes form dimers in the $[Ni_{12}Te_{12}(PEt_3)_8]_2[(Lu_3N@C_{80})_2]$ superatomic crystal forming through the reaction between $Ni_9Te_6(PEt_3)_8$ and $Lu_3N@C_{80}$ [381]. DFT calculations reveal that, compared to $(Sc_3N@I_h\text{-}C_{80}^-)_2$ [380], which have similar energies for the [5,6,6] and [6,6,6] isomers, the latter one is energetically more favorable for $(Lu_3N@I_h\text{-}C_{80}^-)_2$. The results are consistent with the single crystal structure, which only has the [6,6,6] intercage connectivity (Fig. 10).

$Sc_3O@C_{80}$ was recently prepared but its structure failed to be fully characterized due to a rather low isolated amount [385]. Detailed DFT calculations suggest that it may bear an $I_h(7)$-C_{80} outer cage with an unpaired electron in the Sc ions. The radical character indicates that it readily forms a dimer and further polymerizes, which may account for its difficult extraction by an organic solvent.

Theoretical studies are also focused on the various properties of EMF dimers. Ono and Hirose studied the electron-conduction property of a $Li@C_{60}$ dimer sandwiched between electrodes by DFT method, and found that it had improved conductivity than the C_{60} dimer due to the filled unoccupied state around the molecule junction [386]. Recently, Zhao et al. investigated the electronic transport properties of $Li@C_{60}$ dimers under finite biases by combining DFT and the nonequilibrium Green function method [387]. The *I-V* curve shows that the $Li@C_{60}$ dimer exhibits obvious negative differential resistance (NDR) behavior: there is a quick increase followed by a decrease of current with increasing applied bias.

2.10. Coordination reaction

Coordination with transition metals has been reported for $Li^+@C_{60}$ [388], $Sc_2@C_{3v}(8)$-C_{82} [389], $Sc_3N@C_{80}$ [390], $Sc_2C_2@C_{3v}(8)$-C_{82} [391], $Sc_2C_2@C_{2v}(5)$-C_{80} [389] and $Sc_2O@C_s(6)$-C_{82} [389].

The coordination of $Li^+@C_{60}$ toward transition metals is expected to afford very stable complexes due to its higher electron-accepting ability than C_{60}. The room-temperature reaction between $[Li^+@C_{60}](PF_6^-)$ and $[IrCl(CO)(PPh_3)_2]$ in o-DCB afforded a $[\{\eta^2\text{-}(Li^+@C_{60})\}IrCl(CO)(PPh_3)_2](PF_6^-)$ mononuclear complex [388]. In addition, $[Li^+@C_{60}](PF_6^-)$ can react with $[(\eta^2\text{-}C_2H_4)Pt(PPh_3)_2]$ and first yield polynuclear complexes $[(Li^+@C_{60})\{Pt(PPh_3)_2\}_n](PF_6^-)$ $(n \geq 2)$, which further react with undissolved $[Li^+@C_{60}](PF_6^-)$ to give mononuclear $[(Li^+@C_{60})Pt(PPh_3)_2](PF_6^-)$. By adding 1,1′-bis(diphenylphosphino)ferrocene (dppf) to an o-DCB solution of $[(Li^+@C_{60})Pt(PPh_3)_2](PF_6^-)$, phosphine ligands were exchanged to give $[\{\eta^2\text{-}(Li^+@C_{60})\}Pt(dppf)](PF_6^-)$. X-ray crystal structure analysis reveals that the Ir or Pt is coordinated to a [6,6] cage bond in a η^2 fashion with the Li^+ staying adjacent to them (Fig. 11). The Li^+ ion enhances the π back-donation from the transition metal center to the carbon cage, and it resides close to the transition metals due to the electrostatic attraction from the negatively charged carbons near the outer metals. Recent DFT calculations found that the η^2[6,6]-addition pattern is energetically favorable for the coordination of $Li^+@C_{60}$ with $M(Cl)(CO)(PPh_3)_2$ (M = Rh, Ir) or $M(PPh_3)_2$ (M = Pd, Pt) fragments [392]. The

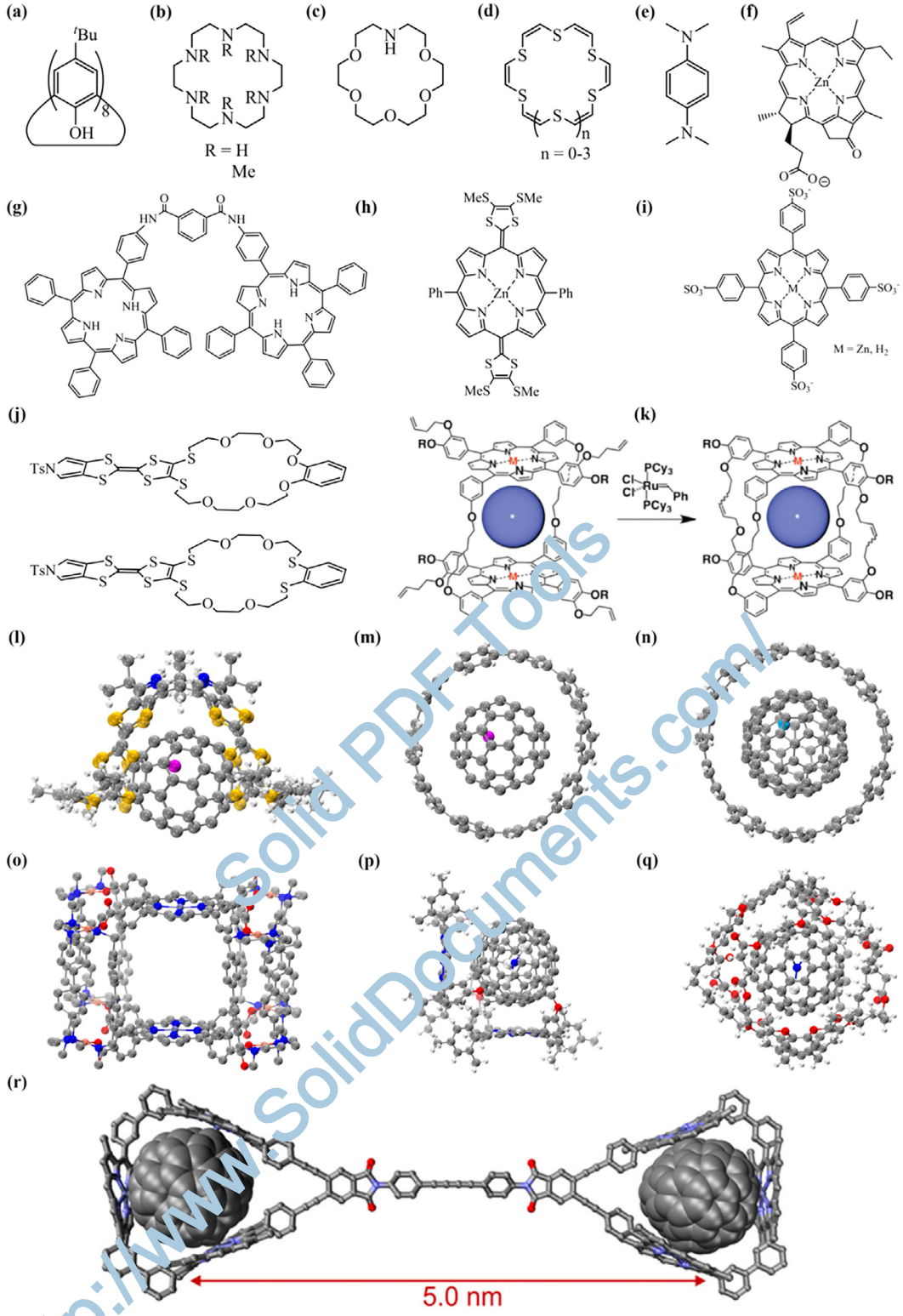

Fig. 12. (a)-(j) Molecules employed to form noncovalent systems with EMFs from Refs. [395,396,399,402,413–415,418,419] (k) *cyclo*-$[P_{Cu}]_2 \supset La@C_{82}$ and *cage*-$[P_{Cu}]_2 - \supset La@C_{82}$ from Ref. [421] (l) $Li^+@C_{60}$-TTF-C4P from Ref. [400] (m) $Li^+@C_{60} \subset$ [10]CPP from Ref. [409] (n) $La@C_{82} \subset$ [11]CPP from Ref. [424] (o) supramolecular nanocapsule from Ref. [23](p) complex of $Sc_3N@C_{80}$ with cyclic porphyrin dimer from Ref. [428](q) hemicarceplexe $Sc_3N@C_{80}$ in cyclotriveratrylene-based molecular cage [431](r) complex formed by cyclic porphyrin trimer receptor and $Y@C_{82}$ from Ref [422]. Reprinted with permission from Ref. [422]. Copyright 2018 American Chemical Society (r).

reaction between $[CpRu(CO)_2]_2$ or $Re_2(CO)_8(PMe_3)_2$ with $Li^+@C_{60}$ is theoretically predicted to yield novel η^1-coordinated metal-fullerene complexes [393].

The photo-induced mononuclear coordination reaction of either $Sc_3N@I_h$-C_{80} or $Sc_3N@D_{5h}$-C_{80} with excess $W(CO)_4(Ph_2PC_2H_4PPh_2)$ affords only one monoadduct with high regioselectivity [390].

XRD reveal that the tungsten center coordinates to a [6,6] bond of the cage far from the inner metals in a η^2 fashion, forming a closed three-membered ring on the $Sc_3N@C_{80}$ cage for the first time (Fig. 11). The two organometallic EMF complexes are air-stable despite weak π back-donation from the W center to the fullerene ligand.

An air-stable complex [(μ-H)$_3$Re$_3$(CO)$_9$-(η^2, η^2, η^2-$Sc_2C_2@C_{3v}(8)$-C_{82})] was obtained by treating $Sc_2C_2@C_{3v}(8)$-C_{82} with [(μ-H)$_3$Re$_3$(CO)$_{11}$-(NCMe)] in chlorobenzene [391]. The addition took place at the sumanene-like hexagonal ring in a highly regioselective manner (Fig. 11). Afterwards, the analogue complexes for $Sc_2@C_{3v}(8)$-C_{82}, $Sc_2C_2@C_{2v}(5)$-C_{80}, and $Sc_2O@C_s(6)$-C_{82} were also synthesized [389].

3.11. Noncovalent modification

The formation of EMF-based supramolecular systems is very attractive due to the possible presence of electron and energy transfer [394]. The reported EMFs include $Li^+@C_{60}$ [395–412], $M@C_{82}$ (M = Y, La, Gd, Dy, Ho, Tm, Lu$_2$) [413–426], $M_2@I_h(7)$-C_{80} (M = La, U) [427], $M_3N@I_h$-C_{80} (M = Sc, Lu) [428–432], $Sc_2CU@I_h(7)$-C_{80} [23], $DySc_2N@C_{80}$ [176], $Sc_3C_2@C_{80}$ [433] and $Y_2@C_{79}N$ [434,435].

Recently, stable $[K^+(18\text{-crown-6})][M@C_{2v}(9)\text{-}C_{82}]^-$ (M = Y and Ho) complexes were synthesized by the redox reaction of $M@C_{2v}$-C_{82} with potassium perchlorotriphenylmethide $[K^+(18\text{-crown-6})][C(C_6Cl_5)_3]^-$ salt as a result of the electron transfer from the $[C(C_6Cl_5)_3]^-$ anion to the EMF [416,417]. $Li^+@C_{60}$ was found can form inclusion complexes with the benzo- and dithiabenzo-crown ether functionalized monopyrrolotetrathiafulvalene (Fig. 12j) [395].

It has been reported before that $La@C_{82}$ can also form a stable 1:1 complex with a cyclic porphyrin trimer in toluene, which is the first record of EMFs' binding to a molecular receptor [421]. The receptor exhibits a high binding affinity for La@C_{82} with three porphyrins simultaneously chelated to the same EMF molecule. Two cyclic porphyrin trimers can be further connected by a rigid linker (features a central butadiyne) to form a two-site receptor and encapsulate two $Y@C_{82}$ with a center-to-center distance of 5.0 nm (Fig. 12r) [422].

Supramolecular complexes composed of $Li^+@C_{60}$ and sulphonated *meso*-tetraphenylporphyrin ($MTPPS^{4-}$: M = Zn, Fb) (Fig. 12i) were reported, and show strong binding due to the favorable cation–anion and π–π interactions [396–398]. Metalloporphyrins linked with the 1,3-dithiol-2-ylidene substituent of tetrathiafulvalene, e.g. ZnTTFP (Fig. 12h), have been synthesized and complexed with $Li^+@C_{60}$ [399]. The donor–acceptor complexes of $Li^+@C_{60}$ with tetrathiafulvalene calix[4]pyrrole (TTF-C4P, Fig. 12l) [400], and supramolecular triad composed of $Li^+@C_{60}$, a porphyrin anion and the radical cation of tetrathiafulvalene calix[4]pyrrole were also achieved [401]. A supramolecular complex was also formed by combining $Li^+@C_{60}$ and an anionic zinc chlorin carboxylate ($ZnCh^-$) (Fig. 12f) [402,403]. Different phthalocyanines possessing carboxylate groups can form supramolecular complexes with $Li^+@C_{60}$ [404]. A free base and nickel complex of a cyclic porphyrin dimer (M-CPD_{Py}, M = H_4 and Ni_2) can host $Li^+@C_{60}$ to form stable supramolecules ($Li^+@C_{60}\subset$M-CPD_{Py}) in benzonitrile [405]. The complexation of $Li^+@C_{60}$ with a phenothiazine-bridged cyclic free-base porphyrin dimer was also reported and exhibits a rather long charge-separated lifetime [406]. The supramolecular complexes between $Li^+@C_{60}$ and free base porphyrin polypeptides are successfully constructed, and feature multiple photosynthetic reaction centres [407]. Efficient charge separation can be realized in these $Li^+@C_{60}$-based noncovalent systems due to the enhanced reactivity of $Li^+@C_{60}$ in photoinduced electron-transfer reduction with various electron donors [408].

An EMF can be selectively extracted from a metallofullerene mixture in solution by complexing with extended π -conjugated systems such as cycloparaphenylene (CPP) [423]. For example, $M_x@C_{2v}$-C_{82}(M = Gd, Tm, Lu, x = 1 or 2) can be strongly captured by the [11]CPP nanoring due to the perfect size matching. Clearly, the selectivity is insensitive to the inner species. $La@C_{82}\subset$[11]CPP is the first host–guest complex comprising an EMF and a metal-free organic molecule whose structure was established by X-ray single crystal analysis (Fig. 12n) [424]. Electrochemical analysis and DFT calculations revealed that a partial charge-transfer occurs due to the strong electron-acceptor properties of $La@C_{82}$, leading to the formation of $(La@C_{82})^{\delta-}\subset[11]CPP^{\delta+}$ polar complex. It is also theoretically suggested that $Tb@C_{2v}(4348)$-C_{66} can form a stable π- π complex with [10]-CPP for its efficient isolation [436].

$Li^+@C_{60}$ is also a potential guest to complex with [10]CPP featuring strong intermolecular charge-transfer interactions. Recently, Itami et al. synthesized an ionic donor–acceptor supramolecule $Li^+@C_{60}\subset[10]CPP{\cdot}X^-$ complex (X = bis(trifluoromethanesulfonyl)imide (NTf_2) or tetrakis[3,5-bis(trifluoromethyl)-phenyl]borate (TFPB)) for the first time [409]. X-ray crystallography unambiguously characterized the structure of 1:1 complex and formation of the ionic crystal from the cationic complex and $TFPB^-$ (Fig. 12m). The binding constant in dichloromethane was estimated to be $4.8\times10^4(\pm6.6\times10^3)$ M^{-1}. Their electrochemical measurement and spectroscopic study reveal that there is strong charge-transfer interaction between the [10]CPP and $Li^+@C_{60}$ complexes, resulting in totally delocalized positive charge on the whole complex. The unique ionic compound may find applications as an electrolyte, dielectric substance, and single-molecular memories. $Li^+@C_{60}$ can bind with (12,8)-[4]*cyclo*-2,8-chrysenylene in *o*DCB at room temperature with a binding constant (log K_a) of 9.2, which is slightly smaller than that of C_{60} (log K_a = 9.6) [410]. The weakened binding affinity is explained by the metal's expanding effect on the cage size. The intriguing three-body molecular interaction in the finite single-wall carbon nanotube could be finely tuned by changing the metal species. In addition, its complex with corannulene, namely $[Li@C_{60}@C_{20}H_{10}]^+$ was observed in benzonitrile [411], and may have applications in nonlinear optical materials [437]. In the hypothetical $[Li@C_{60}@(C_6H_4)_{10}]^+$ Saturn-like complex, $[Li@C_{60}]^+$, C_{60} accepts ca. 0.12 *e* from the ring due to the substantial donor–acceptor interactions between the π orbitals of phenyl groups and the π^* orbitals of the carbon cage [438].

Graphene oxide (GO) was also used for the formation of noncovalent systems. A donor–acceptor composite was constructed by combining $Li^+@C_{60}$ with GO in neat water [412]. DFT calculations reveal that the association was mainly due to the electrostatic interactions between Li ion and electron-rich oxygen functional groups of GO. Electron transfer from GO to the triplet state of $Li^+@C_{60}$ under photoirradiation enhanced the photocurrent generation of the OTE/SnO_2 electrode. Water-soluble GO-$Gd@C_{82}$ nanohybrids were also synthesized with strong π–π stacking interactions between GO and the cage surface [425,426]. The GO-$Gd@C_{82}$ exhibits relaxation effects even higher than $Gd@C_{82}(OH)_x$ probably due to the spin electron transfer from the Gd^{3+} ion to the hydrophilic groups on the GO nanosheet. The 2D planar structure of GO and large number of hydrophilic groups on its surface also induce slow rotational correlation times.

The stable complexes of $Sc_3N@C_{80}$ and tweezers-like bis-tetraphenylporphyrin conjugates were reported to form bis-prophyrin$^{\cdot+}$-$Sc_3N@C_{80}^{\cdot-}$ charge separation states in organic and aqueous media with lifetimes of ca. 400 ps [430].

DFT calculations on the $M_3N@C_{80}$(M = Sc, Y)-Zntetraphenyl porphyrin dyads formed mainly via van del Waals interactions reveal small amounts of charge transfer from the ZnTPP to the EMF parts [439]. The internal cluster orientation does not affect the ground state charge transfer, whereas the charge transfer excitation

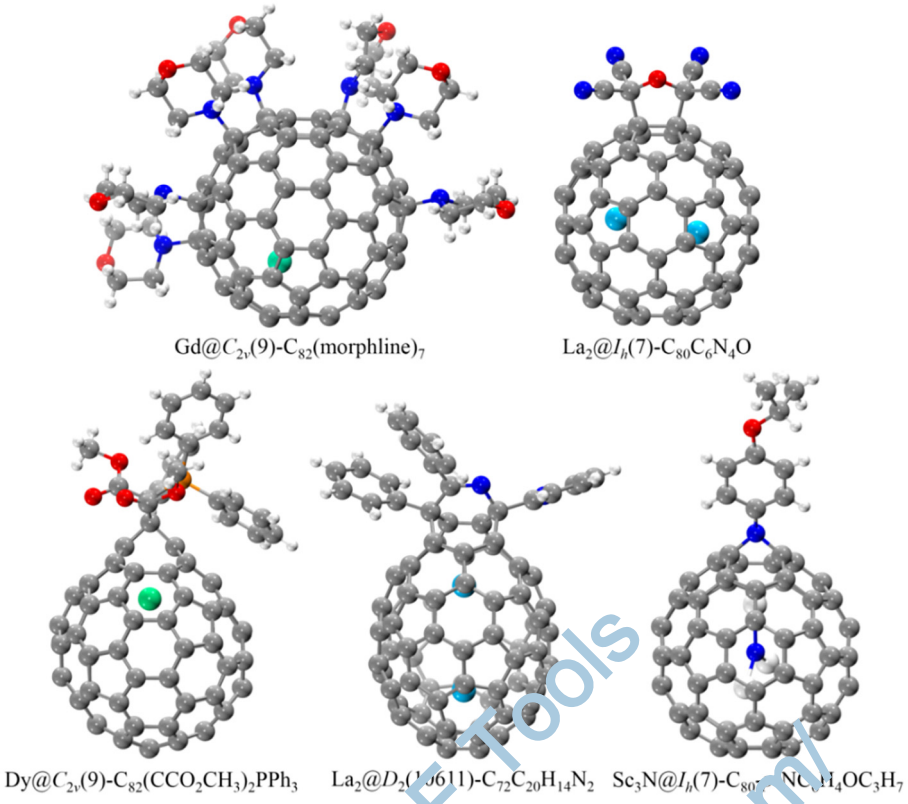

Fig. 13. Functionalized EMFs reported in Refs. [456,446,457,447,448].

energy increases from $Sc_3N@C_{80}$-ZnTPP to $Y_3N@C_{80}$-ZnTPP. The ground and exited states of the non-covalent complexes of $Sc_3N@C_{80}$ with metal-free and zinc-phthalocyanine chromophores were also investigated at the DFT level [440]. $Sc_3N@C_{68}$ and/or $Sc_3N@C_{80}$ supported on the graphene nanoflakes and various concave receptors were predicted by theory as well [441,442].

$Sc_3N@I_h$-C_{80} and $Sc_3N@D_{5h}$-C_{80} can be readily differentiated by ^1H and ^{13}C NMR spectroscopy *via* their formation of hemicarcerplexes with cyclotriveratrylene-based molecular cages (Fig. 12n) [431]. A Cu(II)-based tetragonal prismatic supramolecular nanocapsule was prepared and used to purify the two $Sc_3N@C_{80}$ isomers from EMFs soot in a single step via forming host–guest complexes [432]. Very recently, $U_2@I_h(7)$-C_{80} and the first mixed-metal actinide-based EMF $Sc_2CU@I_h(7)$-C_{80} were isolated stepwise and purified from a crude soot (also containing other EMFs such as $Sc_3N@I_h(7)$-C_{80}) by using a similar nanocapsule (Fig. 12o) [23]. It is very interesting to see that the nanocapsule can distinguish EMFs with identical outer cages but different internal species.

Besides $DySc_2N@C_{80}$ [176], paramagnetic $Sc_3C_2@C_{80}$ was successfully incorporated into the hexagonal pores of MOF-177 via an absorption method [433]. The EPR signals of $Sc_3C_2@C_{80}$ show anisotropic properties due to the restricted motion of $Sc_3C_2@C_{80}$ caused by strong π–π interaction. The spin-active $Y_2@C_{79}N$ was also incarcerated into the pores of MOF-177 crystals *via* a bottom-up approach [434,435]. In the formed host–guest complex, $Y_2@C_{79}N$ tends to situate along the *c*-axis of the crystal lattice due to the π–π interactions between its N-containing hexagonal ring and the triphenylbenzene in the MOF. It exhibits axisymmetric paramagnetic properties at low temperatures. This solid spin system may have potential applications in quantum information storage.

3.12. Miscellaneous reactions

Several other reactions have been previously reported. Liu et al. conducted the ion–molecule reactions between EMFs and small organic cations in gas phase and reported the production of $[M@C_{82}\text{-}C_2H_3O]^+$, $[M_2@C_{80}\text{-}C_2H_3O]^+$, $[M@C_{82}\text{-}C_6H_6]^+$ and $[M@C_{82}\text{-}COCH_3]^+$ (M = Ce, Nd or Tb) adducts [443–445]. Li et al. reported the reaction of Dy@C_{2v}(9)-C_{82} with triphenylphosphine (PPh_3) and dimethyl acetylenedicarboxylate (DMAD) (Fig. 13) [446]. Akasaka et al. reported the thermal [3+2] cycloaddition reaction between $La_2@I_h$-C_{80} and tetracyanoethylene oxide (TCNEO) (Fig. 13) [447]. $Sc_3N@I_h$-C_{80} can undergo thermal and photochemical reactions with 4-isopropoxyphenyl azide to afford azafulleroids $Sc_3N@I_h$-C_{80}-*p*-$NC_6H_4OC_3H_7$ (Fig. 13) [448]. By using the electrosynthetic method, Li et al. found that $[Lu_3N@I_h\text{-}C_{80}]^{2-}$ or $[Sc_3N@I_h\text{-}C_{80}]^{3-}$ can react with excess electrophile benzal bromide ($PhCHBr_2$) [449,450]. The selective reactivity of metallofullerenes with Lewis acids was used to effectively separate EMFs and their derivatives from empty fullerenes [267,451–453], and even other EMFs [454,455].

Huang et al. reported that the reaction of Gd@C_{2v}(9)C_{82} with excess morpholine in the presence of N-fluorobenzenesulfonimide affords an isomerically pure hepta-amino adduct, Gd@C_{82}(morpholine)$_7$ [456]. As indicated by the X-ray structure (Fig. 13), the additions occurred at [5,6,6] sites in a 1,4-pattern with the morpholine groups forming a continuous ribbon of edge-sharing *para*-$C_6(C_4H_8NO)_2$ hexagons.

Recently, Akasaka et al. conducted the thermal reaction of non-IPR La$_2$@D_2(10611)-C_{72} with excess 5,6-diphenyl-3-(2-pyridyl)-1,2,4-triazine and obtained two products [457]. The adsorption and NMR spectra suggest that they have the same addition patterns.

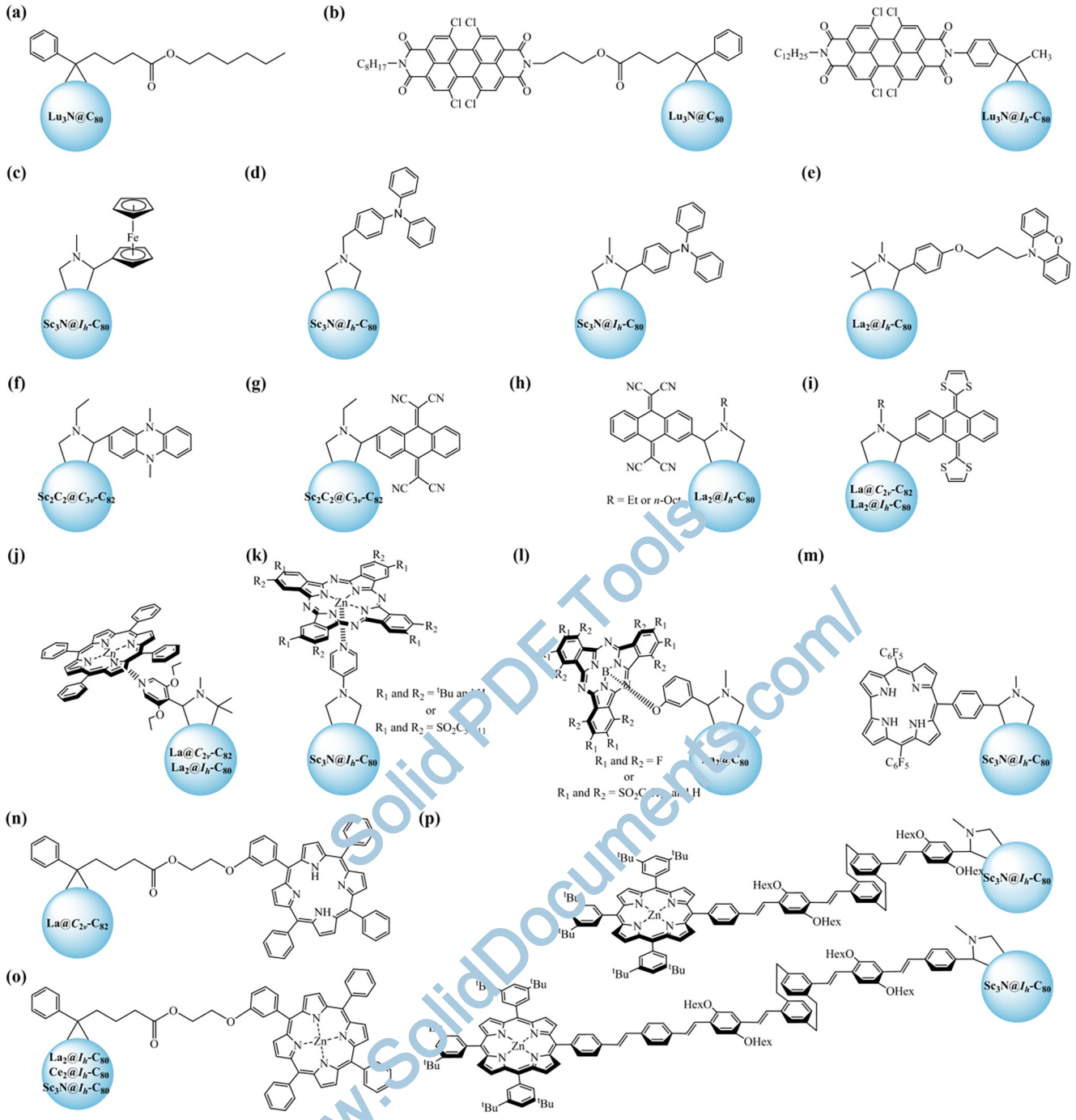

Fig. 14. Some EMF-based donor – acceptor conjugates. (a) $Lu_3N@C_{80}$-PCBH from Ref. [481] (b) $Lu_3N@C_{80}$-PDI from Refs. [479] (left) and [480] (right) (c) $Sc_3N@C_{80}$-pyrrolidine-ferrocene from Ref. [474] (d) two $Sc_3N@C_{80}$-pyrrolidine-TPA dyads from Ref. [477] (e) $La_2@I_h(7)$-C_{80}-POZ from Ref. [485] (f) $Sc_2C_2@C_{3v}(8)$-C_{82}-DDPA (g) $Sc_2C_2@C_{3v}(8)$-C_{82}-TCAQ from Ref. [489] (h) $La_2@C_{80}$-TCAQ from Ref. [471] (i) EMF-pyrrolidine-exTTF from Ref. [466] (j) EMF-Py-ZnP from Ref. [476] (k) $Sc_3N@I_h(7)$-C_{80}-Zn(II) Pcs from Ref. [486] (l) $La_2@C_{80}$–SubPc from Ref. [484] (m) $Sc_3N@C_{80}$-corrole conjugate from Ref. [487] (n) La@C_{82}-H_2Por from Ref. [472] (o) EMF-ZnP conjugate (p) $Sc_3N@C_{80}$-pyrrolidine-ZnP dyads from Ref. [478].

X-ray analysis of one isomer shows that the addition occurs at the [5,5] bond junction of one end in a highly regioselective manner and the derivative is a bisfulleroid with three seven-membered ring orifices on the elongated cage (Fig. 13).

On the theoretical side, Zhao and co-workers studied the addition of methyl azide to $Sc_2@C_{2v}(4059)$-C_{66} by means of DFT calculations [458]. They found that the [5,5] bond located on the unsaturated linear triquinane moiety is the best reaction site due to high local steric strains caused by fused pentagons. Similar regioselectivity was also suggested for the addition of 1,3-dipolar 4-isopropoxyphenyl azide. To find new anticancer inhibitors, Gutiérrez-Flores et al. theoretically explored the [2+2] cycloaddition reaction of epoxide of oestradiol for $Sc_2C_2@C_{72}$, $Sc_2@C_{76}$ and $Sc_2@C_{80}$, and proposed the possible reactive sites with the aid of molecular electrostatic potential (MEP) analysis [459].

Oxygen adducts were among the first fullerene derivatives, but are scarcely reported for EMFs [460]. The first oxide derivative of clusterfullerene, $Lu_3N@C_{80}O$, was recently synthesized by

photochemical reaction, and preliminary characterization confirmed its oxygen bridge structure [461].

The covalent bonding between $Sc_3N@C_{80}$ and pristine graphene (not common GO) was successfully achieved quite recently. The graphite was first subjected to potassium intercalation, and the negatively charged sheets were exfoliated using ultrasonication to obtain activated graphene. It then reacted with the diazonium salts of $Sc_3N@C_{80}$ obtained by Prato reaction and diazotization to get the final graphene-EMF hybrid structures [462].

4. Potential applications

4.1. Photovoltaics

The application of EMFs in photovoltaic materials will be introduced here through some recent examples, except for those mentioned above (e.g., the $Li^+@C_{60}$-based systems). The reported photoinduced electron transfer and long-lived charge separation state promise their potential towards high-efficiency organic solar cells [463–465].

Some potential systems are recently proposed, such as: the electron donor–acceptor conjugates of La@C_{2v}-C_{82}/$La_2@I_h$-C_{80} with π-extended tetrathiafulvalene (exTTF) (Fig. 14i) [466–468]; the $Ce_2@I_h$-C_{80}-ZnP conjugate (ZnP = zinc tetraphenylporphyrin) (Fig. 14o) [469] and its $La_2@I_h$-C_{80} analogue [470]; $La_2@C_{80}$ linked with the electron-withdrawing 11,11,12,12-tetracyano-9,10-anthra-*p*-quinodimethane(TCAQ) (Fig. 14h) [471]; 5,10,15,20-tetraphenylporphyrin (H_2Por)–La@C_{82} hybrids (Fig. 14n) [472] and similar systems of $Ce_2@I_h$-C_{80} [473]; [5,6] ferrocenylpyrrolidine adducts of $Sc_3N@I_h$-C_{80} (Fig. 14c) [474]; dyads composed of $M_3N@C_{80}$ (M = Sc, Y) with exTTF, Fc or phthalocyanine (Pc) derivatives [475]; 1:1 hybrid of ZnP with La@C_{2v}-C_{82}Py and $La_2@I_h$-C_{80}Py (Py = pyridyl functional group) (Fig. 14j) [476]; triphenylamine (TPA)-$Sc_3N@I_h$-C_{80} conjugates (Fig. 14d) [477]; $Sc_3N@I_h$-C_{80}-ZnP dyads with long center-to-center distances (Fig. 14p) [478]; $Lu_3N@C_{80}$ and 1,6,7,12-tetrachloro-3,4,9,10-perylenediimide (PDI) donor–acceptor conjugate (Fig. 14b left) [479]; linear $Lu_3N@I_h$-C_{80}-PDI conjugate (Fig. 14b right) [480]; $Lu_3N@C_{80}$-PCBX (X = M(methyl), B (butyl), H(hexyl), O(octyl)) (Fig. 14a) [481,482] and 1-[3-(2-ethyl) hexoxy carbonyl]propyl-1-phenyl-$Lu_3N@C_{80}$ [483].

Subphthalocyanines (SubPcs) are aromatic chromophores and their light adsorption covers most of the visible part of the spectrum. Based on the electron-donating character of $La_2@C_{80}$, Feng et al. synthesized two conjugates comprising $La_2@C_{80}$ and electron-deficient (dodecafluoro)/hexa(pentylsulfanyl)SubPc by the Prato reaction (Fig. 14l) [484]. ^{1}H NMR and COSY measurements as well as DFT calculations suggest that the reaction site is the [5,6] junction. While the ground state electronic interactions between the two moieties are negligible, the $La_2@C_{80}$-SubPc conjugates exhibit intramolecular electron transfer in the excited state.

Recently, a [5,6]-$La_2@I_h$(7)-C_{80}-phenoxazine (POZ) conjugate with possible folded conformation was prepared using the Prato reaction (Fig. 14e) [485]. Time-resolved absorption spectroscopic studies confirmed that the low-lying $(La_2@C_{80})^{\bullet-}$-$(POZ)^{\bullet+}$ radical-ion-pair state is formed due to ultrafast through-space electron transfer under photoexcitation.

N-pyridyl-substituted $Sc_3N@I_h$(7)-C_{80} was prepared and axially connected to electron-deficient or electron-rich Zn(II)phthalocyanines (Zn(II)Pcs, Fig. 14k) [486]. Depending on the electronic nature of the Zn(II)Pcs supramolecular counterpart, the formed phthalocyanine – $Sc_3N@I_h$ – C_{80} complexes show unprecedented bidirectional photoinduced electron transfer.

Liu et al. first synthesized a $Sc_3N@C_{80}$-corrole conjugate (in 38% yield) by the 1,3-dipolar reaction of $Sc_3N@C_{80}$ with corrole and sarcosine in o-DCB at 130 °C (Fig. 14m) [487]. ^{1}H NMR spectroscopy and electrochemical results suggest that the reaction most likely occurs at a [5,6] double bond. A $[Sc_3N@C_{80}]^{\bullet-}$-$[corrole]^{\bullet+}$ radical ion pair state was formed from the fast electron transfer deactivation of the photoexcited corrole.

The photoinduced charge separation (CS) of TPA-M@I_h(7)-C_{80} (M = Sc_3N, Sc_3CH, Sc_3NC, Sc_4O_2, and Sc_4O_3) were systematically investigated by theoretical calculations [488]. The driving force for the CS reaction, defined as the energy difference between the lowest locally excited (LE_1) and charge-separated (CS_1) states, is highly cluster-dependent and the process is energetically favorable for M = Sc_3N, Sc_3CH, and Sc_4O_3.

By using the Prato reaction, Wu et al. synthesized $Sc_2C_2@C_{3v}$(8)-C_{82}-2,2′-(anthracene-9,10-diylidene)dimalononitrile ($Sc_2C_2@C_{3v}$(8)-C_{82}-TCAQ, Fig. 14g) and $Sc_2C_2@C_{3v}$(8)-C_{82}-5,10-dimethyl-5,10-dihydrophenazine ($Sc_2C_2@C_{3v}$(8)-C_{82}-DDPA, Fig. 14f) as electron acceptor- and electron donor-engrafted examples, respectively [489]. Using ultrafast transient absorption spectroscopy, the substituent effects on the visible-light photoexcited electron dynamics were then investigated. Modifying the fullerene cage with an electron-donor group made long-lived triplet excitons possible.

4.2. Nanomaterials

In recent years, EMF peapods have rendered more complex electronic structures when compared with single-walled carbon nanotubes (SWNTs) filled with empty fullerenes [490–494], owing to the charge transfer and hybridization between metal and cages. EMF peapods are generally prepared by the gas phase doping reaction [495], and the nanotube ends opened by heat treatment to accommodate the EMF molecules.

There are also numerous reports for functionalized EMFs. La@C_{82}Ad can be aligned to form a nanorod with *p*-type FET property [496]. It also forms semi-metallic single crystals with high electron mobility of 10 $cm^2 V^{-1} s^{-1}$, showing its potential as an organic conductor [497,498]. Subsequently, the prepared nanorods were greatly extended to M@C_{82} (M = La, Ce), M@C_{82}Ad (M = Ce, Y), $La_2@C_{80}$Ad, and $Sc_3C_2@C_{80}$Ad [499]. Interestingly, under a magnetic field, all the nanorods are aligned with the axis perpendicular or in parallel to the field, suggesting a novel approach toward the fabrication of EMFs-based low-dimensional nanomaterials (Fig. 15a). Note that La@C_{82} (perpendicular) and its Ad adduct (parallel) show different orientations with the magnetic field. Thus the exohedral modification may switch the magnetic anisotropy of the EMF nanorods.

Gimenez-Lopez et al. synthesized *N*-methyl-2-(4-(liponyloxy)-benzyl)- [5,6]-$Sc_3N@C_{80}$ fulleropyrrolidine, inserted it into nanotubes at room temperature, and imaged the structures with aberration-corrected high-resolution transmission electron microscopy (AC-HRTEM). [500,501].The functionalized $Sc_3N@C_{80}$ form a cage-to-tail chain within the SWNT with folded functional groups (Fig. 15 b-d). Xu et al. fabricated the hexagonal nanorods of $Sc_3N@I_h$(7)-C_{80} contained in zinc *meso*-tetra(4-pyridyl) porphyrin (ZnTPyP) via a supramolecular approach [502].

Metallofullerene polymeric derivatives have been rarely reported. In 2010, Sun et al. first synthesized several Gd@C_{82}-containing copolymers through radical bulk copolymerization [503]. The polymerization reaction was conducted at 65 °C by dissolving Gd@C_{82} in styrene with benzoyl peroxide as the radical initiator to obtain black Gd@C_{82}-styrene copolymers. UV–vis, FTIR spectra and ^{13}C NMR confirmed that Gd@C_{82} has been successfully attached to the polymer chains. With a higher EA than C_{60}, Gd@C_{82} exhibited a stronger radical-scavenging ability and was more reactive during the polymerization. In 2012, Ruan et al. first synthesized the Gd@C_{82}-grafted poly(N-vinylcarbazole) (PVK) via free radical polymerization [504]. Absorption spectra confirmed that the fullerene has been covalently connected to

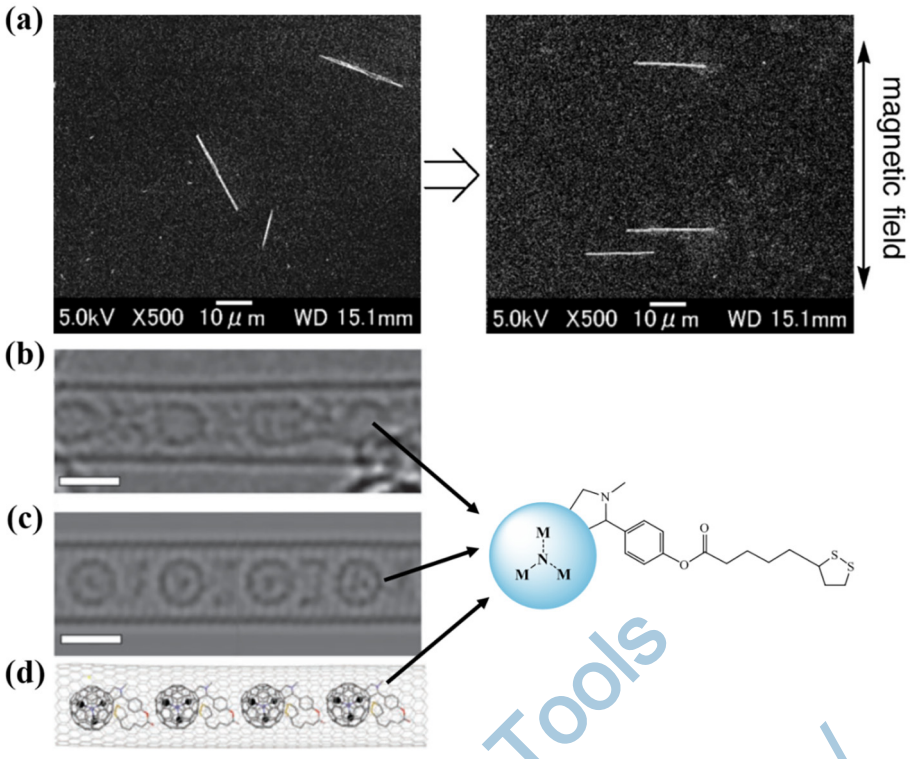

Fig. 15. (a) SEM evidence for the magnetic orientation of La@C_{82}(Ad) nanorods from Ref. [496]. (b) Experimental AC-HRTEM image, (c) simulated image and (d) structural diagram of *N*-methyl-2-(4-(liponyloxy)-benzyl)- [5,6]-Sc_3N@C_{80}@SWNT (scale bars: 2 nm). Copyright 2008 American Chemical Society (a). Adapted from Ref. [500] with permission of The Royal Society of Chemistry (b)-(d).

the PVK and grafted to its backbone. The grafted fullerenes affected the fluorescence properties of the polymer, because of the formation of electron donor–acceptor systems. Recently, they further used Gd@C_{82}-PVK in the ITO/Gd@C_{82}-PVK/Al sandwich structures to fabricate the first metallofullerene-based memory device [505]. Interestingly, DFT calculations suggest that the metal in Gd@C_{82} may accept electrons from the VK group through the cage, rendering Gd@C_{82}-PVK a novel charge-transfer complex which integrates conventional organic and inorganic charge transfer complexes.

Toth et al. synthesized the first TNT-EMF-based liquid crystal by linking Y_3N@C_{80} to two oligo(phenylene ethynylene) (OPE) arms [506]. The Bingel addition was conducted by the reaction of Y_3N@C_{80} with malonate bearing double OPE units (dOPE) or mono-brominated dOPE. The product should be a [5,6]-bridged fulleroid, and it can self-organize into liquid-crystalline mesophase during heating.

4.3. Biomedicine

Since the application of functionalized EMFs in the biomedical field has been reviewed very recently [507,508], we only selectively introduce some examples (see Subsection 3.8 for others).

Water-soluble Gd-based EMF derivatives can be employed as excellent MRI contrast reagents. For example, Gd@$C_{82}(OH)_{40}$ shows a much higher value than the commonly used Gd-DTPA (DTPA = diethylenetriaminepentaacetic acid) (81 mM^{-1} s^{-1} vs. 3.9 mM^{-1} s^{-1}) [361].

Gd@$C_{82}(OH)_{22}$ nanoparticles can inhibit lipid peroxidation, scavenge free radicals, , and have the potential for cell protection [509]. They exhibit excellent antitumor activity [510,511]. Gd@C_{82} forms a transparent complex (diameter: ca. 20–30 nm) with poly(ethylene glycol)-block-poly(2-(N,N-diethylamino)ethyl methacrylate) (PEG-PAMA), which acts as a surfactant to solubilize Gd@C_{82} via the interaction between the fullerene surface and hydrophobic PAMA segment [512]. The complex can be used in neutron capture therapy due to the high neutron capture cross sections of Gd. The tumor vascular-targeting therapeutic technique was realized by triggering the radiofrequency induced phase transition of $(Gd@C_{82})_m(OH)_n$ nanocrystals penetrated into the leaky tumor blood vessels [513].

Ho-based EMFs such as $^{166}Ho_x$@$C_{82}(OH)_y$ can be used as radiotracers and therapeutic radiopharmaceuticals [363]. The malonic ester derivatives of ^{212}Pb@C_{60} were recently prepared [514]. Compared to the ployhydroxylated radiofullerenes and conventional polyaminocarboxylate chelators for ^{212}Pb, the lead in C_{60} did not accumulate in bone, indicating a tight bond to the fullerene cage, which is favorable for targeted delivery of ^{212}Pb.

Gd_3N@C_{80} functionalized by hydroxyl and carboxyl groups was radiolabeled by ^{177}Lu and tetraazacyclododecane tetraacetic acid (DOTA) to prepare ^{177}Lu-DOTA-f-Gd_3N@C_{80}, which can serve as a novel theranostic agent [515,516]. Recently, radioactive $^{177}Lu_xLu_{(3-x)}N$@C_{80} was first functionalized to $^{177}Lu_xLu_{(3-x)}N$@C_{80}-PCBM, which was then conjugated with mPEG(5000)–NH_2 [517]. The $^{177}Lu_xLu_{(3-x)}N$@C_{80}–PCBPEG derivative shows remarkable affinity toward tumors in mice and can be metabolized at a reasonable rate, rendering itself a promising tumor-targeted theranostic agent.

The amino-functionalized Gd_3N@C_{80} (Gd_3N@C_{80}-NH_2) and PEG were conjugated to the surface of PDA (polydopamine) NPs to construct a radionuclide-^{64}Cu-labeled doxorubicin (DOX)-loaded PDA–Gd_3N@C_{80} core. This satellite nanotheranostic is promising for MR/photoacoustic/positron emission tomography and multimodal imaging-guided combination cancer therapy [518].

5. Concluding remarks

In summary, compared with empty fullerenes, which are mainly electron acceptors, EMFs are attractive and can serve as electron donors or acceptors. Their rich functionalizations not only help stabilize the missing members [519], but also confer tunable properties and turn them into versatile materials. The detailed structure and properties of an EMF derivative are determined by the delicate interplay between metal cluster, carbon cage and exohedral addends. The presence of internal metals and intramolecular electron transfer induces chemical properties dramatically different from those of empty fullerenes.

Several aspects affect the reactivity of EMFs in functionalization reactions: (1) the type of endohedral metal cluster; (2) the size of the metal cluster; (3) the size and isomerism of the outer cage; (4) the charge state of the EMF and (5) the reaction types and reagents.

High regioselectivity is frequently observed due to strong metal-cage interactions. Theoretically, the candidate addition sites usually feature: (1) short C–C bonds; (2) high pyramidalization angles; (3) appropriately shaped HOMOs/LUMOs; (4) more positive/negative charges, (6) suitable MEP distribution and/or (6) large spin density (for open-shelled systems). These calculated results, together with the consideration of aromaticity, are useful for interpreting/predicting the regioselectivity of a certain reaction. A more reliable approach (but very time-consuming) is to perform thorough thermodynamic and kinetic analysis for all the possible reactive sites. Occasionally, a reaction may afford different kinetic and thermodynamic products, whose interconversion can be tuned by temperature.

The cluster-addend mutual communication is intriguing: the type, composition, position, orientation and electron transfer of a metal cluster largely affect the regioselectivity and addition pattern. In turn, the exohedral modification will regulate the location, configuration, orientation, motion, electronic state and bonding state of the internal metallic species.

Compared to the well-established C_{60} chemistry, however, EMF research is still in its infancy. Particularly for actinide EMFs [16–23], their reactivity in various functionalization reactions remains untouched thus far. The design and synthesis of various EMF derivatives via exohedral modification are essential to achieve applicable materials. It can be foreseen that functionalized EMFs involving novel metal clusters, new carbon cages and chemical reactions will be achieved soon, and will deepen our understanding of the mysterious EMF world.

Acknowledgments

Financial support in China by National Natural Science Foundation of China (No. 21103224) and in USA by National Science Foundation-Centers of Research Excellence in Science and Technology (NSF-CREST Center) for Innovation, Research and Education in Environmental Nanotechnology (CIRE2N) (Grant No. HRD-1736093) is gratefully acknowledged.

Appendix A. Supplementary data

Supplementary data to this article can be found online at https://doi.org/10.1016/j.ccr.2019.02.028.

References

[1] A.A. Popov, S. Yang, L. Dunsch, Endohedral fullerenes, Chem. Rev. 113 (2013) 5989–6113.
[2] X. Lu, L. Feng, T. Akasaka, S. Nagase, Current status and future developments of endohedral metallofullerenes, Chem. Soc. Rev. 41 (2012) 7723–7760.
[3] S. Yang, T. Wei, F. Jin, When metal clusters meet carbon cages: endohedral clusterfullerenes, Chem. Soc. Rev. 46 (2017) 5005–5058.
[4] P. Jin, C. Tang, Z. Chen, Carbon atoms trapped in cages: metal carbide clusterfullerenes, Coord. Chem. Rev. 270–271 (2014) 89–111.
[5] J. Zhao, X. Huang, P. Jin, Z. Chen, Magnetic properties of atomic clusters and endohedral metallofullerenes, Coord. Chem. Rev. 289–290 (2015) 315–340.
[6] L. Bao, P. Peng, X. Lu, Bonding inside and outside Fullerene Cages, Acc. Chem. Res. 51 (2018) 810–815.
[7] Y. Chai, T. Guo, C. Jin, R.E. Haufler, L.P.F. Chibante, J. Fure, L. Wang, J.M. Alford, R.E. Smalley, Fullerenes with metals inside, J. Phys. Chem. 95 (1991) 7564–7568.
[8] J.M. Campanera, C. Bo, J.M. Poblet, General rule for the stabilization of fullerene cages encapsulating trimetallic nitride templates, Angew. Chem. Int. Ed. 44 (2005) 7230–7233.
[9] R. Valencia, A. Rodríguez-Fortea, J.M. Poblet, Understanding the stabilization of metal carbide endohedral fullerenes $M_2C_2@C_{82}$ and related systems, J. Phys. Chem. A. 112 (2008) 4550–4555.
[10] M.N. Chaur, R. Valencia, A. Rodríguez-Fortea, J.M. Poblet, L. Echegoyen, Trimetallic nitride endohedral fullerenes: experimental and theoretical evidence for the $M_3N^{6+}@C_{2n}^{6-}$ model, Angew. Chem. Int. Ed. 48 (2009) 1425–1428.
[11] A. Rodríguez-Fortea, A.L. Balch, J.M. Poblet, Endohedral metallofullerenes: a unique host–guest association, Chem. Soc. Rev. 40 (2011) 3551–3563.
[12] B.Q. Mercado, M.M. Olmstead, C.M. Beavers, M.L. Easterling, S. Stevenson, M. A. Mackey, C.E. Coumbe, J.D. Phillips, J.P. Phillips, J.M. Poblet, A.L. Balch, A seven atom cluster in a carbon cage, the crystallographically determined structure of $Sc_4(\mu_3\text{-}O)_3@I_h\text{-}C_{80}$, Chem. Commun. 46 (2010) 279–281.
[13] H.W. Kroto, The stability of the fullerenes C_n, with n = 24, 28, 32, 36, 50, 60 and 70, Nature 329 (1987) 529–531.
[14] T.K. Zywietz, H. Jiao, P.v.R. Schleyer, A. de Meijere, Aromaticity and antiaromaticity in oligocyclic annelated five-membered ring systems, J. Org. Chem. 63 (1998) 3417–3422.
[15] Y.-Z. Tan, S.-Y. Xie, R.-B. Huang, L.-S. Zheng, The stabilization of fused-pentagon fullerene molecules, Nat. Chem. 1 (2009) 450–460.
[16] Y. Chen, R. Morales-Martínez, X. Zhang, W. Yang, Y. Wang, A. Rodríguez-Fortea, J.M. Poblet, L. Feng, S. Wang, N. Chen, Unique four-electron metal-to-cage charge transfer of Th to a C_{82} fullerene cage: complete structural characterization of $Th@C_{3v}(8)\text{-}C_{82}$, J. Am. Chem. Soc. 139 (2017) 5110–5116.
[17] W. Cai, R. Morales-Martínez, X. Zhang, D. Najera, E. Romero, A.J. Metta Magana, A. Rodríguez-Fortea, S. Fortier, N. Chen, J.M. Poblet, L. Echegoyen, Single crystal structures and theoretical calculations of uranium endohedral metallofullerenes ($U@C_{2n}$, 2n = 74, 82) show cage isomer dependent oxidation states for U, Chem. Sci. 8 (2017) 5282–5290.
[18] P. Jin, C. Liu, Y. Li, L. Li, L. Zhao, Th@C76., Computational characterization of larger actinide endohedral fullerenes, Int. J. Quantum Chem. 118 (2018) e25501.
[19] P. Zhao, X. Zhang, M. Ehara, Theoretical insights into monometallofullerene $Th@C_{76}$: the covalent interaction between thorium and the carbon cage, Inorg. Chem. 57 (2018) 2961–2964.
[20] Y. Li, Y. Yang, C. Liu, Q. Hou, P. Jin, X. Lu, Th-based endohedral metallofullerenes: anomalous metal position and significant metal-cage covalent interactions with the involvement of Th 5f orbitals, Inorg. Chem. 57 (2018) 7142–7150.
[21] X. Zhang, Y. Wang, R. Morales-Martínez, J. Zhong, C. de Graaf, A. Rodríguez-Fortea, J.M. Poblet, L. Echegoyen, L. Feng, N. Chen, $U_2@I_h(7)\text{-}C_{80}$: crystallographic characterization of a long-sought dimetallic actinide endohedral fullerene, J. Am. Chem. Soc. 140 (2018) 3907–3915.
[22] X. Zhang, W. Li, L. Feng, X. Chen, A. Hansen, S. Grimme, S. Fortier, D.-C. Sergentu, T.J. Duignan, J. Autschbach, S. Wang, Y. Wang, G. Velkos, A.A. Popov, N. Aghdassi, S. Duhm, X. Li, J. Li, L. Echegoyen, W.H.E. Schwarz, N. Chen, A diuranium carbide cluster stabilized inside a C_{80} fullerene cage, Nat. Commun. 9 (2018) 2753.
[23] C. Fuertes-Espinosa, A. Gómez-Torres, R. Morales-Martínez, A. Rodríguez-Fortea, C. García-Simón, F. Gándara, I. Imaz, J. Juanhuix, D. Maspoch, J.M. Poblet, L. Echegoyen, X. Ribas, Purification of uranium-based endohedral metallofullerenes (EMFs) by selective supramolecular encapsulation and release, Angew. Chem. Int. Ed. 57 (2018) 11294–11299.
[24] M.M. Alvarez, E.G. Gillan, K. Holczer, R.B. Kaner, K.S. Min, R.L. Whetten, La_2C_{80}: a soluble dimetallofullerene, J. Phys. Chem. 95 (1991) 10561–10563.
[25] S. Stevenson, G. Rice, T. Glass, K. Harich, F. Cromer, M.R. Jordan, J. Craft, E. Hadju, R. Bible, M.M. Olmstead, K. Maitra, A.J. Fisher, A.L. Balch, H.C. Dorn, Small-bandgap endohedral metallofullerenes in high yield and purity, Nature 401 (1999) 55–57.
[26] J. Zhang, S. Stevenson, H.C. Dorn, Trimetallic nitride template endohedral metallofullerenes: discovery, structural characterization, reactivity, and applications, Acc. Chem. Res. 46 (2013) 1548–1557.
[27] C.-R. Wang, T. Kai, T. Tomiyama, T. Yoshida, Y. Kobayashi, E. Nishibori, M. Takata, M. Sakata, H. Shinohara, A scandium carbide endohedral metallofullerene: $(Sc_2C_2)@C_{84}$, Angew. Chem. Int. Ed. 40 (2001) 397–399.
[28] M. Krause, F. Ziegs, A.A. Popov, L. Dunsch, Entrapped bonded hydrogen in a fullerene: the five-atom cluster Sc_3CH in C_{80}, ChemPhysChem 8 (2007) 537–540.
[29] T.-S. Wang, L. Feng, J.-Y. Wu, W. Xu, J.-F. Xiang, K. Tan, Y.-H. Ma, J.-P. Zheng, L. Jiang, X. Lu, C.-Y. Shu, C.-R. Wang, Planar quinary cluster inside a fullerene cage: synthesis and structural characterizations of $Sc_3NC@C_{80}\text{-}I_h$, J. Am. Chem. Soc. 132 (2010) 16362–16364.
[30] P. Jin, Z. Zhou, C. Hao, Z. Gao, K. Tan, X. Lu, Z. Chen, NC unit trapped by fullerenes: a density functional theory study on $Sc_3NC@C_{2n}$ (2n = 68, 78 and 80), Phys. Chem. Chem. Phys. 12 (2010) 12442–12449.

[31] T. Wang, J. Wu, Y. Feng, Scandium carbide/cyanide alloyed cluster inside fullerene cage synthesis and structural studies of $Sc_3(\mu_3\text{-}C_2)(\mu_3\text{-}CN)@I_h\text{-}C_{80}$, Dalton Trans. 43 (2014) 16270–16274.

[32] S. Stevenson, M.A. Mackey, M.A. Stuart, J.P. Phillips, M.L. Easterling, C.J. Chancellor, M.M. Olmstead, A.L. Balch, A distorted tetrahedral metal oxide cluster inside an icosahedral carbon cage. Synthesis, isolation, and structural characterization of $Sc_4(\mu_3\text{-}O)_2@I_h\text{-}C_{80}$, J. Am. Chem. Soc. 130 (2008) 11844–11845.

[33] L. Dunsch, S. Yang, L. Zhang, A. Svitova, S. Oswald, A.A. Popov, Metal sulfide in a C_{82} fullerene cage: a new form of endohedral clusterfullerenes, J. Am. Chem. Soc. 132 (2010) 5413–5421.

[34] W. Xu, L. Feng, M. Calvaresi, J. Liu, Y. Liu, B. Niu, Z. Shi, Y. Lian, F. Zerbetto, An experimentally observed trimetallofullerene $Sm_3@I_h\text{-}C_{80}$, J. Am. Chem. Soc. 135 (2013) 4187–4190.

[35] M.N. Chaur, F. Melin, A.L. Ortiz, L. Echegoyen, Chemical, electrochemical, and structural properties of endohedral metallofullerenes, Angew. Chem. Int. Ed. 48 (2009) 7514–7538.

[36] M. Yamada, T. Akasaka, S. Nagase, Endohedral metal atoms in pristine and functionalized fullerene cages, Acc. Chem. Res. 43 (2010) 92–102.

[37] T. Tsuchiya, T. Akasaka, S. Nagase, New vistas in fullerene endohedrals: Functionalization with compounds from main group elements, Pure Appl. Chem. 82 (2010) 505–521.

[38] Y. Maeda, T. Tsuchiya, X. Lu, Y. Takano, T. Akasaka, S. Nagase, Current progress on the chemical functionalization and supramolecular chemistry of $M@C_{82}$, Nanoscale 3 (2011) 2421–2429.

[39] S. Osuna, M. Swart, M. Solà, The reactivity of endohedral fullerenes. What can be learnt from computational studies?, Phys Chem. Chem. Phys. 13 (2011) 3585–3603.

[40] X. Lu, T. Akasaka, S. Nagase, Chemistry of endohedral metallofullerenes: the role of metals, Chem. Commun. 47 (2011) 5942–5957.

[41] C.M. Cardona, Functionalization of endohedral metallofullerenes, Curr. Org. Chem. 16 (2012) 1095–1108.

[42] X. Lu, L. Bao, T. Akasaka, S. Nagase, Recent progress in the chemistry of endohedral metallofullerenes, Chem. Commun. 50 (2014) 14701–14715.

[43] M.R. Cerón, L. Echegoyen, Recent progress in the synthesis of regio-isomerically pure bis-adducts of empty and endohedral fullerenes, J. Phys. Org. Chem. 29 (2016) 613–619.

[44] M.R. Cerón, V. Maffeis, S. Stevenson, L. Echegoyen, Endohedral fullerenes: synthesis, isolation, mono and bis-functionalization, Inorg. Chim. Acta 468 (2017) 16–27.

[45] P.W. Fowler, D.E. Manolopoulos, An Atlas of Fullerenes, Clarendon Oxford, 1995.

[46] T. Akasaka, T. Wakahara, S. Nagase, K. Kobayashi, M. Waelchli, K. Yamamoto, M. Kondo, S. Shirakura, S. Okubo, Y. Maeda, T. Kato, M. Kako, Y. Nakadaira, R. Nagahata, X. Gao, E.V. Caemelbecke, K.M. Kadish, $La@C_{82}$ bis(silyl) addition: An unusually stable metallofullerene, J. Am. Chem. Soc. 122 (2000) 9316–9317.

[47] P. Jin, C. Hao, S. Li, W. Mi, Z. Sun, J. Zhang, Q. Hou, Theoretical study on the motion of a La atom inside a C_{82} cage, J. Phys. Chem. A 111 (2007) 167–169.

[48] S. Stevenson, P. Burbank, K. Harich, Z. Sun, H.C. Dorn, F.J.M. van Loosdrecht, M.S. deVries, J.R. Salem, C.-H. Kiang, R.D. Johnson, D.S. Bethune, $La_2@C_{72}$: metal-mediated stabilization of a carbon cage, J. Phys. Chem. A. 102 (1998) 2833–2837.

[49] H. Kato, A. Taninaka, T. Sugai, H. Shinohara, Structure of a missing-caged metallofullerene: $La_2@C_{72}$, J. Am. Chem. Soc. 125 (2003) 7782–7783.

[50] Z. Slanina, Z. Chen, P.v.R. Schleyer, F. Uhlík, X. Lu, S. Nagase, $La_2@C_{72}$ and $Sc_2@C_{72}$: computational characterizations, J. Phys. Chem. A 110 (2006) 2231–2234.

[51] P. Jin, W. Mi, C. Hao, S. Li, Z. Gao, Relativistic density functional theory study on the ^{139}La chemical shifts and electronic spectra of $La_2@C_{72}$, Comput. Theor. Nanosci. 6 (2009) 434–438.

[52] X. Lu, H. Nikawa, T. Nakahodo, T. Tsuchiya, M.O. Ishitsuka, Y. Maeda, T. Akasaka, M. Toki, H. Sawa, Z. Slanina, N. Mizorogi, S. Nagase, Chemical understanding of a non-IPR metallofullerene: stabilization of encaged metals on fused-pentagon bonds in $La_2@C_{72}$, J. Am. Chem. Soc. 130 (2008) 9129–9136.

[53] X. Lu, H. Nikawa, T. Tsuchiya, Y. Maeda, M.O. Ishitsuka, T. Akasaka, M. Toki, H. Sawa, Z. Slanina, N. Mizorogi, S. Nagase, Bis-carbene adducts of non-IPR $La_2@C_{72}$: localization of high reactivity around fused pentagons and electrochemical properties, Angew. Chem. Int. Ed. 47 (2008) 8642–8645.

[54] B. Cao, T. Wakahara, T. Tsuchiya, M. Kondo, Y. Maeda, G.M.A. Rahman, T. Akasaka, K. Kobayashi, S. Nagase, K. Yamamoto, Isolation, characterization, and theoretical study of $La_2@C_{78}$, J. Am. Chem. Soc. 126 (2004) 9164–9165.

[55] B. Cao, H. Nikawa, T. Nakahodo, T. Tsuchiya, Y. Maeda, T. Akasaka, H. Sawa, Z. Slanina, N. Mizorogi, S. Nagase, Addition of adamantylidene to $La_2@C_{78}$: isolation and single-crystal X-ray structural determination of the monoadducts, J. Am. Chem. Soc. 130 (2008) 983–989.

[56] K. Kobayashi, S. Nagase, T. Akasaka, A theoretical study of C_{80} and $La_2@C_{80}$, Chem. Phys. Lett. 245 (1995) 230–236.

[57] T. Akasaka, S. Nagase, K. Kobayashi, M. Wälchli, K. Yamamoto, H. Funasaka, M. Kato, T. Hoshino, T. Erata, ^{13}C and ^{139}La NMR studies of $La_2@C_{80}$: first evidence for circular motion of metal atoms in endohedral dimetallofullerene, Angew. Chem., Int. Ed. Engl. 36 (1997) 1643–1645.

[58] J. Zhang, C. Hao, S. Li, W. Mi, P. Jin, Which configuration is more stable for $La_2@C_{80}$, D_{3d} or D_{2h}? Recomputation with ZORA methods within ADF, J. Phys. Chem. C 111 (2007) 7862–7867.

[59] E. Nishibori, M. Takata, M. Sakata, A. Taninaka, H. Shinohara, Pentagonal-dodecahedral La_2 charge density in $[80\text{-}I_h]$fullerene: $La_2@C_{80}$, Angew. Chem. Int. Ed. 40 (2001) 2998–2999.

[60] H. Shimotani, T. Ito, Y. Iwasa, A. Taninaka, H. Shinohara, E. Nishibori, M. Takata, M. Sakata, Quantum chemical study on the configurations of encapsulated metal ions and the molecular vibration modes in endohedral dimetallofullerene $La_2@C_{80}$, J. Am. Chem. Soc. 126 (2004) 364–369.

[61] K. Kobayashi, S. Nagase, T. Akasaka, Endohedral dimetallofullerenes $Sc_2@C_{84}$ and $La_2@C_{80}$. Are the metal atoms still inside the fullerene cages?, Chem Phys. Lett. 261 (1996) 502–506.

[62] J.C. Duchamp, A. Demortier, K.R. Fletcher, D. Dorn, E.B. Iezzi, T. Glass, H.C. Dorn, An isomer of the endohedral metallofullerene $Sc_3N@C_{80}$ with D_{5h} symmetry, Chem. Phys. Lett. 375 (2003) 655–659.

[63] M. Krause, L. Dunsch, Isolation and characterisation of two $Sc_3N@C_{80}$ isomers, ChemPhysChem 5 (2004) 1445–1449.

[64] T. Cai, L. Xu, M.R. Anderson, Z. Ge, T. Zuo, X. Wang, M.M. Olmstead, A.L. Balch, H.W. Gibson, H.C. Dorn, Structure and enhanced reactivity rates of the D_{5h} $Sc_3N@C_{80}$ and $Lu_3N@C_{80}$ metallofullerene isomers: the importance of the pyracylene motif, J. Am. Chem. Soc. 128 (2006) 8581–8589.

[65] S. Stevenson, P.W. Fowler, T. Heine, J.C. Duchamp, G. Rice, T. Glass, K. Harich, E. Hajdu, R. Bible, H.C. Dorn, A stable non-classical metallofullerene family, Nature 408 (2000) 427–428.

[66] M.M. Olmstead, H.M. Lee, J.C. Duchamp, S. Stevenson, D. Marciu, H.C. Dorn, A. L. Balch, $Sc_3N@C_{68}$: folded pentalene coordination in an endohedral fullerene that does not obey the isolated pentagon rule, Angew. Chem., Int. Ed. 42 (2003) 900–903.

[67] M.H. Olmstead, A. de Bettencourt-Dias, J.C. Duchamp, S. Stevenson, D. Marciu, H.C. Dorn, A.L. Balch, Isolation and structural characterization of the endohedral fullerene $Sc_3N@C_{78}$, Angew. Chem. Int. Ed. 40 (2001) 1223–1225.

[68] J.M. Campanera, C. Bo, M.M. Olmstead, A.L. Balch, J.M. Poblet, Bonding within the endohedral fullerenes $Sc_3N@C_{78}$ and $Sc_3N@C_{80}$ as determined by density functional calculations and reexamination of the crystal structure of $\{Sc_3N@C_{78}\}Co(OEP)\}1.5(C_6H_6)0.3(CHCl_3)$, J. Phys. Chem. A 106 (2002) 12356–12364.

[69] Y. Iiduka, T. Wakahara, T. Nakahodo, T. Tsuchiya, A. Sakuraba, Y. Maeda, T. Akasaka, K. Yoza, E. Horn, T. Kato, M.T.H. Liu, N. Mizorogi, K. Kobayashi, S. Nagase, Structural determination of metallofullerene Sc_3C_{82} revisited: a surprising finding, J. Am. Chem. Soc. 127 (2005) 12500–12501.

[70] H. Fang, H. Cong, M. Suzuki, Q. Bao, B. Yu, Y. Xie, N. Mizorogi, M.M. Olmstead, A.L. Balch, S. Nagase, T. Akasaka, X. Lu, Regioselective benzyl radical addition to an open-shell cluster metallofullerene. crystallographic studies of cocrystallized $Sc_3C_2@I_h\text{-}C_{80}$ and its singly bonded derivative, J. Am. Chem. Soc. 136 (2014) 10534–10540.

[71] K. Tan, X. Lu, Electronic structure and redox properties of the open-shell metal–carbide endofullerene $Sc_3C_2@C_{80}$: a density functional theory investigation, J. Phys. Chem. A 110 (2006) 1171–1176.

[72] X. Lu, K. Nakajima, Y. Iiduka, H. Nikawa, N. Mizorogi, Z. Slanina, T. Tsuchiya, S. Nagase, T. Akasaka, Structural elucidation and regioselective functionalization of an unexplored carbide cluster metallofullerene $Sc_2C_2@C_s(6)\text{-}C_{82}$, J. Am. Chem. Soc. 133 (2011) 19553–19558.

[73] Y. Iiduka, T. Wakahara, K. Nakajima, T. Nakahodo, T. Tsuchiya, Y. Madeda, T. Akasaka, K. Yoza, M.T.H. Liu, N. Mizorogi, S. Nagase, Experimental and theoretical studies of the scandium carbide endohedral metallofullerene $Sc_2C_2@C_{82}$ and its carbene derivative, Angew. Chem., Int. Ed. 46 (2007) 5562–5564.

[74] H. Kurihara, X. Lu, Y. Iiduka, H. Nikawa, M. Hachiya, N. Mizorogi, Z. Slanina, T. Tsuchiya, S. Nagase, T. Akasaka, X-ray structures of $Sc_2C_2@C_{2n}$ ($n = 40$–42): in-depth understanding of the core-shell interplay in carbide cluster metallofullerenes, Inorg. Chem. 51 (2012) 746–750.

[75] X. Lu, K. Nakajima, Y. Iiduka, H. Nikawa, T. Tsuchiya, N. Mizorogi, Z. Slanina, S. Nagase, T. Akasaka, The long-believed $Sc_2@C_{2v}(17)\text{-}C_{84}$ is actually $Sc_2C_2@C_{2v}(9)\text{-}C_{82}$: unambiguous structure assignment and chemical functionalization, Angew. Chem. Int. Ed. 51 (2012) 5889–5892.

[76] M. Kako, S. Nagase, T. Akasaka, Functionalization of endohedral metallofullerenes with reactive silicon and germanium compounds, Molecules 22 (2017) 1179.

[77] T. Akasaka, T. Kato, K. Kobayashi, S. Nagase, K. Yamamoto, H. Funasaka, T. Takahashi, Exohedral adducts of $La@C_{82}$, Nature 374 (1995) 600–601.

[78] S. Nagase, K. Kobayashi, The ionization energies and electron affinities of endohedral metallofullerenes MC_{82}(M = Sc, Y, La): density functional calculations, J. Chem. Soc. Chem. Commun. 1837–1838 (1994).

[79] T. Suzuki, Y. Maruyama, T. Kato, K. Kikuchi, Y. Achiba, Electrochemical properties of $La@C_{82}$, J. Am. Chem. Soc. 115 (1993) 11006–11007.

[80] T. Kato, T. Akasaka, K. Kobayashi, S. Nagase, K. Kikuchi, Y. Achiba, T. Suzuki, K. Yamamoto, Chemical reactivities of endohedral metallofullerenes, J. Phys. Chem. Solids 58 (1997) 1779–1783.

[81] T. Akasaka, T. Kato, S. Nagase, K. Kobayashi, K. Yamamoto, H. Funasaka, T. Takahashi, Chemical derivatization of endohedral metallofullerene $La@C_{82}$ with digermirane, Tetrahedron 52 (1996) 5015–5020.

[82] M. Yamada, L. Feng, T. Wakahara, T. Tsuchiya, Y. Maeda, Y. Lian, M. Kako, T. Akasaka, T. Kato, K. Kobayashi, S. Nagase, Synthesis and characterization of exohedrally silylated $M@C_{82}$ (M = Y and La), J. Phys. Chem. B 109 (2005) 6049–6051.

[83] T. Wakahara, J.-I. Kobayashi, M. Yamada, Y. Maeda, T. Tsuchiya, M. Okamura, T. Akasaka, M. Waelchli, K. Kobayashi, S. Nagase, T. Kato, M. Kako, K.

Yamamoto, K.M. Kadish, Characterization of Ce@C_{82} and its anion, J. Am. Chem. Soc. 126 (2004) 4883–4887.
[84] T. Akasaka, S. Okubo, M. Kondo, Y. Maeda, T. Wakahara, T. Kato, T. Suzuki, K. Yamamoto, K. Kobayashi, S. Nagase, Isolation and characterization of two Pr@C_{82} isomers, Chem. Phys. Lett. 319 (2000) 153–156.
[85] T. Akasaka, S. Nagase, K. Kobayashi, T. Suzuki, T. Kato, K. Yamamoto, H. Funasaka, T. Takahashi, Exohedral derivatization of an endohedral metallofullerene Gd@C_{82}, J. Chem. Soc., Chem. Commun. (1995) 1343–1344.
[86] T. Kato, T. Akasaka, K. Kobayashi, S. Nagase, K. Yamamoto, H. Funasaka, T. Takahashi, ESR study on the reactivity of two isomers of LaC_{82} with disilirane, Appl. Magn. Reson. 11 (1996) 293–300.
[87] Y. Maeda, J. Miyashita, T. Hasegawa, T. Wakahara, T. Tsuchiya, L. Feng, Y. Lian, T. Akasaka, K. Kobayashi, S. Nagase, M. Kato, K. Yamamoto, K.M. Kadish, Chemical reactivities of the cation and anion of M@C_{82} (M = Y, La, and Ce), J. Am. Chem. Soc. 127 (2005) 2143–2146.
[88] J. Ruan, Y. Xie, W. Cai, Z. Slanina, N. Mizorogi, S. Nagase, T. Akasaka, X. Lu, Chemical properties of divalent metallofullerenes Yb@D_{3h}(1)-C_{74} and Yb@C_2(13)-C_{84}, Fuller. Nanotub. Carbon Nanostruct. 22 (2014) 138–146.
[89] M. Yamada, T. Wakahara, T. Tsuchiya, Y. Maeda, M. Kako, T. Akasaka, K. Yoza, E. Horn, N. Mizorogi, S. Nagase, Location of the metal atoms in Ce_2@C_{78} and its bis-silylated derivative, Chem. Commun. 558–560 (2008).
[90] X. Aparicio-Anglès, N. Alegret, A. Clotet, A. Rodríguez-Fortea, J.M. Poblet, Endohedral metallofullerenes containing lanthanides: a robust yet simple computational approach, J. Phys. Chem. C 117 (2013) 12916–12921.
[91] T. Akasaka, S. Nagase, K. Kobayashi, T. Suzuki, T. Kato, K. Kikuchi, Y. Achiba, K. Yamamoto, H. Funasaka, T. Takahashi, Synthesis of the first adducts of the dimetallofullerenes La_2@C_{80} and Sc_2@C_{84} by addition of a disilirane, Angew. Chem. Int. Ed. Engl. 34 (1995) 2139–2141.
[92] K. Kobayashi, S. Nagase, Y. Maeda, T. Wakahara, T. Akasaka, La_2@C_{80}: is the circular motion of two La atoms controllable by exohedral addition?, Chem Phys. Lett. 374 (2003) 562–566.
[93] T. Wakahara, M. Yamada, S. Takahashi, T. Nakahodo, T. Tsuchiya, Y. Maeda, T. Akasaka, M. Kako, K. Yoza, E. Horn, N. Mizorogi, S. Nagase, Two-dimensional hopping motion of encapsulated La atoms in silylated La_2@C_{80}, Chem. Commun. (2007) 2680–2682.
[94] M. Yamada, T. Nakahodo, T. Wakahara, T. Tsuchiya, Y. Maeda, T. Akasaka, M. Kako, K. Yoza, E. Horn, N. Mizorogi, K. Kobayashi, S. Nagase, Positional control of encapsulated atoms inside a fullerene cage by exohedral addition, J. Am. Chem. Soc. 127 (2005) 14570–14571.
[95] M. Yamada, M. Minowa, S. Sato, M. Kako, Z. Slanina, N. Mizorogi, T. Tsuchiya, Y. Maeda, S. Nagase, T. Akasaka, Thermal carbosilylation of endohedral dimetallofullerene La_2@I_h-C_{80} with silirane, J. Am. Chem. Soc. 132 (2010) 17953–17960.
[96] M. Yamada, N. Mizorogi, T. Tsuchiya, T. Akasaka, S. Nagase, Synthesis and characterization of the D_{5h} isomer of the endohedral dimetallofullerene Ce_2@C_{80}: two-dimensional circulation of encapsulated Ce atoms inside a fullerene cage, Chem. Eur. J. 15 (2009) 9486–9493.
[97] Y. Iiduka, O. Ikenaga, A. Sakuraba, T. Wakahara, T. Tsuchiya, Y. Maeda, T. Nakahodo, T. Akasaka, M. Kako, N. Mizorogi, S. Nagase, Chemical reactivity of Sc_3N@C_{80} and La_2@C_{80}, J. Am. Chem. Soc. 127 (2005) 9956–9957.
[98] T. Wakahara, Y. Iiduka, O. Ikenaga, T. Nakahodo, A. Sakuraba, T. Tsuchiya, Y. Maeda, M. Kako, T. Akasaka, K. Yoza, E. Horn, N. Mizorogi, S. Nagase, Characterization of the bis-silylated endofullerene Sc_3N@C_{80}, J. Am. Chem. Soc. 128 (2006) 9919–9925.
[99] K. Sato, M. Kako, M. Suzuki, N. Mizorogi, T. Tsuchiya, M.M. Olmstead, A.L. Balch, T. Akasaka, S. Nagase, Synthesis of silylene-bridged endohedral metallofullerene $Lu_3N@I_h$-C_{80}, J. Am. Chem. Soc. 134 (2012) 1603–1609.
[100] K. Sato, M. Kako, N. Mizorogi, T. Tsuchiya, T. Akasaka, S. Nagase, Bis-silylation of $Lu_3N@I_h$-C_{80}: considerable variation in the electronic structures, Org. Lett. 14 (2012) 5908–5911.
[101] M. Kako, K. Miyabe, K. Sato, M. Suzuki, N. Mizorogi, W. Wang, M. Yamada, Y. Maeda, M.M. Olmstead, A.L. Balch, S. Nagase, T. Akasaka, Preparation, Structural Determination, and Characterization of Electronic Properties of Bis-silylated and Bis-germylated $Lu_3N@C_{80}$, Chem. Eur. J. 21 (2015) 16411–16420.
[102] M. Kako, T. Sugiura, T. Akasaka, Photochemical addition of silirane to endohedral metallofullerene: electronic properties of carbosilylated $Sc_3N@I_h$-C_{80}, Phosphorus Sulfur Silicon Relat. Elem. 191 (2016) 201–206.
[103] M. Kako, T. Sugiura, K. Miyabe, M. Suzui, M. Yamada, Y. Maeda, J.-D. Guo, S. Nagase, T. Akasaka, Preparation, structural determination, and characterization of electronic properties of [5,6]- and [6,6]-carbosilylated $Sc_3N@I_h$-C_{80}, Chem. Asian J. 12 (2017) 1391–1399.
[104] M. Kako, K. Minami, T. Morozova, S. Fukazawa, Y. Arikawa, M. Yamada, Y. Maeda, Q.-Z. Li, S. Nagase, T. Akasaka, Photoreactions of endohedral metallofullerene $Lu_3N@I_h$-C_{80} with disiliranes: electronic properties of carbosilylated $Lu_3N@I_h$-C_{80}, Molecules 22 (2017) 850.
[105] M. Kako, F. Ozeki, S. Kanzawa, S. Fukazawa, K. Sato, M. Yamada, Y. Maeda, M. Furukawa, T. Akasaka, Photoreactions of $Sc_3N@I_h$-C_{80} and $Lu_3N@I_h$-C_{80} with disilirane: Isolation and characterization of labile 1,2-adducts, Heteroatom Chem. 29 (2018) e21477.
[106] T. Wakahara, A. Sakuraba, Y. Iiduka, M. Okamura, T. Tsuchiya, Y. Maeda, T. Akasaka, S. Okubo, T. Kato, K. Kobayashi, S. Nagase, K.M. Kadish, Chemical reactivity and redox property of Sc_3@C_{82}, Chem. Phys. Lett. 398 (2004) 553–556.
[107] T. Akasaka, X. Lu, Structural and electronic properties of endohedral metallofullerenes, Chem. Rec. 12 (2012) 256–269.
[108] E.B. Iezzi, J.C. Duchamp, K. Harich, T.E. Glass, H.M. Lee, M.M. Olmstead, A.L. Balch, H.C. Dorn, A symmetric derivative of the trimetallic nitride endohedral metallofullerene, $Sc_3N@C_{80}$, J. Am. Chem. Soc. 124 (2002) 524–525.
[109] H.M. Lee, M.M. Olmstead, E. Iezzi, J.C. Duchamp, H.C. Dorn, A.L. Balch, Crystallographic characterization and structural analysis of the first organic functionalization product of the endohedral fullerene $Sc_3N@C_{80}$, J. Am. Chem. Soc. 124 (2002) 3494–3495.
[110] H. Kawakami, H. Okada, Y. Matsuo, Efficient Diels-Alder addition of cyclopentadiene to lithium ion encapsulated [60]fullerene, Org. Lett. 15 (2013) 4466–4469.
[111] H. Ueno, H. Kawakami, K. Nakagawa, H. Okada, N. Ikuma, S. Aoyagi, K. Kokubo, Y. Matsuo, T. Oshima, Kinetic study of the diels-alder reaction of Li^+@C_{60} with cyclohexadiene: greatly increased reaction rate by encapsulated Li^+, J. Am. Chem. Soc. 136 (2014) 11162–11167.
[112] Y. Maeda, J. Miyashita, T. Hasegawa, T. Wakahara, T. Tsuchiya, T. Nakahodo, T. Akasaka, N. Mizorogi, K. Kobayashi, S. Nagase, T. Kato, N. Ban, H. Nakajima, Y. Watanabe, Reversible and regioselective reaction of La@C_{82} with cyclopentadiene, J. Am. Chem. Soc. 127 (2005) 12190–12191.
[113] Y. Maeda, S. Sato, K. Inada, H. Nikawa, M. Yamada, N. Mizorogi, T. Hasegawa, T. Tsuchiya, T. Akasaka, T. Kato, Z. Slanina, S. Nagase, Regioselective exohedral functionalization of La@C_{82} and its 1,2,3,4,5-pentamethylcyclopentadiene and adamantylidene adducts, Chem. Eur. J. 16 (2010) 2193–2197.
[114] M. Garcia-Borràs, J.M. Luis, M. Swart, M. Solà, Diels-Alder and retro-Diels–Alder cycloadditions of (1,2,3,4,5-pentamethyl)cyclopentadiene to La@C_{2v}-C_{82}: regioselectivity and product stability, Chem. Eur. J. 19 (2013) 4468–4479.
[115] S. Sato, Y. Maeda, J.-D. Guo, M. Yamada, N. Mizorogi, S. Nagase, T. Akasaka, Mechanistic study of the Diels-Alder reaction of paramagnetic endohedral metallofullerene reaction of La@C_{82} with 1,2,3,4,5-pentamethylcyclopentadiene, J. Am. Chem. Soc. 135 (2013) 5582–5587.
[116] Y. Takano, Y. Nagashima, M.Á. Herranz, N. Martín, T. Akasaka, Thermodynamically stable [4+2] cycloadducts of lanthanum-encapsulated endohedral metallofullerenes, Beilstein J. Org. Chem. 10 (2014) 714–721.
[117] Z. Zhang, Y. Zhang, W. Xue, Z. Guo, P. Cui, Diels-Alder reactivity of metallofullerene $Sc_3N@C_{78}$ and structure elucidation on its products, ChemistrySelect 2 (2017) 8880–8885.
[118] S. Stevenson, R.R. Stephen, T.M. Amos, V.R. Cadorette, J.E. Reid, J.P. Phillips, Synthesis and purification of a trimetallic nitride fullerene bisadduct: exploring the reactivity of $Gd_3N@C_{80}$, J. Am. Chem. Soc. 127 (2005) 12776–12777.
[119] Z. Zhang, W. Xue, W. Jiang, Z. Wang, J. Zhang, Y. Zhang, L. Wang, Z. Guo, P. Cui, Endohedral regulator for metallofullerene chemical property: Diels-Alder reaction studies of $Sc_xY_{3-x}N@C_{80}$-I_h(x = 0–3), ChemistrySelect 3 (2018) 1495–1498.
[120] W. Fu, J. Zhang, T. Fuhrer, H. Champion, K. Furukawa, T. Kato, J.E. Mahaney, B. G. Burke, K. A. Williams, K. Walker, C. Dixon, J. Ge, C. Shu, K. Harich, H.C. Dorn, Gd_2@$C_{79}N$ isolation, characterization, and monoadduct formation of a very stable heterofullerene with a magnetic spin state of S = 15/2, J. Am. Chem. Soc. 133 (2011) 9741–9750.
[121] D. Wang, H. Li, H. Wang, L. Li, Counter anion in Li^+-encapsulated C_{60} can further enhance the rate of Diels-Alder reaction: a DFT study, Int. J. Quantum Chem. 116 (2016) 1846–1850.
[122] C.-X. Cui, Y.-J. Liu, Role of encapsulated metal cation in the reactivity and regioselectivity of the C_{60} Diels–Alder reaction, J. Phys. Chem. A 119 (2015) 3098–3106.
[123] Y. García-Rodeja, M. Solà, F.M. Bickelhaupt, I. Fernández, Understanding the reactivity of ion-encapsulated fullerenes, Chem. Eur. J. 23 (2017) 11030–11036.
[124] T. Debnath, T. Ash, J.K. Saha, A.K. Das, Mechanistic insight into the enhancement of reactivity of C_{60}^+ in comparison with neutral C_{60} and EMFs towards different fundamental reactions: a DFT approach, ChemistrySelect 2 (2017) 4039–4053.
[125] P. Ravinder, V. Subramanian, Role of Encapsulation of Na^+ and F^- Ions on the Diels-Alder Reactivity of C_{32}, J. Phys. Chem. A 116 (2012) 6870–6878.
[126] S. Osuna, M. Swart, J.M. Campanera, J.M. Poblet, M. Solà, Chemical reactivity of D_{3h} $_{C7}$8 (metallo)fullerene: regioselectivity changes induced by S_c3N encapsulation, J. Am. Chem. Soc. 130 (2008) 6206–6214.
[127] S. Osuna, M. Swart, M. Solà, The Diels-Alder reaction on endohedral $Y_3N@C_{78}$: the importance of the fullerene strain energy, J. Am. Chem. Soc. 131 (2009) 129–139.
[128] M. Garcia-Borràs, S. Osuna, J.M. Luis, M. Swart, M. Solà, The exohedral Diels-Alder reactivity of the titanium carbide endohedral metallofullerene Ti_2C_2@D_{3h}-C_{78}: comparison with D_{3h}–C_{78} and $M_3N@D_{3h}$-C_{78} (M = Sc and Y) reactivity, Chem. Eur. J. 18 (2012) 7141–7154.
[129] M. Garcia-Borràs, A. Romero-Rivera, S. Osuna, J.M. Luis, M. Swart, M. Solà, The frozen cage model: a computationally low-cost tool for predicting the exohedral regioselectivity of cycloaddition reactions involving endohedral metallofullerenes, J. Chem. Theor. Comput. 8 (2012) 1671–1683.
[130] F.M. Bickelhaupt, M. Solà, I. Fernández, Understanding the reactivity of endohedral metallofullerenes: C_{78} versus $Sc_3N@C_{78}$, Chem. Eur. J. 21 (2015) 5760–5768.
[131] S. Osuna, R. Valencia, A. Rodríguez-Fortea, M. Swart, M. Solà, J.M. Poblet, Full exploration of the Diels-Alder cycloaddition on metallofullerenes $M_3N@C_{80}$ (M = Sc, Lu, Gd): the D_{5h} versus I_h isomer and the influence of the metal cluster, Chem. Eur. J. 18 (2012) 8944–8956.
[132] M. Garcia-Borràs, S. Osuna, J.M. Luis, M. Swart, M. Solà, A complete guide on the influence of metal clusters in the Diels-Alder regioselectivity of I_h-C_{80} endohedral metallofullerenes, Chem. Eur. J. 19 (2013) 14931–14940.

[133] T. Yang, X. Zhao, S. Nagase, T. Akasaka, Diels-Alder reaction on free C_{68} fullerene and endohedral $Sc_3N@C_{68}$ fullerene violating the isolated pentagon rule importance of pentagon adjacency, Chem. Asian J. 9 (2014) 2604–2611.

[134] P. Zhao, X. Zhao, M. Ehara, Regioselectivity of $Sc_2C_2@C_{3v}(8)$-C_{82}: role of the sumanene-type hexagon in Diels-Alder reaction, J. Org. Chem. 81 (2016) 8169–8174.

[135] R.C. Haddon, π-Electrons in three dimensions, Acc. Chem. Res. 21 (1988) 243–249.

[136] R. Zhao, K. Yuan, S. Zhao, X. Zhao, M. Ehara, Quantum chemical insight into La_2C_{96}: metal carbide fullerene $La_2C_2@C_{94}$ versus dimetallofullerene $La_2@C_{96}$, Inorg. Chem. 56 (2017) 11883–11890.

[137] C.-X. Cui, Y.-J. Liu, Y. Zhang, L.-B. Qu, Z.-P. Zhang, Theoretical study on the reactivity and regioselectivity of the Diels-Alder reaction of fullerene: effects of charges and encapsulated lanthanum on the bis-functionalization of C_{70}, J. Phys. Chem. A 121 (2017) 523–531.

[138] Z. Ge, J.C. Duchamp, T. Cai, H.W. Gibson, H.C. Dorn, Purification of endohedral trimetallic nitride fullerenes in a single, facile step, J. Am. Chem. Soc. 127 (2005) 16292–16298.

[139] B. Cao, T. Wakahara, Y. Maeda, A. Han, T. Akasaka, T. Kato, K. Kobayashi, S. Nagase, Lanthanum endohedral metallofulleropyrrolidines: synthesis, isolation, and EPR characterization, Chem. Eur. J. 10 (2004) 716–720.

[140] N. Crivillers, Y. Takano, Y. Matsumoto, J. Casado-Montenegro, M. Mas-Torrent, C. Rovira, T. Akasaka, J. Veciana, Electrochemical and magnetic properties of a surface-grafted novel endohedral metallofullerene derivative, Chem. Commun. 49 (2013) 8145–8147.

[141] Y. Takano, Z. Slanina, J. Mateos, T. Tsuchiya, H. Kurihara, F. Uhlík, M.Á. Herranz, N. Martín, S. Nagase, T. Akasaka, Unprecedented chemical reactivity of a paramagnetic endohedral metallofullerene $La@C_s$-C_{82} that leads hydrogen addition in the 1,3-dipolar cycloaddition reaction, J. Am. Chem. Soc. 136 (2014) 17537–17546.

[142] X. Lu, X. He, L. Feng, Z. Shi, Z. Gu, Synthesis of pyrrolidine ring-fused metallofullerene derivatives, Tetrahedron 60 (2004) 3713–3716.

[143] L. Feng, X. Lu, X. He, Z. Shi, Z. Gu, Reactions of endohedral metallofullerenes with azomethine ylides: an efficient route toward metallofullerene-pyrrolidines, Inorg. Chem. Commun. 7 (2004) 1010–1013.

[144] M. Yamada, T. Wakahara, T. Nakahodo, T. Tsuchiya, Y. Maeda, T. Akasaka, K. Yoza, E. Horn, N. Mizorogi, S. Nagase, Synthesis and structural characterization of endohedral pyrrolidinodimetallofullerenes: $La_2@C_{80}(CH_2)_2NTrt$, J. Am. Chem. Soc. 128 (2006) 1402–1403.

[145] M. Yamada, M. Okamura, S. Sato, C.I. Someya, N. Mizorogi, T. Tsuchiya, T. Akasaka, T. Kato, S. Nagase, Two regioisomers of endohedral pyrrolidinodimetallofullerenes $M_2@I_h$-$C_{80}(CH_2)_2NTrt$ (M = La, Ce; Trt = trityl): control of metal atom positions by addition positions, Chem. Eur. J. 15 (2009) 10533–10542.

[146] M. Yamada, Z. Slanina, N. Mizorogi, A. Muranaka, Y. Maeda, S. Nagase, T. Akasaka, N. Kobayashi, Application of MCD spectroscopy and TD-DFT to endohedral metallofullerenes, Phys. Chem. Chem. Phys. 15 (2013) 3593–3601.

[147] T. Cai, L. Xu, H.W. Gibson, H.C. Dorn, C.J. Chancellor, M.M. Olmstead, A.L. Balch, $Sc_3N@C_{78}$: encapsulated cluster regiochemical adduct docking on an ellipsoidal metallofullerene sphere, J. Am. Chem. Soc. 129 (2007) 10795–10800.

[148] T. Cai, Z. Ge, E.B. Iezzi, T.E. Glass, K. Harich, H.W. Gibson, H.C. Dorn, Synthesis and characterization of the first trimetallic nitride templated pyrrolidino endohedral metallofullerenes, Chem. Commun. 3594–3596 (2005).

[149] C.M. Cardona, A. Kitaygorodskiy, A. Ortiz, M.Á. Herranz, L. Echegoyen, The first fulleropyrrolidine derivative of $Sc_3N@C_{80}$: pronounced chemical shift differences of the geminal protons on the pyrrolidine ring, J. Org. Chem. 70 (2005) 5092–5097.

[150] T. Cai, C. Slebodnick, L. Xu, K. Harich, T.E. Glass, C. Chancellor, J.C. Fettinger, M. M. Olmstead, A.L. Balch, H.W. Gibson, H.C. Dorn, A pivotal hinge on a metallofullerene sphere: interconversion of isomers of a trityl pyrrolidino I_h $Sc_3N@C_{80}$, J. Am. Chem. Soc. 128 (2006) 6486–6492.

[151] S. Osuna, A. Rodríguez-Fortea, J.M. Poblet, M. Sola, M. Swart, Product formation in the Prato reaction on $Sc_3N@D_{5h}$-C_{80} preference for [5,6]-bonds, and not pyracylenic bonds, Chem. Commun. 48 (2012) 2486–2488.

[152] Y. Maeda, M. Kimura, C. Ueda, M. Yamada, T. Kawabata, M. Suzuki, W.-W. Wang, N. Mizorogi, N. Karousis, N. Tagmatarchis, H. Isobe, E. Nakamura, M.M. Olmstead, A.L. Balch, S. Nagase, T. Akasaka, Isolation and characterization of [5,6]-pyrrolidino-$Sc_3N@I_h$-C_{80} diastereomers, Chem. Commun. 50 (2014) 12552–12555.

[153] B. Liu, H. Cong, X. Li, B. Yu, L. Bao, Y. Cai, Y. Xie, X. Lu, Highly regioselective 1,3-dipolar cycloaddition of diphenylnitrilimine to $Sc_3N@I_h$-C_{80} affording a very stable, unprecedented pyrrole-ring fused derivative of endohedral metallofullerenes, Chem. Commun. 50 (2014) 12710–12713.

[154] L. Bao, M. Chen, W. Chen, C. Tan, K.B. Ghiassi, M.M. Olmstead, A.L. Balch, T. Akasaka, X. Lu, Regioselective synthesis and crystallographic characterization of isoxazoline-ring-fused derivatives of $Sc_3N@I_h$-C_{80} and C_{60}, Inorg. Chem. 55 (2016) 4075–4077.

[155] C.M. Cardona, A. Kitaygorodskiy, L. Echegoyen, Trimetallic nitride endohedral metallofullerenes: reactivity dictated by the encapsulated metal cluster, J. Am. Chem. Soc. 127 (2005) 10448–10453.

[156] C.M. Cardona, B. Elliott, L. Echegoyen, Unexpected chemical and electrochemical properties of $M_3N@C_{80}$ (M = Sc, Y, Er), J. Am. Chem. Soc. 128 (2006) 6480–6485.

[157] A. Rodríguez-Fortea, J.M. Campanera, C.M. Cardona, L. Echegoyen, J.M. Poblet, Dancing on a fullerene surface: isomerization of $Y_3N@$(N-ethylpyrrolidino-C_{80}) from the 6,6 to the 5,6 regioisomer, Angew. Chem., Int. Ed. 45 (2006) 8176–8180.

[158] L. Echegoyen, C.J. Chancellor, C.M. Cardona, B. Elliott, J. Rivera, M.M. Olmstead, A.L. Balch, X-Ray crystallographic and EPR spectroscopic characterization of a pyrrolidine adduct of $Y_3N@C_{80}$, Chem. Commun. (2006) 2653–2655.

[159] B. Elliott, A.D. Pykhova, J. Rivera, C.M. Cardona, L. Dunsch, A.A. Popov, L. Echegoyen, Spin density and cluster dynamics in $Sc_3N@C_{80}$ upon [5,6] exohedral functionalization: an ESR and DFT study, J. Phys. Chem. C 117 (2013) 2344–2348.

[160] M.d.C. Gimenez-Lopez, J.A. Gardener, A.Q. Shaw, A. Iwasiewicz-Wabnig, K. Porfyrakis, C. Balmer, G. Dantelle, M. Hadjipanayi, A. Croosley, N.R. Champness, M.R. Castell, G.A.D. Briggs, A.N. Khlobystov, Endohedral metallofullerenes in self-assembled monolayers, Phys. Chem. Chem. Phys. 12 (2010) 123–131.

[161] Z. Zhou, J. Zhang, R. Sadler, J. Yang, A. Coleman, Synthesis of trimetasphere pyrrolidino derivatives reaction of $Lu_3N@C_{80}$ with N-ethylglycine in the presence and absence of aldehyde, ECS Trans. 2 (2007) 103–117.

[162] N. Chen, J.R. Pinzón, L. Echegoyen, Influence of the encapsulated clusters on the electrochemical behaviour of endohedral fullerene derivatives: comparative study of N-tritylpyrrolidino derivatives of $Sc_3N@I_h$-C_{80} and $Lu_3N@I_h$-C_{80}, ChemPhysChem 12 (2011) 1422–1425.

[163] Y. Li, T. Wang, C. Zhao, Y. Qin, H. Meng, M. Nie, L. Jiang, C. Wang, A magnetoreception system constructed by a dysprosium metallofullerene and nitroxide radical, Dalton Trans. 46 (2017) 8938–8941.

[164] N. Martín, M. Altable, S. Filippone, A. Martín-Domenech, L. Echegoyen, C.M. Cardona, Retro-cycloaddition reaction of pyrrolidinofullerenes, Angew. Chem. Int. Ed. 45 (2006) 110–114.

[165] O. Lukoyanova, C.M. Cardona, M. Altable, S. Filippone, A.M. Domenech, N. Martin, L. Echegoyen, Selective electrochemical retro-cycloaddition reaction by pyrrolidinofullerenes, Angew. Chem., Int. Ed. 45 (2006) 7430–7433.

[166] B. Wu, T. Wang, Z. Zhang, Y. Feng, L. Gan, L. Jiang, C. Wang, An effective retro-cycloaddition of $M_3N@C_{80}$ (M = Sc, Lu, Ho) metallofulleropyrrolidines, Chem. Commun. 49 (2013) 10489–10491.

[167] S. Aroua, M. Garcia-Borràs, M.F. Bölter, S. Osuna, Y. Yamakoshi, Endohedral metal-induced regioselective formation of bis-prato adduct of $Y_3N@I_h$-C_{80} and $Gd_3N@I_h$-C_{80}, J. Am. Chem. Soc. 137 (2015) 58–61.

[168] M.R. Cerón, M. Izquierdo, M. Garcia-Borràs, S.S. Lee, S. Stevenson, S. Osuna, L. Echegoyen, Bis-1,3-dipolar cycloadditions on endohedral fullerenes $M_3N@I_h$-C_{80} (M = Sc, Lu): remarkable endohedral-cluster regiochemical control, J. Am. Chem. Soc. 137 (2015) 11778–11782.

[169] S. Aroua, Y. Yamakoshi, Prato reaction of $M_3N@I_h$-C_{80} (M = Sc, Lu, Y, Gd) with reversible isomerization, J. Am. Chem. Soc. 134 (2012) 20242–20245.

[170] S. Aroua, M. Garcia-Borràs, S. Osuna, K. Yamakoshi, Essential factors for control of the equilibrium in the reversible rearrangement of $M_3N@I_h$-C_{80} fulleropyrrolidines: exohedral functional groups versus endohedral metal clusters, Chem. Eur. J. 20 (2014) 14032–14039.

[171] Y. Feng, T. Wang, J. Xiang, L. Gan, B. Wu, L. Jiang, C. Wang, Tuneable dynamics of a scandium nitride cluster inside an I_h-C_{80} cage, Dalton Trans. 44 (2015) 2057–2060.

[172] C. Shu, W. Xu, C. Slebodnick, H. Champion, W. Fu, J.E. Reid, H. Azurmendi, C. Wang, K. Harich, H.C. Dorn, Syntheses and structures of phenyl-C_{81}-butyric acid methyl esters (PCBMs) from $M_3N@C_{80}$, Org. Lett. 11 (2009) 1753–1756.

[173] B. Wu, Y. Li, L. Jiang, C. Wang, T. Wang, Spin-paramagnet communication between nitroxide radical and metallofullerene, J. Phys. Chem. C 120 (2016) 6252–6255.

[174] N. Chen, E. Zhang, K. Tan, C.-R. Wang, X. Lu, Size effect of encaged clusters on the exohedral chemistry of endohedral fullerenes: a case study on the pyrrolidino reaction of $Sc_xGd_{3-x}N@C_{80}$ (x = 0–3), Org. Lett. 9 (2007) 2011–2013.

[175] N. Chen, L.-Z. Fan, K. Tan, Y.-Q. Wu, C.-Y. Shu, X. Lu, C.-R. Wang, Comparative spectroscopic and reactivity studies of $Sc_{3-x}Y_xN@C_{80}$ (x = 0–3), J. Phys. Chem. C 111 (2007) 11823–11828.

[176] Y. Li, T. Wang, H. Meng, C. Zhao, M. Nie, L. Jiang, C. Wang, Controlling the magnetic properties of dysprosium metallofullerene within metal–organic frameworks, Dalton Trans. 45 (2016) 19226–19229.

[177] C.-H. Chen, D.S. Krylov, S.M. Avdoshenko, F. Liu, L. Spree, R. Westerstrom, C. Bulbucan, M. Studniarek, J. Dreiser, A.U.B. Wolter, B. Buchner, A.A. Popov, Magnetic hysteresis in self-assembled monolayers of Dy-fullerene single molecule magnets on gold, Nanoscale 10 (2018) 11287–11292.

[178] W. Cai, M. Chen, L. Bao, Y. Xie, T. Akasaka, X. Lu, In-depth understanding of the chemical properties of rarely explored carbide cluster metallofullerenes: a case study of $Sc_2C_2@C_{3v}(8)$-C_{82} that reveals a general rule, Chem. Eur. J. 21 (2015) 3449–3454.

[179] T. Wang, J. Wu, W. Xu, J. Xiang, X. Lu, B. Li, L. Jiang, C. Shu, C. Wang, Spin divergence induced by exohedral modification: ESR study of $Sc_3C_2@C_{80}$ fulleropyrrolidine, Angew. Chem. Int. Ed. 49 (2010) 1786–1789.

[180] T. Wang, J. Wu, Y. Feng, Y. Ma, L. Jiang, C. Shu, C. Wang, Preparation and ESR study of $Sc_3C_2@C_{80}$ bis-addition fulleropyrrolidines, Dalton Trans. 41 (2012) 2567–2570.

[181] B. Wu, T. Wang, Y. Feng, Z. Zhang, L. Jiang, C. Wang, Molecular magnetic switch for a metallofullerenes, Nat. Commun. 6 (2015) 6468.

[182] H. Meng, C. Zhao, M. Nie, C. Wang, T. Wang, Triptycene molecular rotor mounted on metallofullerene $Sc_3C_2@C_{80}$ and their spin-rotation couplings, Nanoscale 10 (2018) 18119–18123.

[183] Y. Ma, T. Wang, J. Wu, Y. Feng, L. Jiang, C. Shu, C. Wang, Susceptible electron spin adhering to an yttrium cluster inside an azafullerene $C_{79}N$, Chem. Commun. 48 (2012) 11570–11572.

[184] T. Akasaka, T. Kono, Y. Matsunaga, T. Wakahara, T. Nakahodo, M.O. Ishitsuka, Y. Maeda, T. Tsuchiya, T. Kato, M.T.H. Liu, N. Mizorogi, Z. Slanina, S. Nagase, Isolation and characterization of carbene derivatives of La@$C_{82}(C_s)$, J. Phys. Chem. A 112 (2008) 1294–1297.

[185] N. Tagmatarchis, A. Taninaka, H. Shinohara, Production and EPR characterization of exohedrally perfluoroalkylated paramagnetic lanthanum metallofullerenes: (La@C_{82})–(C_8F_{17})$_2$, Chem. Phys. Lett. 355 (2002) 226–232.

[186] C.R. Wang, T. Kai, T. Tomiyama, T. Yoshida, Y. Kobayashi, E. Nishibori, M. Takata, M. Sakata, H. Shinohara, C_{66} fullerene encaging a scandium dimer, Nature 408 (2000) 426–427.

[187] M. Yamada, H. Kurihara, M. Suzuki, J.D. Guo, M. Waelchli, M.M. Olmstead, A.L. Balch, S. Nagase, Y. Maeda, T. Hasegawa, X. Lu, T. Akasaka, Sc_2@C_{66} revisited: an endohedral fullerene with scandium ions nestled within two unsaturated linear triquinanes, J. Am. Chem. Soc. 136 (2014) 7611–7614.

[188] Q.-Z. Li, J.-J. Zheng, X. Zhao, Bingel-Hirsch reaction on Sc_2@C_{66}: a highly regioselective bond neighboring to unsaturated linear triquinanes, J. Phys. Chem. C 119 (2015) 26196–26201.

[189] S.M. Avdoshenko, Fullerene faraday cage keeps magnetic properties of inner cluster pristine, J. Comput. Chem. 39 (2018) 1594–1598.

[190] Y. Zhang, K.B. Ghiassi, Q. Deng, N.A. Samoylova, M.M. Olmstead, A.L. Balch, A. A. Popov, Synthesis and structure of $LaSc_2N$@C_s(hept)-C_{80} with one heptagon and thirteen pentagons, Angew. Chem. Int. Ed. 54 (2015) 495–499.

[191] Q. Deng, A.A. Popov, Prato and Bingel-Hirsch cycloaddition to heptagon-containing $LaSc_2N$@C_s(hept)-C_{80}: importance of pentalene units, Chem. Commun. 51 (2015) 5637–5640.

[192] J.-Y. Wang, C.-S. Lin, M.-Y. Zhang, G.-L. Chai, W.-D. Cheng, Theoretical study on the one-, two-, and three-photon absorption properties of exohedral functionalized derivative of Sc_3N@C_{80}, Int. J. Quantum. Chem. 112 (2012) 1198–1208.

[193] R. Valencia, A. Rodríguez-Fortea, A. Clotet, C. de Graaf, M.N. Chaur, L. Echegoyen, J.M. Poblet, Electronic structure and redox properties of metal nitride endohedral fullerenes M_3N@C_{2n} (M = Sc, Y, La, and Gd; 2n = 80, 84, 88, 92, 96), Chem. Eur. J. 15 (2009) 10997–11009.

[194] R.D. Bolskar, A.F. Benedetto, L.O. Husebo, R.E. Price, E.F. Jackson, S. Wallace, L. J. Wilson, J.M. Alford, First soluble M@C_{60} derivatives provide enhanced access to metallofullerenes and permit in vivo evaluation of Gd@C_{60}[C(COOH)$_2$]$_{10}$ as a MRI contrast agent, J. Am. Chem. Soc. 125 (2003) 5471–5478.

[195] L. Feng, T. Nakahodo, T. Wakahara, T. Tsuchiya, Y. Maeda, T. Akasaka, T. Kato, E. Horn, K. Yoza, N. Mizorogi, S. Nagase, A singly bonded derivative of endohedral metallofullerene: La@C_{82}CBr(COOC$_2$H$_5$)$_2$, J. Am. Chem. Soc. 127 (2005) 17136–17137.

[196] L. Feng, T. Wakahara, T. Nakahodo, T. Tsuchiya, Q. Piao, Y. Maeda, Y. Lian, T. Akasaka, E. Horn, K. Yoza, T. Kato, N. Mizorogi, S. Nagase, The bingel monoadducts of La@C_{82}: synthesis, characterization, and electrochemistry, Chem. Eur. J. 12 (2006) 5578–5586.

[197] L. Feng, T. Tsuchiya, T. Wakahara, T. Nakahodo, Q. Piao, Y. Maeda, T. Akasaka, T. Kato, K. Yoza, E. Horn, N. Mizorogi, S. Nagase, Synthesis and characterization of a bisadduct of La@C_{82}, J. Am. Chem. Soc. 128 (2006) 5990–5991.

[198] R. He, H. Zhao, J. Liu, Y. Jiao, Y. Liang, X. Li, C. Chen, Synthesis and aggregation studies of Bingel-Hirsch monoadducts of gadofullerene, Fuller. Nanotub. Carbon Nanostruct. 21 (2013) 549–559.

[199] R. He, G. Xing, X. Wang, Y. Jiao, H. Zhao, H. Yuan, S. Wang, J. Dong, H. Lei, Synthesis and evaluation of Bingel-Hirsch multiadducts of paramagnetic gadofullerene as potential magnetic resonance imaging contrast agents, J. Nanosci. Nanotechnol. 13 (2013) 1549–1554.

[200] C.Y. Shu, C.R. Wang, J.F. Zhang, H.W. Gibson, H.C. Dorn, F.D. Corwin, P.P. Fatouros, T.J.S. Dennis, Organophosphonate functionalized Gd@C_{82} as a magnetic resonance imaging contrast agent, Chem. Mater. 20 (2008) 2106–2108.

[201] O. Lukoyanova, C.M. Cardona, J. Rivera, L.Z. Lugo-Morales, C.J. Chancellor, M. M. Olmstead, A. Rodríguez-Fortea, J.M. Poblet, A.L. Balch, L. Echegoyen, "Open Rather than Closed" malonate methano-fullerene derivatives. The formation of methanofulleroid adducts of Y_3N@C_{80}, J. Am. Chem. Soc. 129 (2007) 10423–10430.

[202] J.R. Pinzón, T. Zuo, L. Echegoyen, Synthesis and electrochemical studies of Bingel-Hirsch derivatives of M_3N@I_h-C_{80} (M = Y, Lu), Chem. Eur. J. 16 (2010) 4864–4869.

[203] N. Alegret, R. Rodríguez-Fortea, J.M. Poblet, Bingel-Hirsch addition on endohedral metallofullerenes: kinetic versus thermodynamic control, Chem. Eur. J. 19 (2013) 5061–5068.

[204] T. Wei, M. Eugenia Pérez-Gómez, A. Hirsch, The first molecular dumbbell consisting of an endohedral Sc_3N@C_{80} and an empty C_{60}-fullerene building block, Chem. Commun. 53 (2017) 7886–7889.

[205] M. Garcia-Borràs, M. Osuna, S. Osuna, M. Izquierdo, J.M. Luis, L. Echegoyen, M. Solà, The regioselectivity of Bingel-Hirsch cycloadditions on isolated pentagon rule endohedral metallofullerenes, Angew. Chem. Int. Ed. 55 (2016) 2374–2377.

[206] M.N. Chaur, F. Melin, A.J. Athans, B. Elliott, K. Walker, B.C. Holloway, L. Echegoyen, The influence of cage size on the reactivity of trimetallic nitride metallofullerenes: a mono- and bis-methanoadduct of Gd_3N@C_{80} and a monoadduct of Gd_3N@C_{84}, Chem. Commun. 2665–2667 (2008).

[207] N. Alegret, M.N. Chaur, E. Santos, A. Rodríguez-Fortea, L. Echegoyen, J.M. Poblet, Bingel–Hirsch reactions on non-IPR Gd_3N@C_{2n} (2n = 82 and 84), J. Org. Chem. 75 (2010) 8299–8302.

[208] N. Alegret, P. Salvadó, A. Rodríguez-Fortea, J.M. Poblet, Bingel-Hirsch addition on non-isolated-pentagon-rule Gd_3N@C_{2n} (2n = 82 and 84): metallofullerenes products under kinetic control, J. Org. Chem. 78 (2013) 9986–9990.

[209] S. Yang, C. Chen, X. Li, T. Wei, F. Liu, S. Wang, Bingel-Hirsch monoadducts of $TiSc_2N$@I_h-C_{80} versus Sc_3N@I_h-C_{80}: reactivity improvement via internal metal atom substitution, Chem. Commun. 49 (2013) 10844–10846.

[210] S. Wang, J. Huang, C. Gao, F. Jin, Q. Li, S. Xie, S. Yang, Singly bonded monoadduct rather than methanofullerene: manipulating the addition pattern of trimetallic nitride clusterfullerene through one endohedral metal atom substitution, Chem. Eur. J. 22 (2016) 8309–8315.

[211] T. Cai, L. Xu, C. Shu, H.A. Champion, J.E. Reid, C. Anklin, M.R. Anderson, H.W. Gibson, H.C. Dorn, Selective formation of a symmetric Sc_3N@C_{78} bisadduct: adduct docking controlled by an internal trimetallic nitride cluster, J. Am. Chem. Soc. 130 (2008) 2136–2137.

[212] T. Cai, L. Xu, C. Shu, J.E. Reid, H.W. Gibson, H.C. Dorn, Synthesis and characterization of a non-IPR fullerene derivative: Sc_3N@C_{68}[C(COOC$_2$H$_5$)$_2$], J. Phys. Chem. C 112 (2008) 19203–19208.

[213] Y. Ma, T. Wang, J. Wu, Y. Feng, H. Li, L. Jiang, C. Shu, C. Wang, Electron spin manipulation via encaged cluster: differing anion radicals of Y_2@C_{82}-C_s, Y_2C_2@C_{82}-C_s, and Sc_2C_2@C_{82}-C_s, J. Phys. Chem. Lett. 4 (2013) 464–467.

[214] J.P. Martínez, M. Garcia-Borràs, S. Osuna, J. Poater, F.M. Bickelhaupt, M. Solà, Reaction mechanism and regioselectivity of the bingel-hirsch addition of dimethyl bromomalonate to La@C_{2v}-C_{82}, Chem. Eur. J. 22 (2016) 5953–5962.

[215] P. Zhao, J.-S. Dang, X. Zhao, Bingel-Hirsch reaction mechanisms on $TiSc_2N$@I_h-C_{80}: role of the endohedral titanium nitride, Phys. Chem. Chem. Phys. 18 (2016) 9709–9714.

[216] M. Garcia-Borràs, S. Osuna, J.M. Luis, M. Swart, M. Solà, The role of aromaticity in determining the molecular structure and reactivity of (endohedral metallo)fullerenes, Chem. Soc. Rev. 43 (2014) 5089–5105.

[217] M. Garcia-Borràs, J.M. Luis, M. Solà, S. Osuna, The key role of aromaticity in the structure and reactivity of C_{60} and endohedral metallofullerenes, Inorg. Chim. Acta 468 (2017) 38–48.

[218] M. Garcia-Borràs, S. Osuna, M. Swart, J.M. Luis, L. Echegoyen, M. Solà, Aromaticity as the driving force for the stability of non-IPR endohedral metallofullerene Bingel-Hirsch adducts, Chem. Commun. 49 (2013) 8767–8769.

[219] B. Sitharaman, R.D. Bolskar, I. Rusakova, L.J. Wilson, Gd@C_{60}[C(COOH)$_2$]$_{10}$ and Gd@C_{60}(OH)x: nanoscale aggregation studies of two metallofullerene MRI contrast agents in aqueous solution, Nano Lett. 4 (2004) 2373–2378.

[220] B. Sitharaman, L.A. Tran, C.P. Pham, R.D. Bolskar, R. Muthupillai, S.D. Flamm, A.G. Mikos, L.J. Wilson, Gadofullerenes as nanoscale magnetic labels for cellular MRI, Contrast Media Mol. Imaging 2 (2007) 139–146.

[221] M. Yamada, T. Akasaka, S. Nagase, Carbene additions to fullerenes, Chem. Rev. 113 (2013) 7209–7264.

[222] T. Suzuki, Y. Maruyama, T. Kato, T. Akasaka, K. Kobayashi, S. Nagase, K. Yamamoto, H. Funasaka, T. Takahashi, Chemical reactivity of a metallofullerene: EPR study of diphenylmethano-La@C_{82} radicals, J. Am. Chem. Soc. 117 (1995) 9606–9607.

[223] H. Ueno, H. Okada, M. Maruyama, H. Sato, H. Tobita, Y. Ono, K. Omote, K. Kawachi, Y. Kasama, Covalently chemical modification of lithium ion-encapsulated fullerene synthesis and characterization of [Li$^+$@PCBM]PF$_6^-$, Org. Lett. 14 (2012) 3784–3787.

[224] H. Ueno, H. Okada, S. Aoyagi, Y. Matsuo, Synthesis and crystal structure of Li$^+$@Fluoreno[60]fullerene: effect of encapsulated lithium ion on electrochemistry of spiroannelated fullerene, J. Org. Chem. 82 (2017) 11631–11635.

[225] H. Okada, H. Kawakami, S. Aoyagi, Y. Matsuo, Crystallographic structure determination of both [5,6]- and [6,6]-isomers of lithium-ion-containing dipheylmethano[60]fullerene, J. Org. Chem. 82 (2017) 5868–5872.

[226] L. Feng, X. Zhang, Z. Yu, J. Wang, Z. Gu, Chemical modification of Tb@C_{82} by copper(I)-catalyzed cycloadditions, Chem. Mater. 14 (2002) 4021–4022.

[227] Y. Maeda, Y. Matsunaga, T. Wakahara, S. Takahashi, T. Tsuchiya, M.O. Ishitsuka, T. Hasegawa, T. Akasaka, M.T.H. Liu, K. Kokura, E. Horn, K. Yoza, T. Kato, S. Okubo, K. Kobayashi, S. Nagase, K. Yamamoto, Isolation and characterization of a carbene derivative of La@C_{82}, J. Am. Chem. Soc. 126 (2004) 6858–6859.

[228] T. Akasaka, T. Kono, Y. Takematsu, H. Nikawa, T. Nakahodo, T. Wakahara, M.O. Ishitsuka, T. Tsuchiya, Y. Maeda, M.T.H. Liu, K. Yoza, T. Kato, K. Yamamoto, N. Mizorogi, Z. Slanina, S. Nagase, Does Gd@C_{82} have an anomalous endohedral structure? Synthesis and single crystal X-ray structure of the carbene adduct, J. Am. Chem. Soc. 130 (2008) 12840–12841.

[229] X. Lu, H. Nikawa, L. Feng, T. Tsuchiya, Y. Maeda, T. Akasaka, N. Mizorogi, Z. Slanina, S. Nagase, Location of the yttrium atom in Y@C_{82} and its influence on the reactivity of cage carbons, J. Am. Chem. Soc. 131 (2009) 12066–12067.

[230] Y. Takano, M. Aoyagi, M. Yamada, H. Nikawa, Z. Slanina, N. Mizorogi, M.O. Ishitsuka, T. Tsuchiya, Y. Maeda, T. Akasaka, T. Kato, S. Nagase, Anisotropic magnetic behavior of anionic Ce@C_{82} carbene adducts, J. Am. Chem. Soc. 131 (2009) 9340–9346.

[231] M. Hachiya, H. Nikawa, N. Mizorogi, T. Tsuchiya, X. Lu, T. Akasaka, Exceptional chemical properties of Sc@C_{2v}(9)-C_{82} probed with adamantylidene carbene, J. Am. Chem. Soc. 134 (2012) 15550–15555.

[232] Q. Zhou, H. Li, Y. Wang, Y. Lian, Formation of the first derivatives of praseodymium-containing metallofullerenes via regioselective carbene addition to Pr@C_{2v}(9)-C_{82}, Phys. Status Solidi A-Appl. Mat. 211 (2014) 2735–2738.

[233] Q. Zhou, H. Li, Y. Lian, M. Suzuki, L. Bao, W. Cai, W. Wang, S. Nagase, X. Lu, T. Akasaka, Regioselective synthesis and molecular structure of the first

derivative of praseodymium-containing metallofullerenes, Chem. Commun. 50 (2014) 9876–9878.
[234] M.O. Ishitsuka, H. Enoki, T. Tsuchiya, Z. Slanina, N. Mizorogi, S. Nagase, M.T.H. Liu, T. Akasaka, Chemical modification of endohedral metallofullerene La@C_{82} with 3-chloro-3-phenyldiazirine, Phosphorus Sulfur Silicon Relat. Elem. 185 (2010) 1124–1130.
[235] Y. Xie, M. Suzuki, W. Cai, N. Mizorogi, S. Nagase, T. Akasaka, X. Lu, Highly regioselective addition of adamantylidene carbene to Yb@C_{2v}(3)-C_{80} to afford the first derivative of divalent metallofullerenes, Angew. Chem. Int. Ed. 52 (2013) 5142–5145.
[236] W. Zhang, M. Suzuki, Y. Xie, L. Bao, W. Cai, Z. Slanina, S. Nagase, M. Xu, T. Akasaka, X. Lu, Molecular structure and chemical property of a divalent metallofullerene Yb@C_2(13)-C_{84}, J. Am. Chem. Soc. 135 (2013) 12730–12735.
[237] Y. Zhao, H. Yu, Y. Lian, Experimental and theoretical evaluation of structures of Pr_2@C_{72} and its functionalized adduct with adamantylidene carbene, RSC Adv. 6 (2016) 115113–115119.
[238] M. Yamada, C.I. Someya, T. Nakahodo, Y. Maeda, T. Tsuchiya, T. Akasaka, Synthesis of endohedral metallofullerene glycoconjugates by carbene addition, Molecules 16 (2011) 9495–9504.
[239] M.O. Ishitsuka, S. Sano, H. Enoki, S. Sato, H. Nikawa, T. Tsuchiya, Z. Slanina, N. Mizorogi, M.T.H. Liu, T. Akasaka, S. Nagase, Regioselective bis-functionalization of endohedral dimetallofullerene, La_2@C_{80}: extremal La–La distance, J. Am. Chem. Soc. 133 (2011) 7128–7134.
[240] M. Yamada, C. Someya, T. Wakahara, T. Tsuchiya, Y. Maeda, T. Akasaka, K. Yoza, E. Horn, M.T.H. Liu, N. Mizorogi, S. Nagase, Metal atoms collinear with the spiro carbon of 6,6-open adducts, M_2@C_{80}(Ad) (M = La and Ce, Ad = adamantylidene), J. Am. Chem. Soc. 130 (2008) 1171–1176.
[241] W. Shen, L. Yang, Y. Wu, L. Bao, Y. Li, P. Jin, H. Fang, Y. Xie, X. Lu, Reactions between N-heterocyclic carbene and lutetium-metallofullerenes: high regioselectivity directed by electronic effect in addition to steric hindrance, J. Org. Chem. 84 (2019) 606–612.
[242] M. Izquierdo, M.R. Cerón, M.M. Olmstead, A.L. Balch, L. Echegoyen, [5,6]-Open methanofullerene derivatives of I_h-C_{80}, Angew. Chem. Int. Ed. 52 (2013) 11826–11830.
[243] M. Yamada, T. Abe, C. Saito, T. Yamazaki, S. Sato, N. Mizorogi, Z. Slanina, F. Uhlík, M. Suzuki, Y. Maeda, Y. Lian, X. Lu, M.M. Olmstead, A.L. Balch, S. Nagase, T. Akasaka, Adamantylidene addition to M_3N@I_h-C_{80} (M = Sc, Lu) and Sc_3N@D_{5h}-C_{80}: synthesis and crystallographic characterization of the [5,6]-open and [6,6]-open adducts, Chem. Eur. J. 23 (2017) 6552–6561.
[244] M. Chen, L. Bao, M. Ai, W. Shen, X. Lu, Sc_3N@I_h-C_{80} as a novel lewis acid: an abnormal N-heterocyclic carbene unprecedented formation of a singly bonded [6, 6, 6]-adduct, Chem. Sci. 7 (2016) 2331–2334.
[245] M. Chen, W. Shen, P. Peng, L. Bao, S. Zhao, Y. Xie, P. Jin, H. Fang, F. Li, X. Lu, Evidence of oxygen activation in the reaction between an N-heterocyclic carbene and M_3N@I_h(7)–C_{80}: an unexpected method of steric hindrance release, J. Org. Chem. 82 (2017) 3500–3505.
[246] M.R. Cerón, M. Izquierdo, N. Alegret, J.A. Valdez, A. Rodríguez-Fortea, M.M. Olmstead, A.L. Balch, J.M. Poblet, L. Echegoyen, Reactivity differences of Sc_3N@C_{2n} (2n = 68 and 80). Synthesis of the first methanofullerene derivatives of Sc_3N@D_{5h}-C_{80}, Chem. Commun. 52 (2016) 64–67.
[247] H. Kurihara, X. Lu, Y. Iiduka, N. Mizorogi, Z. Slanina, T. Tsuchiya, T. Akasaka, S. Nagase, Sc_2C_2@C_{80} rather than Sc_2@C_{82}: templated formation of unexpected C_{2v}(5)-C_{80} and temperature-dependent dynamic motion of internal Sc_2C_2 cluster, J. Am. Chem. Soc. 133 (2011) 2382–2385.
[248] H. Kurihara, X. Lu, Y. Iiduka, H. Nikawa, N. Mizorogi, Z. Slanina, T. Tsuchiya, S. Nagase, T. Akasaka, Chemical understanding of carbide cluster metallofullerenes: a case study on Sc_2C_2@C_{2v}(5)–C_{80} with complete X-ray crystallographic characterizations, J. Am. Chem. Soc. 134 (2012) 3139–3144.
[249] L. Bao, M. Chen, W. Shen, L. Yang, P. Jin, X. Lu, Lewis acid–base adducts of Sc_2C_2@C_{3v}(8)-C_{82}/N-heterocyclic carbene: toward isomerically pure metallofullerene derivatives, Inorg. Chem. 56 (2017) 4711–14750.
[250] H. Kurihara, Y. Iiduka, Y. Rubin, M. Waelchli, N. Mizorogi, Z. Slanina, T. Tsuchiya, S. Nagase, T. Akasaka, Unexpected formation of a Sc_3C_2@C_{80} bisfulleroid derivative, J. Am. Chem. Soc. 134 (2012) 4092–4095.
[251] M. Yamada, Y. Tanabe, J.-S. Dang, S. Sato, N. Mizorogi, M. Hachiya, M. Suzuki, T. Abe, H. Kurihara, Y. Maeda, X. Zhao, Y. Lian, S. Nagase, T. Akasaka, D_{2d}(23)-C_{84} versus Sc_2C_2@D_{2d}(23)-C_{84}: impact of endohedral Sc_2C_2 doping on chemical reactivity in the photolysis of diazirine, J. Am. Chem. Soc. 138 (2016) 16523–16532.
[252] Y. Wang, Q. Zhou, Y. Zhao, W. Dong, Y. Lian, Formation of the first derivatives of endohedral diterbium fullerenes via carbene addition to a large carbon cage, Fuller. Nanotub. Carbon Nanostruct. 23 (2015) 1018–1023.
[253] H. Li, C. Risko, J.H. Seo, C. Campbell, G. Wu, J.-L. Brédas, G.C. Bazan, Fullerene-carbene lewis acid-base adducts, J. Am. Chem. Soc. 133 (2011) 12410–12413.
[254] P. Jin, S. Nagase, Density functional theory study of fullerene-carbene lewis acid-base adducts: critical role of dispersion interactions, RSC Adv. 3 (2013) 10177–10180.
[255] M. Li, M. Su, The addition reactions between N-heterocyclic carbenes and fullerenes (C_{60} and C_{70}): a density functional study, Theor. Chem. Acc. 134 (2015) 38.
[256] P. Jin, L. Yang, C. Liu, M. Chen, Q. Hou, L. Li, Y. Zhao, A comparative study on the N-heterocyclic carbene adducts of I_h-C_{60}, D_{5h}–C_{70} and Sc_3N@I_h-C_{80}, Phys. Chem. Chem. Phys. 19 (2017) 17598–17606.
[257] X. Lu, J. Xu, X. He, Z. Sh, Z. Gu, Addition of benzyne to Gd@C_{82}, Chem. Mater. 16 (2004) 953–955.
[258] X. Lu, H. Nikawa, T. Tsuchiya, T. Akasaka, M. Toki, H. Sawa, N. Mizorogi, S. Nagase, Nitrated benzyne derivatives of La@C_{82}: addition of NO_2 and its positional directing effect on the subsequent addition of benzynes, Angew. Chem. Int. Ed. 49 (2010) 594–597.
[259] F.-F. Li, J.R. Pinzón, B.Q. Mercado, M.M. Olmstead, A.L. Balch, L. Echegoyen, [2+2] cycloaddition reaction to Sc_3N@I_h-C_{80}. The formation of very stable [5,6]- and [6,6]-adducts, J. Am. Chem. Soc. 133 (2011) 1563–1571.
[260] G.-W. Wang, T.-X. Liu, M. Jiao, N. Wang, S.-E. Zhu, C. Chen, S. Yang, F.L. Bowles, C.M. Beavers, M.M. Olmstead, B.Q. Mercado, A.L. Balch, The cycloaddition reaction of I_h-Sc_3N@C_{80} with 2-amino-4,5-diisopropoxybenzoic acid and isoamyl nitrite to produce an open-cage metallofullerene, Angew. Chem. Int. Ed. 50 (2011) 4658–4662.
[261] C.-G. Liu, Electronic structures and second-order nonlinear optical properties of a series of functionalized Sc_3N@I_h-C_{80} derivatives, Comput. Theor. Chem. 996 (2012) 51–56.
[262] A.A. Popov, A.D. Pykhova, I.N. Ioffe, F.-F. Li, L. Echegoyen, Anion radicals of isomeric [5,6] and [6,6] benzoadducts of Sc_3N@C_{80}: remarkable differences in endohedral cluster spin density and dynamics, J. Am. Chem. Soc. 136 (2014) 13436–13441.
[263] T. Yang, S. Nagase, T. Akasaka, J.M. Poblet, K.N. Houk, M. Ehara, X. Zhao, (2 + 2) cycloaddition of benzyne to endohedral metallofullerenes M_3N@C_{80} (M = Sc, Y): a rotating-intermediate mechanism, J. Am. Chem. Soc. 137 (2015) 6820–6828.
[264] S. Li, C. Tang, X. Zhang, How will the benzyne group $-C_6H_4$ affect the structure, electronic and optical properties of M_3N@C_{80} (M = Sc, Y), Comput. Theor. Chem. 1084 (2016) 17–24.
[265] A. Moreno-Vicente, M. Mulet-Gas, P.W. Dunk, J.M. Poblet, A. Rodríguez-Fortea, Probing the formation of halogenated endohedral metallofullerenes: predictions confirmed by experiments, Carbon 129 (2018) 750–757.
[266] A. Nakagawa, M. Nishino, H. Niwa, K. Ishino, Z. Wang, H. Omachi, K. Furukawa, S. Yamaguchi, T. Kato, S. Bandow, J. Rio, C. Ewels, S. Aoyagi, H. Shinohara, Crystalline functionalized endohedral C_{60} metallofullerides, Nat. Commun. 9 (2018) 3073.
[267] Z. Wang, Y. Nakanishi, S. Noda, H. Niwa, J. Zhang, R. Kitaura, H. Shinohara, Missing small-bandgap metallofullerenes: their isolation and electronic properties, Angew. Chem. Int. Ed. 52 (2013) 11770–11774.
[268] Z. Wang, S. Aoyagi, H. Omachi, R. Kitaura, H. Shinohara, Isolation and structure determination of a missing endohedral fullerene La@C_{70} through in situ trifluoromethylation, Angew. Chem. Int. Ed. 55 (2016) 199–202.
[269] T. Wakahara, H. Nikawa, T. Kikuchi, T. Nakahodo, G.M.A. Rahman, T. Tsuchiya, Y. Maeda, T. Akasaka, K. Yoza, E. Horn, K. Yamamoto, N. Mizorogi, Z. Slanina, S. Nagase, La@C_{72} having non-IPR carbon cage, J. Am. Chem. Soc. 128 (2006) 14228–14229.
[270] C. Tang, W. Shen, K. Deng, How will the dichlophenyl group affect the geometric structure, electronic properties, and static linear polarizability of La@C_{72}?, J. Mol. Struct. (Theochem) 894 (2009) 112–116.
[271] K. Sawada, Y. Takano, M. Izquierdo, S. Filippone, N. Martín, Z. Slanina, N. Mizorogi, M. Waelchli, T. Tsuchiya, T. Akasaka, S. Nagase, Enantioselective synthesis of endohedral metallofullerenes, J. Am. Chem. Soc. 133 (2011) 17746–17752.
[272] Y.-L. Zhao, Q. Zhou, Y.-F. Lian, H.-T. Yu, Molecular structures of Pr@C_{72} and Pr@C_{72}($C_6H_3Cl_2$): a combined experimental–theoretical investigation, RSC Adv. 5 (2015) 97568–97578.
[273] Y. Maeda, T. Tsuchiya, T. Kikuchi, H. Nikawa, T. Yang, X. Zhao, Z. Slanina, M. Suzuki, M. Yamada, Y. Lian, S. Nagase, X. Lu, T. Akasaka, Effective derivatization and extraction of insoluble missing lanthanum metallofullerenes La@C_{2n} (n = 36–38) with iodobenzene, Carbon 98 (2016) 67–73.
[274] H. Nikawa, T. Kikuchi, T. Wakahara, T. Nakahodo, T. Tsuchiya, G.M.A. Rahman, T. Akasaka, Y. Maeda, K. Yoza, E. Horn, K. Yamomoto, N. Mizorogi, S. Nagase, Missing metallofullerene La@C_{74}, J. Am. Chem. Soc. 127 (2005) 9684–9685.
[275] X. Lu, H. Nikawa, T. Kikuchi, N. Mizorogi, Z. Slanina, T. Tsuchiya, S. Nagase, T. Akasaka, Radical derivatives of insoluble La@C_{74}: X-ray structures, metal positions, and isomerization, Angew. Chem. Int. Ed. 50 (2011) 6356–6359.
[276] C. Tang, K. Deng, W. Tan, Y. Yuan, Y. Liu, H. Wu, D. Huang, F. Hu, J. Yang, X. Wang, Influence of a dichlophenyl group on the geometric structure, electronic properties, and static linear polarizability of La@C_{74}, Phys. Rev. A 76 (2007) 013201.
[277] Y.-L. Zhao, Q. Zhou, Y.-F. Lian, H.-T. Yu, Experimental and theoretical investigation of structures and relative reactivity of Pr@C_{74} and Pr@C_{74}($C_6H_3Cl_2$), Diam. Relat. Mater. 64 (2016) 110–118.
[278] H. Nikawa, T. Yamada, B. Cao, N. Mizorogi, Z. Slanina, T. Tsuchiya, T. Akasaka, K. Yoza, S. Nagase, Missing metallofullerene with C_{80} Cage, J. Am. Chem. Soc. 131 (2009) 10950–10954.
[279] I.E. Kareev, V.P. Bubnov, E.B. Yagubskii, Trifluoromethyl derivatives of cerium endohedral metallofullerenes, Russ. Chem. Bull., Int. Ed. 60 (2011) 1058–1062.
[280] Y. Takano, A. Yomogida, H. Nikawa, M. Yamada, T. Wakahara, T. Tsuchiya, M. O. Ishitsuka, Y. Maeda, T. Akasaka, T. Kato, Z. Slanina, N. Mizorogi, S. Nagase, Radical coupling reaction of paramagnetic endohedral metallofullerene La@C_{82}, J. Am. Chem. Soc. 130 (2008) 16224–16230.
[281] Y. Takano, M.O. Ishitsuka, T. Tsuchiya, T. Akasaka, T. Kato, S. Nagase, Retro-reaction of singly bonded La@C_{82} derivatives, Chem. Commun. 46 (2010) 8035–8036.
[282] N. Tagmatarchis, A. Taninaka, H. Shinohara, M. Prato, Synthesis and EPR characterization of exohedrally perfluoroalkylated paramagnetic lanthanum

metallofullerenes: a fluorous phase approach, AIP Conf. Proc. 633 (2002) 12–16.
[283] I.E. Kareev, V.P. Bubnov, E.B. Yagubskii, Endohedral gadolinium-containing metallofullerenes in the trifluoromethylation reaction, Russ. Chem. Bull., Int. Ed. 57 (2008) 1486–1491.
[284] B.L. Tumanskii, V.V. Bashilov, S.P. Solodovnikov, V.I. Sokolov, V.P. Bubnov, E.E. Laukhina, Ya.I. Estrin, V.K. Kol'tover, E.B. Yagubskii, EPR study of reactivity of endohedral metallofullerenes La@C_{82} and Y@C_{82}, Fullerene Sci. Technol. 6 (1998) 445–451.
[285] Z. Slanina, F. Uhlík, S.-L. Lee, L. Adamowicz, H. Kurihara, H. Nikawa, X. Lu, M. Yamada, S. Nagase, T. Akasaka, Computations on metallofullerenes derivatized during extraction La@C_{80}-$C_6H_3Cl_2$ and La@C_{82}-$C_6H_3Cl_2$, Fuller. Nanotub. Carbon Nanostruct. 22 (2014) 173–181.
[286] T. Akasaka, X. Lu, H. Kuga, H. Nikawa, N. Mizorogi, Z. Slanina, T. Tsuchiya, K. Yoza, S. Nagase, Dichlorophenyl derivatives of La@$C_{3v}(7)$-C_{82}: endohedral metal induced localization of pyramidalization and spin on a triple-hexagon junction, Angew. Chem. Int. Ed. 49 (2010) 9715–9719.
[287] Y. Takano, R. Tashita, M. Suzuki, S. Nagase, H. Imahori, T. Akasaka, Molecular location sensing approach by anisotropic magnetism of an endohedral metallofullerene, J. Am. Chem. Soc. 138 (2016) 8000–8006.
[288] I.E. Kareev, S.F. Lebedkin, V.P. Bubnov, E.B. Yagubskii, I.N. Ioffe, P.A. Khavrel, I. V. Kuvychko, S.H. Strauss, O.V. Boltalina, Trifluoromethylated endohedral metallofullerenes: synthesis and characterization of Y@$C_{82}(CF_3)_5$, Angew. Chem., Int. Ed. 44 (2005) 1846–1849.
[289] L. Bao, M. Chen, C. Pan, T. Yamaguchi, T. Kato, M.M. Olmstead, A.L. Balch, T. Akasaka, X. Lu, Crystallographic evidence for direct metal-metal bonding in a stable open-shell $La_2@I_h$-C_{80} derivative, Angew. Chem. Int. Ed. 55 (2016) 4242–4246.
[290] F. Liu, D.S. Krylov, L. Spree, S.M. Avdoshenko, N.A. Samoylova, M. Rosenkranz, A. Kostanyan, T. Greber, A.U.B. Wolter, B. Büchner, A.A. Popov, Single molecule magnet with an unpaired electron trapped between two lanthanide ions inside a fullerene, Nat. Commun. 8 (2017) 16098.
[291] F. Liu, G. Velkos, D.S. Krylov, L. Spree, M. Zalibera, R. Ray, N.A. Samoylova, C.-H. Chen, M. Rosenkranz, S. Schiemenz, F. Ziegs, K. Nenkov, A. Kostanyan, T. Greber, A.U.B. Wolter, M. Richter, B. Büchner, S.M. Avdoshenko, A.A. Popov, Air-stable redox-active nanomagnets with lanthanide spins radical-bridged by a metal–metal bond, Nat. Commun. 10 (2019) 571.
[292] M. Yamada, H. Kurihara, M. Suzuki, M. Saito, Z. Slanina, F. Uhlík, T. Aizawa, T. Kato, M.M. Olmstead, A.L. Balch, Y. Maeda, S. Nagase, X. Lu, T. Akasaka, Hiding and recovering electrons in a dimetallic endohedral fullerene: air-stable products from radical additions, J. Am. Chem. Soc. 137 (2015) 232–238.
[293] X. Ding, J.M. Alford, J.C. Wright, Lanthanide fluorescence from Er^{3+} in $Er_2@C_{82}$, Chem. Phys. Lett. 269 (1997) 72–78.
[294] C. Shu, C. Slebodnick, L. Xu, H. Champion, T. Fuhrer, T. Cai, E. Reid, W. Fu, K. Harich, H.C. Dorn, H.W. Gibson, Highly regioselective derivatization of trimetallic nitride templated endohedral metallofullerenes via a facile photochemical reaction, J. Am. Chem. Soc. 130 (2008) 17755–17760.
[295] C. Shu, T. Cai, L. Xu, T. Zuo, J. Reid, K. Harich, H.C. Dorn, H.W. Gibson, Manganese(III)-catalyzed free radical reactions on trimetallic nitride endohedral metallofullerenes, J. Am. Chem. Soc. 129 (2007) 15710–15717.
[296] N.B. Shustova, A.A. Popov, M.A. Mackey, C.E. Coumbe, J.P. Phillips, S. Stevenson, S.H. Strauss, O.V. Boltalina, Radical trifluoromethylation of $Sc_3N@C_{80}$, J. Am. Chem. Soc. 129 (2007) 11676–11677.
[297] N.B. Shustova, Y.-S. Chen, M.A. Mackey, C.E. Coumbe, J.P. Phillips, S. Stevenson, A.A. Popov, O.V. Boltalina, S.H. Strauss, $Sc_3N@(C_{80}$-$I_h(7))(CF_3)_{14}$ and $Sc_3N@(C_{80}$-$I_h(7))(CF_3)_{16}$. Endohedral metallofullerene derivatives with exohedral addends on four and eight triple-hexagon junctions. Does the Sc_3N cluster control the addition pattern or vice versa?, J Am. Chem. Soc. 131 (2009) 17630–17637.
[298] S. Yang, C. Chen, M.A. Lanskikh, N.B. Tamm, E. Kemnitz, S.I. Troyanov, New isomers of trifluoromethylated derivatives of metallofullerene cluster fullerene: $Sc_3N@C_{80}(CF_3)_n$ (n = 14 and 16), Chem. Asian J. 6 (2011) 505–509.
[299] S. Yang, C. Chen, M. Jiao, N.B. Tamm, M.A. Lanskikh, E. Kemnitz, S.I. Troyanov, Synthesis, isolation, and addition patterns of trifluoromethylated D_{5h} and I_h isomers of $Sc_3N@C_{80}$: $Sc_3N@D_{5h}$-$C_{80}(CF_3)_{18}$ and $Sc_3N@I_h$-$C_{80}(CF_3)_{14}$, Inorg. Chem. 50 (2011) 3766–3771.
[300] T. Wei, N.B. Tamm, S. Yang, S.I. Troyanov, New trifluoromethylated derivatives of metal nitride cluster fullerenes $Sc_3N@I_h$-$C_{80}(CF_3)_{14}$ and $Sc_3N@D_{5h}$-$C_{80}(CF_3)_{16}$, Chem. Asian J. 9 (2014) 2449–2452.
[301] A.A. Popov, N.B. Shustova, A.L. Svitova, M.A. Mackey, C.E. Coumbe, J.P. Phillips, S. Stevenson, S.H. Strauss, O.V. Boltalina, L. Dunsch, Redox-tuning endohedral fullerene spin states: from the dication to the trianion radical of $Sc_3N@C_{80}(CF_3)_2$ in five reversible single-electron steps, Chem. Eur. J. 16 (2010) 4721–4727.
[302] A.A. Popov, L. Dunsch, Charge controlled changes in the cluster and spin dynamics of $Sc_3N@C_{80}(CF_3)_2$: the flexible spin density distribution and its impact on ESR spectra, Phys. Chem. Chem. Phys. 13 (2011) 8977–8984.
[303] N.B. Shustova, D.V. Peryshkov, I.V. Kuvychko, Y.-S. Chen, M.A. Mackey, C.E. Coumbe, D.T. Heaps, B.S. Confait, T. Heine, J.P. Phillips, S. Stevenson, L. Dunsch, A.A. Popov, S.H. Strauss, O.V. Boltalina, Poly(perfluoroalkylation) of metallic nitride fullerenes reveals addition-pattern guidelines: synthesis and characterization of a family of $Sc_3N@C_{80}(CF_3)_n$ (n = 2–16) and their radical anions, J. Am. Chem. Soc. 133 (2011) 2672–2690.
[304] J.M. Campanera, M.I. Heggie, R. Taylor, Analysis of polyaddition levels in *i*-Sc_3NC_{80}, J. Phys. Chem. B 109 (2005) 4024–4031.
[305] F. Jin, N.B. Tamm, S.I. Troyanov, S. Yang, Steering the geometry of butterfly-shaped dimetal carbide cluster within a carbon cage via trifluoromethylation of $Y_2C_2@C_{82}(6)$, J. Am. Chem. Soc. 140 (2018) 3496–3499.
[306] F. Jin, S. Wang, S. Yang, N.B. Tamm, I.N. Ioffe, S.I. Troyanov, Trifluoromethyl derivatives of a monometallic cyanide cluster fullerene, YCN@$C_{82}(6)(CF_3)_{16/18}$, Inorg. Chem. 55 (2016) 12523–12526.
[307] F. Jin, S. Wang, N.B. Tamm, S. Yang, S.I. Troyanov, Synthesis, isolation and trifluoromethylation of two isomers of C_{84}-based monometallic cyanide clusterfullerenes: interplay between the endohedral cluster and the exohedral addends, Angew. Chem. Int. Ed. 56 (2017) 11990–11994.
[308] A.A. Popov, S.M. Avdoshenko, A.M. Pendás, L. Dunsch, Bonding between strongly repulsive metal atoms: an oxymoron made real in a confined space of endohedral metallofullerenes, Chem. Commun. 48 (2012) 8031–8050.
[309] A.A. Popov, Redox-active metal–metal bonds between lanthanides in dimetallofullerenes, Curr. Opin. Electrochem. 8 (2018) 73–80.
[310] A. Velloth, Y. Imamura, M. Hada, Functionalization of endohedral metallofullerenes toward improving barrier height for the relaxation of magnetization for $Dy_2@C_{80}$-X (X = CF_3, $C_3N_3Ph_2$), Inorg. Chem. 58 (2019) 1208–1215.
[311] Z. Wang, R. Kitaura, H. Shinohara, Metal-dependent stability of pristine and functionalized unconventional dimetallofullerene $M_2@I_h$-C_{80}, J. Phys. Chem. C 118 (2014) 13953–13958.
[312] D. Xu, Z. Wang, H. Shinohara, Capturing the unconventional metallofullerene M@C_{66} by trifluoromethylation: a theoretical study, ChemPhysChem 18 (2017) 3007–3011.
[313] J. Guan, D. Tomanek, Can CF_3-functionalized La@C_{60} be isolated experimentally and become superconducting, Nano Lett. 17 (2017) 3402–3408.
[314] A. Suzuki, T. Oku, Electronic structure and magnetic properties of endohedral metallofullerenes based on mixed metal cluster within fullerene cage with trifluoromethyl groups, J. Phys.: Conf. Ser. 433 (2013) 012004.
[315] A. Suzuki, T. Oku, Influence of chemical substitution in $Sc_xY_{3-x}N@C_{80}(CF_3)_n$ endohedral fullerenes on magnetic properties, Physica B 428 (2013) 18–26.
[316] A. Suzuki, T. Oku, Role of scandium atom in $Sc_xY_{3-x}N@C_{80}(CF_3)_n$ (n = 0, 2) on nuclear quadrupole interaction, electric field gradient and asymmetric parameters, Microelectron. Eng. 126 (2014) 113–117.
[317] Y. Abe, A. Suzuki, T. Oku, Electronic structures and magnetic properties of $Sc_4O_2@C_{80}(CF_3)_n$ (n = 2 and 4), J. Appl. Phys. 53 (2014) 05FN02.
[318] R.D. Bolskar, Gadofullerene MRI contrast agents, Nanomedicine 3 (2008) 201–213.
[319] S. Zhang, D. Sun, X. Li, F. Pei, S. Liu, Synthesis and solvent enhanced relaxation property of water-soluble endohedral metallofullerenols, Full. Sci. Techol. 5 (1997) 1635–1643.
[320] J. Zhang, F. Li, X. Miao, J. Zhao, L. Jing, G. Yang, X. Jia, Most stable structures of polyhydroxylated endohedral metallofullerene Gd@$C_{82}(OH)_x$ (x = 1–24) from density functional theory, Chem. Phys. Lett. 492 (2010) 68–70.
[321] Z. Wang, Z. Xu, Y. Zhao, X. Gao, Oxidation-induced water-solubilization and chemical functionalization of fullerenes C_{60}, Gd@C_{60} and Gd@C_{82}: atomistic insight into the formation mechanisms, Nanoscale 7 (2015) 2914–2925.
[322] I.G. Rodríguez-Zavala, I. Padilla-Osuna, R.A. Guirado-López, Modifying the endohedral La-ion location in both neutral and positively charged polyhydroxylated metallofullerenes, Phys. Rev. B 78 (2008) 155426.
[323] X. Gao, B.-Z. Chen, X. Gao, Isolated aromatic patches as a rule to select metallofullerene multiple adducts with high chemical stabilities, Carbon 96 (2016) 980–986.
[324] X.J. Gao, X. Shen, B. Chen, X. Gao, Improved description for the structures of fullerenols $C_{60}(OH)_n$ (n =12-48) and $C_{2v}(9)$–$C_{82}(OH)_x$ (x = 14–58), J. Phys. Chem. C 120 (2016) 11709–11715.
[325] H. He, L. Zheng, P. Jin, M. Yang, The structural stability of polyhydroxylated $C_{60}(OH)_{24}$: density functional theory characterizations, Comput. Theor. Chem. 974 (2011) 16–20.
[326] G. Wu, X.J. Gao, J. Jang, X. Gao, Fullerenes and their derivatives as inhibitors of tumor necrosis factor-α with highly promoted affinities, J. Mol. Model. 22 (2016) 161.
[327] H. Ueno, Y. Nakamura, N. Ikuma, K. Kokubo, T. Oshima, Synthesis of a lithium-encapsulated fullerenol and the effect of the internal lithium cation on its aggregation behavior, Nano Res. 5 (2012) 558–564.
[328] C.-Y. Shu, L.-H. Gan, C.-R. Wang, X.-L. Pei, H.-B. Han, Synthesis and characterization of a new water-soluble endohedral metallofullerene for MRI contrast agents, Carbon 44 (2006) 496–500.
[329] M. Ehrich, R.V. Tassell, Y. Li, Z. Zhou, C.L. Kepley, Fullerene antioxidants decrease organophosphate-induced acetylcholinesterase inhibition in vitro, Toxicol. Vitro 25 (2011) 301–307.
[330] E. Tóth, R.D. Bolskar, A. Borel, G. González, L. Helm, A.E. Merbach, B. Sitharaman, L.J. Wilson, Water-soluble gadofullerenes: toward high-relaxivity, pH-responsive MRI contrast agents, J. Am. Chem. Soc. 127 (2005) 799–805.
[331] V.T. Lebedev, Yu.S. Grushko, D.N. Orlova, A.F. Kim, V.S. Kozlov, V.P. Sedov, S.G. Kolesnik, V.V. Shamanin, E. Yu, Melenevskaya, aggregation in hydroxylated endohedral fullerene solutions, Fuller. Nanotub. Carbon Nanostruct. 18 (2010) 422–426.
[332] E.B. Iezzi, F. Cromer, P. Stevenson, H.C. Dorn, Synthesis of the first water-soluble trimetallic nitride endohedral metallofullerols, Synth. Met. 128 (2002) 289–291.
[333] M. Okumura, M. Mikawa, T. Yokawa, Y. Kanazawa, H. Kato, H. Shinohara, Evaluation of water-soluble metallofullerenes as MRI contrast agents, Acad. Radiol. 9 (2002) S495–S497.

[334] X. Lu, H. Li, B. Sun, Z. Shi, Z. Gu, Selective reduction and extraction of Gd@C_{82} and Gd_2@C_{80} from soot and the chemical reaction of their anions, Carbon 43 (2005) 1546–1549.

[335] C. Shu, F.D. Corwin, J. Zhang, Z. Chen, J.E. Reid, M. Sun, W. Xu, J.H. Sim, C. Wang, P.P. Fatouros, A.R. Esker, H.W. Gibson, H.C. Dorn, Facile preparation of a new gadofullerene-based magnetic resonance imaging contrast agent with high ^{1}H relaxivity, Bioconjugate Chem. 20 (2009) 1186–1193.

[336] H. Kato, Y. Kanazawa, M. Okumura, A. Taninaka, T. Yokawa, H. Shinohara, Lanthanoid endohedral metallofullerenols for MRI contrast agents, J. Am. Chem. Soc. 125 (2003) 4391–4397.

[337] S. Wang, B. Sun, D. Yue, L. Jing, R. He, T. Ren, J. Dong, H. Yuan, G. Xing, J. Wang, Y. Zhao, K. Ibrahim, Surface modification induced shielding effects on electron orbital coupling in metallofullerene, J. Nanosci. Nanotechnol. 10 (2010) 8625–8631.

[338] T. Zou, M. Zhen, J. Li, D. Chen, Y. Feng, R. Li, M. Guan, Y. Zhang, C. Shu, C. Wang, The effect of hemiketals on the relaxivity of endohedral gadofullerenols, RSC Adv. 5 (2015) 96253–96257.

[339] T. Li, S. Murphy, B. Kiselev, K.S. Bakshi, J. Zhang, A. Eltahir, Y. Zhang, Y. Chen, J. Zhu, R.M. Davis, L.A. Madsen, J.R. Morris, D.R. Karolyi, S.M. LaConte, Z. Sheng, H.C. Dorn, A new interleukin-13 amino-coated gadolinium metallofullerene nanoparticle for targeted MRI detection of glioblastoma tumor cells, J. Am. Chem. Soc. 137 (2015) 7881–7888.

[340] D. Sun, H. Huang, S. Yang, Z. Liu, S. Liu, Synthesis and characterization of a water-soluble endohedral metallofullerol, Chem. Mater. 11 (1999) 1003–1006.

[341] J. Zhang, Y. Ye, Y. Chen, C. Pregot, T. Li, S. Balasubramaniam, D.B. Hobart, Y. Zhang, S. Wi, R.M. Davis, L.A. Madsen, J.R. Morris, S.M. LaConte, G.T. Yee, H.C. Dorn, Gd_3N@$C_{84}(OH)_x$: a new egg-shaped metallofullerene magnetic resonance imaging contrast agent, J. Am. Chem. Soc. 136 (2014) 2630–2636.

[342] Y. Zhang, J. Xiang, J. Zhuang, Y. Li, B. Xin, F. Liu, K. Hou, Y. Tang, Synthesis of the first dihydroxyl adduct of Gd@C_{82}, Chem. Lett. 34 (2005) 1264–1265.

[343] B. Sun, Z. Gu, Synthesis and characterization of water-soluble metallofullerene derivatives, Chem. J. Chin. Univ. 24 (2003) 1747–1749.

[344] C. Chen, G. Xing, J. Wang, Y. Zhao, B. Li, J. Tang, G. Jia, T. Wang, J. Sun, L. Xing, H. Yuan, Y. Gao, H. Meng, Z. Chen, F. Zhao, Z. Chai, X. Fang, Multihydroxylated $[Gd@C_{82}(OH)_{22}]_n$ nanoparticles: antineoplastic activity of high efficiency and low toxicity, Nano Lett. 5 (2005) 2050–2057.

[345] Y. Cheng, K.M. Liu, G.M. Xing, H. Yuan, L. Jing, Y.L. Zhao, Study of multihydroxylated processes of Gd@C_{82} by ICP-MASS, J. Radioanal. Nucl. Chem. 272 (2007) 537–540.

[346] H.L. Fillmore, M.D. Shultz, S.C. Henderson, P. Cooper, W.C. Broaddus, Z. Chen, C.-Y. Shu, J. Zhang, J. Ge, H.C. Dorn, F. Corwin, J.I. Hirsch, [illegible] Wilson, Conjugation of functionalized gadolinium metallofullerenes with IL-13 peptides for targeting and imaging glial tumors, Nanomedicine 6 (2011) 449–458.

[347] J. Zheng, Q. Liu, M. Zhen, F. Jiang, C. Shu, C. Jin, Y. Yang, [illegible] A. Alhadlaq, C. Wang, Multifunctional imaging probe based on gadofullerene nanoplatform, Nanoscale 4 (2012) 3669–3672.

[348] L. Xiao, T. Li, M. Ding, J. Yang, J. Rodríguez-Corral, S. LaConte, N. Nacey, D. B. Weiss, L. Jin, H.C. Dorn, X. Li, Detecting chronic post-traumatic osteomyelitis of mouse tibia via an IL-13Rα2 targeted metallofullerene magnetic resonance imaging probe, Bioconjugate Chem. 28 (2017) 649–658.

[349] Y. Zhou, R. Deng, M. Zhen, J. Li, M. Guan, W. Jia, X. Li, Y. Zhang, T. Yu, T. Zou, Z. Lu, J. Guo, L. Sun, C. Shu, C. Wang, Amino acid functionalized gadofullerene nanoparticles with superior antitumor activity via destruction of tumor vasculature in vivo, Biomaterials 133 (2017) 107–118.

[350] T. Li, L. Xiao, J. Yang, M. Ding, Z. Zhou, L. LaConte, L. Jin, H.C. Dorn, X. Li, Trimetallic nitride endohedral fullerenes carboxyl-Gd_3N@C_{80}: a new theranostic agent for combating oxidative stress and resolving inflammation, ACS Appl. Mater. Interfaces 9 (2017) 17681–17689.

[351] J. Tang, G.M. Xing, H. Yuan, W.B. Cao, L. Jing, X.F. Gao, L. Gu, L. Cheng, C. Ye, Y. L. Zhao, Z.F. Chai, K. Ibrahim, H.J. Qian, R. Su, Tuning electronic properties of metallic atom in bondage to a nanospace, J. Phys. Chem. B 109 (2005) 8779–8785.

[352] I.I. Faingold, D.A. Poletaeva, R.A. Kotelnikova, A.S. Kornev, P.A. Troshin, I.E. Kareev, V.P. Bubnov, V.S. Romanova, A.I. Kotelnikov, Membranotropic and relaxation properties of water-soluble gadolinium endometallofullerene derivatives, Russ. Chem. Bull., Int. Ed. 63 (2014) 1107–1112.

[353] D.K. MacFarland, K.L. Walker, R.P. Lenk, S.C. Wilson, K. Kumar, C.L. Kepley, J.R. Garbow, Hydrochalarones: a novel endohedral metallofullerene platform for enhancing magnetic resonance imaging contrast, J. Med. Chem. 51 (2008) 3681–3683.

[354] J. Li, W. Yang, R. Cui, D. Wang, Y. Chang, W. Gu, W. Yin, X. Bai, K. Chen, L. Xia, H. Geng, G. Xing, Metabolism in vivo of fullerenes and metallofullerenes by positron emission tomography, Nanotechnology 27 (2016) 155101.

[355] E.Y. Zhang, C.Y. Shu, C.G. Ying, C.R. Wang, Preparation and characterization of two new water-soluble endohedral metallofullerenes as magnetic resonance imaging contrast agents, J. Phys. Chem. B 111 (2007) 14223–14226.

[356] J. Zhang, P.P. Fatouros, C. Shu, J. Reid, L.S. Owens, T. Cai, H.W. Gibson, G.L. Long, F.D. Corwin, Z.-J. Chen, H.C. Dorn, High relaxivity trimetallic nitride (Gd_3N) metallofullerene MRI contrast agents with optimized functionality, Bioconjugate Chem. 21 (2010) 610–615.

[357] P.P. Fatouros, F.K. Corwin, Z.J. Chen, W.C. Broaddus, J.L. Tatum, B. Kettenmann, Z. Ge, H.W. Gibson, J.L. Russ, A.P. Leonard, J.C. Duchamp, H.C. Dorn, In vitro and in vivo imaging studies of a new endohedral metallofullerene nanoparticle, Radiology 240 (2006) 756–764.

[358] A. Miyamoto, H. Okimoto, H. Shinohara, Y. Shibamoto, Development of water-soluble metallofullerenes as X-ray contrast media, Eur. Radiol. 16 (2006) 1050–1053.

[359] H. Kato, K. Suenaga, W. Mikawa, M. Okumura, N. Miwa, A. Yashiro, H. Fujimura, A. Mizuno, Y. Nishida, K. Kobayashi, H. Shinohara, Syntheses and EELS characterization of water-soluble multi-hydroxyl Gd@C_{82} fullerenols, Chem. Phys. Lett. 324 (2000) 255–259.

[360] S.A. Anderson, K.K. Lee, J.A. Frank, Gadolinium-fullerenol as a paramagnetic contrast agent for cellular imaging, Invest. Radiol. 41 (2006) 332–338.

[361] M. Mikawa, H. Kato, M. Okumura, M. Narazaki, Y. Kanazawa, N. Miwa, H. Shinohara, Paramagnetic water-soluble metallofullerenes having the highest relaxivity for MRI contrast agents, Bioconjugate Chem. 12 (2001) 510–514.

[362] J.-P. Zheng, M.-M. Zhen, J.-C. Ge, Q.-L. Liu, F. Jiang, C.-Y. Shu, H.A. Alhadlaq, C.-R. Wang, Multifunctional gadofulleride nanoprobe for magnetic resonance imagingfluorescent dual modality molecular imaging and free radical scavenging, Carbon 65 (2013) 175–180.

[363] D.W. Cagle, S.J. Kennel, S. Mirzadeh, J.M. Alford, L.J. Wilson, In vivo studies of fullerene-based materials using endohedral metallofullerene radiotracers, Proc. Natl. Acad. Sci. USA 96 (1999) 5182–5187.

[364] C. Li, R. Cui, L. Feng, J. Li, H. huang, H. Yao, X. Guo, J. Dong, G. Xing, Z. Liu, B. Sun, Synthesis of a UCNP@SiO_2@Gadofullerenes nanocomposite and its application in UCLMR Bimodal Imaging, RSC Adv. 6 (2016) 98968–98974.

[365] J. Zhang, K. Liu, G. Xing, T. Ren, S. Wang, Synthesis and in vivo study of metallofullerene based MRI contrast agent, J. Radioanal. Nucl. Chem. 272 (2007) 605–609.

[366] J. Li, T. Wang, Y. Feng, Y. Zhang, M. Zhen, C. Shu, L. Jiang, Y. Wang, C. Wang, A water-soluble gadolinium metallofullerenol: facile preparation, magnetic properties and magnetic resonance imaging application, Dalton Trans. 45 (2016) 8696–8699.

[367] H. Ueno, S. Toyagi, Y. Yamazaki, K. Ohkubo, N. Ikuma, H. Okada, T. Kato, Y. Matsuo, S. Fukuzumi, K. Kokubo, Electrochemical reduction of cationic Li^+@neutral Li^+@C_{60}: isolation and characterisation of endohedral [60]fullerene, Chem. Sci. 7 (2016) 5770–5774.

[368] H. Shinohara, M. Inakuma, M. Kishida, S. Yamzaki, T. Hashizume, T. Sakurai, A. Oriented cluster formation of endohedral Y@C_{82} metallofullerenes on clean surfaces, J. Phys. Chem. 99 (1995) 13769–13771.

[369] Y. Hasegawa, Y. Ling, S. Yamazaki, T. Hashizume, H. Shinohara, T. Sakurai, STM study on one-dimensional cluster formation processes of Y@C_{82} and C_{60} molecules, Mater. Sci. Eng. A 217 (218) (1996) 23–26.

[370] Y. Hasegawa, Y. Ling, S. Yamazaki, T. Hashizume, H. Shinohara, A. Sakai, H.W. Pickering, T. Sakurai, STM study of one-dimensional cluster formation of fullerenes dimerization in Y@C_{82}, Phys. Rev. B 56 (1997) 6470–6473.

[371] N. Lin, H. Huang, S. Yang, N. Cue, Nucleation of endohedral metallofullerene Nd@C_{82} on Cu(111), Phys. Rev. B 58 (1998) 2126–2130.

[372] K. Furukawa, S. Okubo, H. Kato, H. Shinohara, T. Kato, High-field/high-frequency ESR study of Gd@C_{82}-I, J. Phys. Chem. A 107 (2003) 10933–10937.

[373] S. Zhang, J. Dong, B. Yuan, X. Qiu, S. Yang, J. Hao, H. Zhang, H. Yuan, G. Xing, Y. Zhao, B. Sun, Scanning tunneling microscopy investigation of substrate-dependent adsorption and assembly of metallofullerene Gd@C_{82} on Cu(111), J. Phys. Chem. C 115 (2011) 6265–6268.

[374] S.-R. Shi, X.-S. Wang, H. Huang, S.-H. Yang, W. Heiland, N. Cue, Scanning tunneling microscopy of endohedral metallofullerene Tb@C_{82} on C_{60} film and Si(100) 2 × 1 surface, J. Phys. Chem. B 105 (2001) 11414–11418.

[375] M. Suzuki, M. Yamada, Y. Maeda, S. Sato, Y. Takano, F. Uhlík, Z. Slanina, Y. Lian, X. Lu, S. Nagase, M.M. Olmstead, A.L. Balch, T. Akasaka, The unanticipated dimerization of Ce@$C_{2v}(9)$-C_{82} upon co-crystallization with Ni(octaethylporphyrin) and comparison with monomeric M@$C_{2v}(9)$-C_{82} (M = La, Sc, and Y), Chem. Eur. J. 22 (2016) 18115–18122.

[376] L. Bao, C. Pan, Z. Slanina, F. Uhlík, T. Akasaka, X. Lu, Isolation and crystallographic characterization of the labile isomer of Y@C_{82} cocrystallized with Ni(OEP): unprecedented dimerization of pristine metallofullerenes, Angew. Chem. Int. Ed. 55 (2016) 9234–9238.

[377] S. Hu, T. Liu, W. Shen, Z. Slanina, T. Akasaka, Y. Xie, F. Uhlik, W. Huang, X. Lu, Isolation and structural characterization of Er@$C_{2v}(9)$–C_{82} and Er@$C_s(6)$–C_{82}: regioselective dimerization of a pristine endohedral metallofullerene induced by cage symmetry, Inorg. Chem. 58 (2019) 2177–2182.

[378] M. Koshino, Y. Niimi, E. Nakamura, H. Kataura, T. Okazaki, K. Suenaga, S. Iijima, Analysis of the reactivity and selectivity of fullerene dimerization reactions at the atomic level, Nat. Chem. 2 (2010) 117–124.

[379] T. Huang, J. Zhao, M. Feng, H. Petek, S. Yang, L. Dunsch, Superatom orbitals of Sc_3N@C_{80} and their intermolecular hybridization on Cu(110)-(2x1)-O surface, Phys. Rev. B 81 (2010) 085434.

[380] D.V. Konarev, L. Zorina, S.S. Khasanov, A.A. Popov, A. Otsuka, H. Yamochi, G. Saito, R.N. Lyubovskaya, A crystalline anionic complex of scandium nitride endometallofullerene experimental observation of single-bonded (Sc_3N@I_h-C_{80}^-)$_2$ dimers, Chem. Commun. 52 (2016) 10763–10766.

[381] A.A. Voevodin, L. Abella, E. Castro, D.W. Paley, L.M. Campos, A. Rodríguez-Fortea, J.M. Poblet, L. Echegoyen, X. Roy, Dimerization of endohedral fullerene in a superatomic crystal, Chem. Eur. J. 23 (2017) 13305–13308.

[382] Y. Jiang, D. Wang, D. Xu, J. Zhang, Z. Wang, Dimerization of metallofullerenes to obtain materials with enhanced nonlinear optical properties, ChemPhysChem 19 (2018) 2995–3000.

[383] A.A. Popov, S.M. Avdoshenko, G. Cuniberti, L. Dunsch, Dimerization of radical-anions nitride clusterfullerenes versus empty fullerenes, J. Phys. Chem. Lett. 2 (2011) 1592–1600.

[384] P. Rapta, A.A. Popov, S. Yang, L. Dunsch, Charged states of $Sc_3N@C_{68}$: an in situ spectroelectrochemical study of the radical cation and radical anion of a non-IPR fullerene, J. Phys. Chem. A 112 (2008) 5858–5865.

[385] L. Abella, Q. Tang, X. Zhang, Y. Wang, N. Chen, J.M. Poblet, A. Rodríguez-Fortea, $Sc_3O@I_h(7)$-C_{80}: a trimetallic oxide clusterfullerene abundant in the raw soot, J. Phys. Chem. C 120 (2016) 26159–26167.

[386] T. Ono, K. Hirose, First-principles study of electron-conduction properties of C_{60} bridges, Phys. Rev. Lett. 98 (2007) 026804.

[387] P. Zhao, D.S. Liu, Y. Zhang, Y. Su, H.Y. Liu, S.J. Li, G. Chen, Large low bias negative differential resistance in an endohedral $Li@C_{60}$ dimer junction, J. Phys. Chem. C 116 (2012) 7968–7974.

[388] T. Watanabe, M.F. Itoh, T. Komuro, H. Okada, T. Sakai, Y. Ono, K. Kawachi, Y. Kasama, H. Tobita, Iridium and platinum complexes of $Li^+@C_{60}$, Organometallics 33 (2014) 608–611.

[389] C.-H. Chen, D.-Y. Lin, W.-Y. Yeh, Regiospecific coordination of Re_3 clusters with the sumanene-type hexagons on endohedral metallofullerenes and higher fullerenes that provides an efficient separation method, Chem. Eur. J. 20 (2014) 5768–5775.

[390] L. Bao, B. Liu, X. Li, C. Pan, Y. Xie, X. Lu, $W(CO)_3(Ph_2PC_2H_4PPh_2)(\eta^2$-$Sc_3N@I_h$-$C_{80}$/$Sc_3N@D_{5h}$-$C_{80})$ regioselective synthesis and crystallographic characterization of air-stable mononuclear complexes of endohedral fullerenes, Dalton Trans. 45 (2016) 11606–11610.

[391] C.-H. Chen, W.-Y. Yeh, Y.-H. Liu, G.-H. Lee, [(μ -H)$_3$Re$_3$(CO)$_9$(η 2, η2, η^2-$Sc_2C_2@C_{3v}(8)$-C_{82})]: face-capping cluster complex of an endohedral fullerene, Angew. Chem. Int. Ed. 51 (2012) 13046–13049.

[392] M.-C. Yang, A.K. Sharma, W.M.C. Sameera, K. Morokuma, M.-D. Su, Theoretical study of addition reactions of L_4M(M = Rh, Ir) and L_2M(M = Pd, Pt) to $Li^+@C_{60}$, J. Phys. Chem. A. 121 (2017) 2665–2673.

[393] H. Zheng, X. Zhao, S. Sakaki, [2 + 2]-type reaction of metal-metal σ-bond with fullerene forming an η^1-C_{60} metal complex: mechanistic details of formation reaction and prediction of a New η^1-C_{60} metal complex, Inorg. Chem. 56 (2017) 6746–6754.

[394] T. Tsuchiya, T. Akasaka, S. Nagase, Construction of supramolecular systems based on endohedral metallofullerenes, Bull. Chem. Soc. Jpn. 82 (2009) 171–181.

[395] M. Supur, Y. Kawashima, K.R. Larsen, K. Ohkubo, J.O. Jeppesen, S. Fukuzumi, Robust inclusion complexes of crown ether fused tetrathiafulvalenes with $Li^+@C_{60}$ to afford efficient photodriven charge separation, Chem. Eur. J. 20 (2014) 13976–13983.

[396] K. Ohkubo, Y. Kawashima, S. Fukuzumi, Strong supramolecular binding of $Li^+@C_{60}$ with sulfonated meso-tetraphenylporphyrins and long-lived photoinduced charge separation, Chem. Commun. 48 (2012) 4314–4316.

[397] K. Ohkubo, Y. Kawashima, H. Sakai, T. Hasobe, S. Fukuzumi, Enhanced photoelectrochemical performance of composite photovoltaic cells of $Li^+@C_{60}$–sulphonated porphyrin supramolecular nanoclusters, Chem. Commun. 49 (2013) 4474–4476.

[398] Y. Kawashima, K. Ohkubo, H. Okada, Y. Matsuo, S. Fukuzumi, Supramolecular formation of $Li^+@$PCBM fullerene with sulfonated porphyrins and long-lived charge separation, ChemPhysChem 15 (2014) 3785–3790.

[399] N.L. Bill, M. Ishida, S. Bhring, J.M. Lim, S. Lee, C.M. Davis, V.M. Lynch, K.A. Nielsen, J.O. Jeppesen, K. Ohkubo, S. Fukuzumi, D. Kim, J.L. Sessler, Porphyrins fused with strongly electron-donating 1,3-dithiol-2-ylidene moieties: redox control by metal cation complexation and anion binding, J. Am. Chem. Soc. 135 (2013) 10852–10862.

[400] S. Fukuzumi, K. Ohkubo, Y. Kawashima, D.S. Kim, J.S. Park, A. Jana, V.M. Lynch, D. Kim, J.L. Sessler, Ion-controlled on–off switch of electron transfer from tetrathiafulvalene calix[4]pyrroles to $Li^+@C_{60}$, J. Am. Chem. Soc. 133 (2011) 15938–15941.

[401] C.M. Davis, K. Ohkubo, A.D. Lammer, D.S. Kim, Y. Kawashima, J.L. Sessler, S. Fukuzumi, Photoinduced electron transfer in a supramolecular triad produced by porphyrin anion-induced electron transfer from tetrathiafulvalene calix [4] pyrrole to $Li^+@C_{60}$, Chem. Commun. 51 (2015) 9787–9790.

[402] Y. Kawashima, K. Ohkubo, M. Kentaro, S. Fukuzumi, Electron transfer in a supramolecular complex of zinc chlorin carboxylate anion with $Li^+@C_{60}$ affording the long-lived charge-separated state, Phys. Chem. C 117 (2013) 21166–21177.

[403] K. Ohkubo, Y. Kawashima, K. Masek, H. Sakai, T. Hasobe, S. Fukuzumi, Photoelectrochemical properties of supramolecular composites of an anionic zinc chlorin and $Li^+@C_{60}$ on SnO_2 with porphyrins Phthalocyanines 18 (2014) 982–990.

[404] Y. Kawashima, K. Ohkubo, V.M. Blas-Ferrando, H. Sakai, E. Font-Sanchis, J. Ortíz, F. Fernández-Lázaro, T. Hasobe, Á. Sastre-Santos, S. Fukuzumi, Near-infrared photoelectrochemical conversion via photoinduced charge separation in supramolecular complexes of anionic phthalocyanines with $Li^+@C_{60}$, J. Phys. Chem. B 119 (2015) 7690–7697.

[405] T. Kamimura, K. Ohkubo, Y. Kawashima, H. Nobukuni, Y. Naruta, F. Tani, S. Fukuzumi, Sub-millisecond-lived photoinduced charge separation in inclusion complexes composed of $Li^+@C_{60}$ and cyclic porphyrin dimers, Chem. Sci. 4 (2013) 1451–1461.

[406] T. Kamimura, K. Ohkubo, Y. Kawashima, S. Ozako, K.-I. Sakaguchi, S. Fukuzumi, F. Tani, Long-lived photoinduced charge separation in inclusion complexes composed of a phenothiazine-bridged cyclic porphyrin dimer and fullerenes, J. Phys. Chem. C 119 (2015) 25634–25650.

[407] K. Ohkubo, T. Hasegawa, R. Rein, N. Solladié, S. Fukuzumi, Multiple photosynthetic reaction centres of porphyrinic polypeptide–$Li^+@C_{60}$ supramolecular complexes, Chem. Commun. 51 (2015) 17517–17520.

[408] Y. Kawashima, K. Ohkubo, S. Fukuzumi, Efficient charge separation in $Li^+@C_{60}$ supramolecular complexes with electron donors, Chem. Asian J. 10 (2015) 44–54.

[409] H. Ueno, T. Nishihara, Y. Segawa, K. Itami, Cycloparaphenylene-based ionic donor-acceptor supramolecule isolation and characterization of $Li^+@C_{60}$⊂[10] CPP, Angew. Chem. Int. Ed. 54 (2015) 3707–3711.

[410] S. Hitosugi, R. Iizuka, T. Yamasaki, R. Zhang, Y. Murata, H. Isobe, Assessment of fullerene derivatives as rolling journals in a finite carbon nanotube bearing, Org. Lett. 15 (2013) 3199–3201.

[411] M. Yamada, K. Ohkubo, M. Shionoya, S. Fukuzumi, Photoinduced electron transfer in a charge-transfer complex formed between corannulene and $Li^+@C_{60}$ by concave-convex π–π interactions, J. Am. Chem. Soc. 136 (2014) 13240–13248.

[412] M. Supur, Y. Kawashima, K. Ohkubo, H. Sakai, T. Hasobe, S. Fukuzumi, Graphene oxide–$Li^+@C_{60}$ donor–acceptor composites for photoenergy conversion, Phys. Chem. Chem. Phys. 17 (2015) 15732–15738.

[413] S. Yang, S. Yang, Preparation and film formation behavior of the supramolecular complex of the endohedral metallofullerene $Dy@C_{82}$ with calix[8]arene, Langmuir 18 (2002) 8488–8495.

[414] T. Tsuchiya, K. Sato, H. Kurihara, T. Wakahara, T. Nakahodo, Y. Maeda, T. Akasaka, K. Ohkubo, S. Fukuzumi, T. Kato, N. Mizorogi, K. Kobayashi, S. Nagase, Host-guest complexation of endohedral metallofullerene with azacrown ether and its application, J. Am. Chem. Soc. 128 (2006) 6699–6703.

[415] T. Tsuchiya, H. Kurihara, K. Sato, T. Wakahara, T. Akasaka, T. Shimizu, N. Kamigata, N. Mizorogi, S. Nagase, Supramolecular complexes of $La@C_{82}$ with unsaturated thiacrown ethers, Chem. Commun. 3585–3587 (2006).

[416] I.E. Kareev, E. Laukhina, V.P. Bubnov, V.M. Martynenko, V. Lloveras, J. Vidal-Gancedo, M. Mas-Torrent, J. Veciana, C. Rovira, Harnessing electron transfer from the perchlorotriphenylmethide anion to $Y@C_{82}(C_{2v})$ to engineer an endometallofullerene-based salt, ChemPhysChem 14 (2013) 1670–1675.

[417] V.M. Martynov, V.P. Bubnov, V.M. Martynenko, I.E. Kareev, E. Laukhina, J. Veciana, C. Rovira, Synthesis and characterization of endohedral metallofulleride K(18-crown-6)[Ho@$C_{82}(C_{2v})$], Russ. Chem. Bull. Int. Ed. 64 (2015) 2473–2476.

[418] T. Tsuchiya, K. Sato, H. Kurihara, T. Wakahara, Y. Maeda, T. Akasaka, K. Ohkubo, S. Fukuzumi, T. Kato, S. Nagase, Spin-site exchange system constructed from endohedral metallofullerenes and organic donors, J. Am. Chem. Soc. 128 (2006) 14418–14419.

[419] G. Pagona, S.P. Economopoulos, T. Aono, Y. Miyata, H. Shinohara, N. Tagmatarchis, Molecular recognition of $La@C_{82}$ endohedral metallofullerene by an isophthaloyl bridged porphyrin dimer, Tetrahedron Lett. 51 (2010) 5896–5899.

[420] F. Hajjaj, K. Yashiro, H. Nikawa, N. Mizorogi, T. Akasaka, S. Nagase, K. Furukawa, T. Kato, T. Aida, Ferromagnetic spin coupling between endohedral metallofullerene $La@C_{82}$ and a cyclodimeric copper porphyrin upon inclusion, J. Am. Chem. Soc. 133 (2011) 9290–9292.

[421] G. Gil-Ramírez, S.D. Karlen, A. Shundo, K. Porfyrakis, Y. Ito, G.A.D. Briggs, J.J.L. Morton, H.L. Anderson, A cyclic porphyrin trimer as a receptor for fullerenes, Org. Lett. 12 (2010) 3544–3547.

[422] G. Gil-Ramírez, A. Shah, H. El Mkami, K. Porfyrakis, G.A.D. Briggs, J.J.L. Morton, H.L. Anderson, J.E. Lovett, Distance measurement of a noncovalently bound $Y@C_{82}$ pair with double electron electron resonance spectroscopy, J. Am. Chem. Soc. 140 (2018) 7420–7424.

[423] Y. Nakanishi, H. Omachi, S. Matsuura, Y. Miyata, R. Kitaura, Y. Segawa, K. Itami, H. Shinohara, Size-selective complexation and extraction of endohedral metallofullerenes with cycloparaphenylene, Angew. Chem. Int. Ed. 53 (2014) 3102–3106.

[424] T. Iwamoto, Z. Slanina, N. Mizorogi, J. Guo, T. Akasaka, S. Nagase, H. Takaya, N. Yasuda, T. Kato, S. Yamago, Partial charge transfer in the shortest possible metallofullerene peapod, La@C_{82}⊂[11]cycloparaphenylene, Chem. Eur. J. 20 (2014) 14403–14409.

[425] R. Cui, J. Li, H. Huang, M. Zhang, X. Guo, Y. Chang, M. Li, J. Dong, B. Sun, G. Xing, Novel carbon nanohybrids as highly efficient magnetic resonance imaging contrast agents, Nano Res. 8 (2015) 1259–1268.

[426] J. Li, R. Cui, Y. Chang, X. Guo, W. Gu, H. Huang, K. Chen, G. Lin, J. Dong, G. Xing, B. Sun, Adaption of the structure of carbon nanohybrids toward high-relaxivity for a new MRI contrast agent, RSC Adv. 6 (2016) 58028–58033.

[427] T. Tsuchiya, M. Wielopolski, N. Sakuma, N. Mizorogi, T. Akasaka, T. Kato, D.M. Guldi, S. Nagase, Stable radical anions inside fullerene cages formation of reversible electron transfer systems, J. Am. Chem. Soc. 133 (2011) 13280–13283.

[428] L.P. Hernández-Eguia, E.C. Escudero-Adán, J.R. Pinzón, L. Echegoyen, P. Ballester, Complexation of $Sc_3N@C_{80}$ endohedral fullerene with cyclic Zn-bisporphyrins: solid state and solution studies, J. Org. Chem. 76 (2011) 3258–3265.

[429] B. Grimm, J. Schornbaum, C.M. Cardona, J.D. van Paauwe, P.D.W. Boyd, D.M. Guldi, Enhanced binding strengths of acyclic porphyrin hosts with endohedral metallofullerenes, Chem. Sci. 2 (2011) 1530–1537.

[430] V. Strauss, S.G. Radhakrishnan, J. Malig, N. Jux, D.M. Guldi, Catching metallic nitride endohedral fullerenes in organic and aqueous media, J. Porphyrins Phthalocyanines 20 (2016) 1–9.

[431] M.-Y. Ku, S.-J. Huang, S.-L. Huang, Y.-H. Liu, C.-C. Lai, S.-M. Peng, S.-H. Chiu, Hemicarceplex formation allows ready identification of the isomers of the metallofullerene $Sc_3N@C_{80}$ using ^1H and ^{13}C NMR spectroscopy, Chem. Commun. 50 (2014) 11709–11712.

[432] C. Fuertes-Espinosa, C. Garcia-Simon, E. Castro, M. Costas, L. Echegoyen, X. Ribas, A copper-based supramolecular nanocapsule that enables

straightforward purification of Sc_3N-based endohedral metallofullerene soots, Chem. Eur. J. 23 (2017) 3553–3557.
[433] H. Meng, C. Zhao, Y. Li, M. Nie, C. Wang, T. Wang, An implanted paramagnetic metallofullerene probe within a metal–organic framework, Nanoscale 10 (2018) 3291–3298.
[434] Y. Feng, T. Wang, Y. Li, J. Li, J. Wu, B. Wu, L. Jiang, C. Wang, Steering metallofullerene electron spin in porous metal-organic framework, J. Am. Chem. Soc. 137 (2015) 15055–15060.
[435] C. Zhao, H. Meng, M. Nie, L. Jiang, C. Wang, T. Wang, Anisotropic paramagnetic properties of metallofullerene confined in a metal-organic framework, J. Phys. Chem. C 122 (2018) 4635–4640.
[436] Q.-Z. Li, J.-J. Zheng, L. He, S. Nagase, X. Zhao, Stabilization of a chlorinated $^{\#4348}C_{66}$:C_{2v} cage by encapsulating monometal species coordination between metal and double hexagon-condensed pentalenes, Inorg. Chem. 55 (2016) 7667–7675.
[437] L. Wang, W.-Y. Wang, Y. Qiu, H.-Z. Lu, Second-order nonlinear optical response of electron donor-acceptor hybrids formed between corannulene and metallofullerenes, J. Phys. Chem. C 119 (2015) 24965–24975.
[438] H.U. Rehman, N.A. McKee, M.L. McKee, Saturn systems, J. Comput. Chem. 37 (2016) 194–209.
[439] L. Basurto, F. Amerikheirabadi, R. Zope, T. Baruah, The electronic structure and charge transfer excited states of the endohedral trimetallic nitride $C_{80}(I_h)$ fullerenes–Zn-tetraphenyl porphyrin dyads, Phys. Chem. Chem. Phys. 17 (2015) 5832–5839.
[440] F. Amerikheirabadi, C. Diaz, N. Mohan, R.R. Zope, T. Baruah, A DFT analysis of the ground and charge-transfer excited states of $Sc_3N@I_h$–C_{80} fullerene coupled with metal-free and zinc-phthalocyanine, Phys. Chem. Chem. Phys. 20 (2018) 25841–25848.
[441] J.U. Reveles, N.N. Karle, T. Baruah, R.R. Zope, Electronic and structural properties of C_{60} and $Sc_3N@C_{80}$ supported on graphene nanoflakes, J. Phys. Chem. C 120 (2016) 26083–26092.
[442] E.M. Cabaleiro-Lago, J. Rodríguez-Otero, J.A. Carrazana-García, A theoretical study of complexes between fullerenes and concave receptors with interest in photovoltaics, Phys. Chem. Chem. Phys. 19 (2017) 26787–26798.
[443] D. Sun, Z. Liu, Z. Liu, X. Guo, C. Hao, W. Xu, S. Liu, Gas phase derivations of endohedral metallofullerenes by ion-molecular reactions, Full. Sci. Technol. 5 (1997) 1461–1477.
[444] C. Hao, Z. Liu, X. Guo, Z. Liu, W. Xu, Y. Sun, S. Liu, Gas phase derivatization of endohedral metallofullerenes R@C_{82} and R_2@C_{80} (R = Nd, Ce), Rapid Commun. Mass Spectrom. 11 (1997) 1677–1680.
[445] D. Sun, Z. Liu, X. Guo, S. Liu, Synthesis and spectroscopic studies of endohedral metallofullerenes Tb@C_{2n}, Full. Sci. Technol. 6 (1998) 707–713.
[446] X. Li, L. Fan, D. Liu, H.H.Y. Sung, I.D. Williams, S. Yang, K. Tan, X. Lu, Synthesis of a Dy@C_{82} derivative bearing a single phosphorus substituent via a zwitterion approach, J. Am. Chem. Soc. 129 (2007) 10636–10637.
[447] M. Yamada, M. Minowa, S. Sato, Z. Slanina, T. Tsuchiya, Y. Maeda, S. Nagase, T. Akasaka, Regioselective cycloaddition of $La_2@I_h$-C_{80} with tetracyanoethylene oxide: formation of an endohedral dimetallofullerene adduct featuring enhanced electron-accepting character, J. Am. Chem. Soc. 133 (2011) 3796–3799.
[448] T.-X. Liu, T. Wei, S.-E. Zhu, G.-W. Wang, M. Jiao, S. Yang, F.L. Bowles, M.M. Olmstead, A.L. Balch, Azide addition to an endohedral metallofullerene formation of azafulleroids of $Sc_3N@I_h$-C_{80}, J. Am. Chem. Soc. 134 (2012) 11956–11959.
[449] F.-F. Li, A. Rodríguez-Fortea, J.M. Poblet, L. Echegoyen, Reactivity of metallic nitride endohedral metallofullerene anions: electrochemical synthesis of a $Lu_3N@I_h$-C_{80} derivative, J. Am. Chem. Soc. 133 (2011) 2760–2765.
[450] F.-F. Li, A. Rodríguez-Fortea, P. Peng, G.A.C. Chavez, J.M. Poblet, L. Echegoyen, Electrosynthesis of a $Sc_3N@I_h$-C_{80} methano derivative from thermionic $Sc_3N@I_h$-C_{80}, J. Am. Chem. Soc. 134 (2012) 7480–7487.
[451] K. Akiyama, T. Hamano, Y. Nakanishi, E. Takeuchi, S. Noda, Z. Wang, S. Kubuki, H. Shinohara, Non-HPLC rapid separation of metallofullerenes and empty cages with $TiCl_4$ lewis acid, J. Am. Chem. Soc. 134 (2012) 9762–9767.
[452] Z. Wang, Y. Nakanishi, S. Noda, K. Akiyama, H. Shinohara, The origin and mechanism of non-HPLC purification of metallofullerenes with $TiCl_4$, J. Phys. Chem. C 116 (2012) 25563–25567.
[453] Z. Wang, H. Omachi, H. Shinohara, Non-chromatographic purification of endohedral metallofullerenes, Molecules 22 (2017) 718.
[454] S. Stevenson, M.A. Mackey, J.E. Pickens, M.A. Stuart, B.S. Confait, J.P. Phillips, Selective complexation and reactivity of metallic nitride and oxometallic fullerenes with lewis acids and it as an effective purification method, Inorg. Chem. 48 (2009) 11685–11695.
[455] S. Stevenson, K.A. Rottinger, M. Fahim, J.S. Field, B.R. Martin, K.D. Arvola, Tuning the selectivity of Gd_3N cluster endohedral metallofullerene reactions with lewis acids, Inorg. Chem. 53 (2014) 12939–12946.
[456] H. Huang, L. Zhang, X. Cao, X. Guo, R. Cui, B. Xu, J. Dong, Y. Li, L. Gan, F. Chang, X. Gao, B. Sun, Regioselective polyamination of Gd@$C_{2v}(9)$-C_{82} and non-high performance liquid chromatography rapid separation of Gd@C_{82}(morpholine)$_7$, Chem. Mater. 30 (2018) 64–68.
[457] M. Yamada, Y. Muto, H. Kurihara, Z. Slanina, M. Suzuki, Y. Maeda, Y. Rubin, M. M. Olmstead, A.L. Balch, S. Nagase, X. Lu, T. Akasaka, Regioselective cage opening of $La_2@D_2(10611)$-C_{72} with 5,6-diphenyl-3-(2-pyridyl)-1,2,4-triazine, Angew. Chem. Int. Ed. 54 (2015) 2232–2235.
[458] Q.-Z. Li, J.-J. Zheng, X. Zhao, Azide addition to $Sc_2@C_{66}$: Favorable activity on unsaturated linear triquinanes and dramatic reactivity difference compared with free C_{66} cage, Phys. Chem. Chem. Phys. 17 (2015) 20485–20489.
[459] J. Gutiérrez-Flores, A. Moreno, F.J. Vázquez, C. Rios, B. Minutti, G. Morales, A. Suarez, E. Ramos, R. Salcedo, Cycloaddition reactions of pristine and endohedral fullerene molecules: possible anticancer activity, J. Mol. Model. 24 (2018) 268.
[460] A. Lassesson, A. Gromov, H. Jönsson, A. Taninaka, H. Shinohara, E.E.B. Campbell, Oxygen reactivity of La@C_{82} investigated with laser desorption mass spectrometry, Int. J. Mass Spectrom. 228 (2003) 913–920.
[461] J. Zhuang, Y. Wang, J. Yao, T. Yang, N. Chen, Synthesis and characterization of $Lu_3N@C_{80}O$, Chin. J. Chem. 35 (2017) 1459–1462.
[462] T. Wei, O. Martin, S. Yang, F. Hauke, A. Hirsch, Modular covalent graphene functionalization with C_{60} and the endohedral fullerene $Sc_3N@C_{80}$: a facile entry to inter-synthetic-carbon-allotrope-hybrids, Angew. Chem. Int. Ed. 58 (2019) 816–820.
[463] M. Rudolf, S. Wolfrum, D.M. Guldi, L. Feng, T. Tsuchiya, T. Akasaka, L. Echegoyen, Endohedral metallofullerenes—filled fullerene derivatives towards multifunctional reaction center mimics, Chem. Eur. J. 18 (2012) 5136–5148.
[464] M. Rudolf, S.V. Kirner, D.M. Guldi, A multicomponent molecular approach to artificial photosynthesis-the role of fullerenes and endohedral metallofullerenes, Chem. Soc. Rev. 45 (2016) 612–630.
[465] V. Strauss, A. Roth, M. Sekita, D.M. Guldi, Efficient energy-conversion materials for the future: understanding and tailoring charge-transfer processes in carbon nanostructures, Chem 1 (2016) 531–556.
[466] Y. Takano, S. Obuchi, N. Mizorogi, R. García, M.Á. Herranz, M. Rudolf, S. Wolfrum, D.M. Guldi, N. Martin, S. Nagase, T. Akasaka, Stabilizing ion and radical ion pair states in a paramagnetic endohedral metallofullerene/π-extended tetrathiafulvalene conjugate, J. Am. Chem. Soc. 134 (2012) 16103–16106.
[467] Y. Takano, M.Á. Herranz, N. Martín, S.G. Radhakrishnan, D.M. Guldi, T. Tsuchiya, S. Nagase, T. Akasaka, Donor-acceptor conjugates of lanthanum endohedral metallofullerene and π-extended tetrathiafulvalene, J. Am. Chem. Soc. 132 (2010) 8048–8055.
[468] C. Schubert, M. Rudolf, D.M. Guldi, Y. Takano, N. Mizorogi, M.A. Herranz, N. Martín, S. Nagase, T. Akasaka, Rates and energetics of intramolecular electron transfer processes in conjugated metallofullerenes, Philos. Trans. R. Soc., A 371 (2013) 20120490.
[469] D.M. Guldi, L. Feng, S.G. Radhakrishnan, H. Nikawa, M. Yamada, N. Mizorogi, T. Tsuchiya, T. Akasaka, S. Nagase, M.Á. Herranz, N. Martín, A molecular $Ce_2@I_h$-C_{80} switchs-unprecedented oxidative pathway in photoinduced charge transfer reactivity, J. Am. Chem. Soc. 132 (2010) 9078–9086.
[470] L. Feng, S.G. Radhakrishnan, N. Mizorogi, Z. Slanina, H. Nikawa, T. Tsuchiya, T. Akasaka, S. Nagase, N. Martín, D.M. Guldi, Synthesis and charge-transfer chemistry of $La_2@I_h$-C_{80}/$Sc_3N@I_h$-C_{80}–zinc porphyrin conjugates: impact of endohedral cluster, J. Am. Chem. Soc. 133 (2011) 7608–7618.
[471] Y. Takano, S. Obuchi, N. Mizorogi, R. Garcia, M.Á. Herranz, M. Rudolf, D.M. Guldi, N. Martin, S. Nagase, T. Akasaka, An endohedral metallofullerene as a pure electron donor, J. Am. Chem. Soc. 134 (2012) 19401–19408.
[472] L. Feng, Z. Slanina, S. Sato, K. Yoza, T. Tsuchiya, N. Mizorogi, T. Akasaka, S. Nagase, N. Martín, D.M. Guldi, Covalently linked porphyrin–La@C_{82} hybrids: structural elucidation and investigation of intramolecular interactions, Angew. Chem. Int. Ed. 50 (2011) 5909–5912.
[473] M. Rudolf, L. Feng, Z. Slanina, W. Wang, S. Nagase, T. Akasaka, D.M. Guldi, Strong electronic coupling and electron transfer in a $Ce_2@I_h$-C_{80}–H_2P electron donor acceptor conjugate, Nanoscale 8 (2016) 13257–13262.
[474] J.R. Pinzón, M.E. Plonska-Brzezinska, C.M. Cardona, A.J. Athans, S.S. Gayathri, D.M. Guldi, M.Á. Herranz, N. Martín, T. Torres, L. Echegoyen, $Sc_3N@C_{80}$-ferrocene electron-donor/acceptor conjugates as promising materials for photovoltaic applications, Angew. Chem. Int. Ed. 47 (2008) 4173–4176.
[475] J.R. Pinzón, C.M. Cardona, M.Á. Herranz, M.E. Plonska-Brzezinska, A. Palkar, A. J. Athans, N. Martín, A. Rodríguez-Fortea, J.M. Poblet, G. Bottari, T. Torres, S.S. Gayathri, D.M. Guldi, L. Echegoyen, Metal nitride cluster fullerene $M_3N@C_{80}$ (M = Y, Sc) based dyads: synthesis, and electrochemical, theoretical and photophysical studies, Chem. Eur. J. 15 (2009) 864–877.
[476] T. Tsuchiya, M. Rudolf, S. Wolfrum, S.G. Radhakrishnan, R. Aoyama, Y. Yokosawa, A. Oshima, T. Akasaka, S. Nagase, D.M. Guldi, Coordinative interactions between porphyrins and C_{60}, La@C_{82}, and $La_2@C_{80}$, Chem. Eur. J. 19 (2013) 558–565.
[477] J.R. Pinzón, D.C. Gasca, S.G. Sankaranarayanan, G. Bottari, T. Torres, D.M. Guldi, L. Echegoyen, Photoinduced charge transfer and electrochemical properties of triphenylamine I_h-$Sc_3N@C_{80}$ donor acceptor conjugates, J. Am. Chem. Soc. 131 (2009) 7727–7734.
[478] S. Wolfrum, J.R. Pinzón, A. Molina-Ontoria, A. Gouloumis, N. Martín, L. Echegoyen, D.M. Guldi, Utilization of $Sc_3N@C_{80}$ in long-range charge transfer reactions, Chem. Commun. 47 (2011) 2270–2272.
[479] L. Feng, M. Rudolf, S. Wolfrum, A. Troeger, Z. Slanina, T. Akasaka, S. Nagase, N. Martín, T. Ameri, C.J. Brabec, D.M. Guldi, A paradigmatic change linking fullerenes to electron acceptors, J. Am. Chem. Soc. 134 (2012) 12190–12197.
[480] M. Rudolf, L. Feng, Z. Slanina, T. Akasaka, S. Nagase, D.M. Guldi, A metallofullerene electron donor that powers an efficient spin flip in a linear electron donor-acceptor conjugate, J. Am. Chem. Soc. 135 (2013) 11165–11174.
[481] R.B. Ross, C.M. Cardona, D.M. Guldi, S.G. Sankaranarayanan, M.O. Reese, N. Kopidakis, J. Peet, B. Walker, G.C. Bazan, E.V. Keuren, B.C. Holloway, M. Drees, Endohedral fullerenes for organic photovoltaic devices, Nat. Mater. 8 (2009) 208–212.

[482] R.B. Ross, C.M. Cardona, F.B. Swain, D.M. Guldi, S.G. Sandaranarayanan, E.V. Keuren, B.C. Holloway, M. Drees, Tuning conversion efficiency in metallo endohedral fullerene-based organic photovoltaic devices, Adv. Funct. Mater. 19 (2009) 2332–2337.
[483] M. Liedtke, A. Sperlich, H. Kraus, A. Baumann, C. Deibel, M.J.M. Wirix, J. Loos, C.M. Cardona, V. Dyakonov, Triplet exciton generation in bulk-heterojunction solar cells based on endohedral fullerenes, J. Am. Chem. Soc. 133 (2011) 9088–9094.
[484] L. Feng, M. Rudolf, O. Trukhina, Z. Slanina, F. Uhlík, X. Lu, T. Torres, D.M. Guldi, T. Akasaka, Tuning intramolecular electron and energy transfer processes in novel conjugates of $La_2@C_{80}$ and electron accepting Subphthalocyanines, Chem. Commun. 51 (2015) 330–333.
[485] T. Akasaka, A. Nakata, M. Rudolf, W.-W. Wang, M. Yamada, M. Suzuki, Y. Maeda, R. Aoyama, T. Tsuchiya, S. Nagase, D.M. Guldi, Synthesis and photoinduced electron-transfer reactions in a $La_2@I_h$-C_{80}–phenoxazine conjugate, ChemPlusChem 82 (2017) 1067–1072.
[486] O. Trukhina, M. Rudolf, G. Bottari, T. Akasaka, L. Echegoyen, T. Torres, D.M. Guldi, Bidirectional electron transfer capability in phthalocyanine–$Sc_3N@I_h$–C_{80} complexes, J. Am. Chem. Soc. 137 (2015) 12914–12922.
[487] B. Liu, H. Fang, X. Li, W. Cai, L. Bao, M. Rudolf, F. Plass, L. Fan, X. Lu, D.M. Guldi, Synthesis and photophysical properties of a $Sc_3N@C_{80}$-corrole electron donor-acceptor conjugate, Chem. Eur. J. 21 (2015) 746–752.
[488] J.P. Martínez, M. Solà, A.A. Voityuk, The driving force of photoinduced charge separation in metal-cluster-encapsulated triphenylamine-[80]fullerenes, Chem. Eur. J. 22 (2016) 17305–17310.
[489] B. Wu, J. Hu, P. Cui, L. Jiang, Z. Chen, Q. Zhang, C. Wang, Y. Luo, Visible-light photoexcited electron dynamics of scandium endohedral metallofullerenes: the cage symmetry and substituent effects, J. Am. Chem. Soc. 137 (2015) 8769–8774.
[490] O. Vostrowsky, A. Hirsch, Molecular peapods as supramolecular carbon allotropes, Angew. Chem. Int. Ed. 43 (2004) 2326–2329.
[491] A.N. Khlobystov, D.A. Britz, G.A.D. Briggs, Molecules in carbon nanotubes, Acc. Chem. Res. 38 (2005) 901–909.
[492] R. Kitaura, H. Shinohara, Carbon-nanotube-based hybrid materials nanopeapods, Chem. Asian J. 1 (2006) 646–655.
[493] R. Kitaura, H. Shinohara, Endohedral metallofullerenes and nano-peapods, Jpn. J. Appl. Phys. 46 (2007) 881–891.
[494] M. Koshino, Multiple reaction pathways of metallofullerenes investigated by transmission electron microscopy, Dalton Trans. 43 (2014) 7359–7365.
[495] K. Hirahara, K. Suenaga, S. Bandow, H. Kato, T. Okazaki, H. Shinohara, S. Iijima, One-dimensional metallofullerene crystal generated inside single-walled carbon nanotubes, Phys. Rev. Lett. 85 (2000) 5384–5387.
[496] T. Tsuchiya, R. Kumashiro, K. Tanigaki, Y. Matsunaga, M.O. Ishitsuka, T. Wakahara, Y. Maeda, Y. Takano, M. Aoyagi, T. Akasaka, M.T. Liu, T. Kato, K. Suenaga, J.S. Jeong, S. Iijima, F. Kimura, T. Kimura, S. Nagase, Nanorods of endohedral metallofullerene derivative, J. Am. Chem. Soc. 130 (2008) 450–451.
[497] S. Sato, S. Seki, Y. Honsho, L. Wang, H. Nikawa, G. Luo, Lu, M. Haranaka, T. Tsuchiya, S. Nagase, T. Akasaka, Semi-metallic single-component crystal of soluble $La@C_{82}$ derivative with high electron mobility, J. Am. Chem. Soc. 133 (2011) 2766–2771.
[498] M. Yamada, S. Sato, W. Choi, S. Seki, T. Abe, M. Suzuki, Y. Maeda, S. Nagase, T. Akasaka, Temperature dependence of anisotropic transient conductivity of a $La@C_{2v}$-C_{82}(Ad) crystal, Chem. Lett. 46 (2017) 973–975.
[499] M.O. Ishitsuka, H. Nikawa, N. Mizorogi, F. Kimura, T. Kimura, T. Kaneko, S. Nagase, T. Akasaka, Magnetic alignments of endohedral metallofullerene nanorods under magnetic fields, Fuller. Nanotub. Carbon Nanostruct. 23 (2014) 35–39.
[500] M.d.C. Gimenez-Lopez, A. Chuvilin, U. Kaiser, A.N. Khlobystov, Functionalised endohedral fullerenes in single-walled carbon nanotubes, Chem. Commun. 47 (2011) 2116–2118.
[501] A. Chuvilin, E. Bichoutskaia, M.C. Gimenez-Lopez, T.W. Chamberlain, G.A. Rance, N. Kuganathan, J. Biskupek, U. Kaiser, A.N. Khlobystov, Self-assembly of a sulphur-terminated graphene nanoribbon within a single-walled carbon nanotube, Nat. Mater. 10 (2011) 687–692.
[502] Y. Xu, C. He, F. Liu, M. Jiao, S. Yang, Hybrid hexagonal nanorods of metal nitride clusterfullerene and porphyrin using a supramolecular approach, J. Mater. Chem. 21 (2011) 13538–13545.
[503] D. Yue, X. Bai, S. Zhao, X. Miao, M. Li, J. Dong, K. Ibrahim, J. Wang, Y. Zhao, H. Yuan, G. Xing, B. Sun, First endohedral metallofullerene-containing polymer: preparation and characterization of $Gd@C_{82}$-polystyrene, J. Phys. Chem. C 114 (2010) 7631–7636.
[504] X.L. Ruan, D.M. Yue, S.Y. Yang, X.H. Guo, J.Q. Dong, R.L. Cui, B.Y. Sun, Synthesis and characterization of $Gd@C_{82}$-PVK and C_{60}-PVK–a kind of fullerene-grafted polymer, J. Nanosci. Nanotechnol. 12 (2012) 7233–7238.
[505] D. Yue, R. Cui, X. Ruan, H. Huang, X. Guo, Z. Wang, X. Gao, S. Yang, J. Dong, F. Yi, B. Sun, A novel organic electrical memory device based on the metallofullerene-grafted polymer ($Gd@C_{82}$-PVK), Org. Electron. 15 (2014) 3482–3486.
[506] K. Toth, J.K. Molloy, M. Matta, B. Heinrich, D. Guillon, G. Bergamini, F. Zerbetto, B. Donnio, P. Ceroni, D. Felder-Flesch, A strongly emitting liquid-crystalline derivative of $Y_3N@C_{80}$: bright and long-lived near-IR luminescence from a charge transfer state, Angew. Chem. Int. Ed. 52 (2013) 12303–12307.
[507] K.B. Ghiassi, M.M. Olmstead, A.L. Balch, Gadolinium-containing endohedral fullerenes: structures and function as magnetic resonance imaging (MRI) agents, Dalton Trans. 43 (2014) 7346–7358.
[508] T. Li, H.C. Dorn, Biomedical applications of metal-encapsulated fullerene nanoparticles, Small 13 (2017) 1603152.
[509] J.-J. Yin, F. Lao, P.P. Fu, W.G. Wamer, Y. Zhao, P.C. Wang, Y. Qiu, B. Sun, G. Xing, J. Dong, X.-J. Liang, C. Chen, The scavenging of reactive oxygen species and the potential for cell protection by functionalized fullerene materials, Biomaterials 30 (2009) 611–621.
[510] J. Meng, X. Liang, X. Chen, Y. Zhao, Biological characterizations of $[Gd@C_{82}(OH)_{22}]_n$ nanoparticles as fullerene derivatives for cancer therapy, Integ. Biol. 5 (2013) 43–47.
[511] Y. Liu, Y. Chen, P. Qian, X. Lu, B. Sun, X. Zhang, L. Wang, X. Gao, H. Li, Z. Chen, J. Tang, Y. Zhang, J. Dong, R. Bai, P.E. Lobie, Q. Wu, S. Liu, H. Zhang, F. Zhao, M.S. Wicha, T. Zhu, Y. Zhao, Gd-metallofullerenol nanomaterial as non-toxic breast cancer stem cell-specific inhibitor, Nat. Commun. 6 (2015) 5988.
[512] Y. Horiguchi, S. Kudo, Y. Nagasaki, $Gd@C_{82}$ metallofullerenes for neutron capture therapy—fullerene solubilization by poly(ethylene glycol)-block-poly(2-(N, N-diethylamino)ethyl methacrylate) and resultant efficacy in vitro, Sci. Technol. Adv. Mater. 12 (2011) 044607.
[513] M. Zhen, C. Shu, J. Li, G. Zhang, T. Wang, Y. Luo, T. Zou, R. Deng, F. Fang, H. Lei, C. Wang, C. Bai, A highly efficient and tumor vascular-targeting therapeutic technique with size-expansible gadofullerene nanocrystals, Sci. China Mater. 58 (2015) 799–810.
[514] M.D. Diener, J.M. Alford, S.J. Kennel, S. Mirzadeh, $^{212}Pb@C_{60}$ and its water-soluble derivatives synthesis, stability, and suitability for radioimmunotherapy, J. Am. Chem. Soc. 129 (2007) 5131–5138.
[515] M.E. Kueck, J.D. Wilson, C.E. Fuller, J. Zhang, H.C. Dorn, P.P. Fatouros, Metallofullerene-based nanoplatform for brain tumor brachytherapy and longitudinal imaging in a murine orthotopic xenograft model, Radiology 261 (2011) 136–143.
[516] J.D. Wilson, W.C. Broaddus, H.C. Dorn, P.P. Fatouros, C.E. Chalfant, M.D. Shultz, Metallofullerene-nanoplatform-delivered interstitial brachytherapy improved survival in a murine model of glioblastoma multiforme, Bioconjugate Chem. 23 (2012) 1873–1880.
[517] G. Zhang, Z. Sun, H. Song, M. Zhen, M. Guan, T. Chu, S. Luo, C. Wang, C. Shu, Radioactive lutetium metallofullerenes $^{177}Lu_xLu_{(3-x)}N@C_{80}$–PCBPEG derivative: a potential tumor-targeted theranostic agent, J. Mater. Chem. B 3 (2015) 7011–7013.
[518] S. Wang, J. Lin, Z. Wang, Z. Zhou, R. Bai, N. Lu, Y. Liu, X. Fu, O. Jacobson, W. Fan, J. Qu, S. Chen, T. Wang, P. Huang, X. Chen, Core-satellite polydopamine–gadolinium-metallofullerene nanotheranostics for multimodal imaging guided combination cancer therapy, Adv. Mater. 29 (2017) 1701013.
[519] M. Yamada, T. Akasaka, S. Nagase, Salvaging reactive fullerenes from soot by exohedral derivatization, Angew. Chem. Int. Ed. 57 (2018) 13394–13405.